2017

NEUTRON-ANTINEUTRON TRANSITIONS: EXPLORING $B - L$ VIOLATION WITH QUARKS

Xinshuai Yan
University of Kentucky, xinshuaiyan@gmail.com
Digital Object Identifier: https://doi.org/10.13023/ETD.2017.308

STUDENT AGREEMENT:

I represent that my thesis or dissertation and abstract are my original work. Proper attribution has been given to all outside sources. I understand that I am solely responsible for obtaining any needed copyright permissions. I have obtained needed written permission statement(s) from the owner(s) of each third-party copyrighted matter to be included in my work, allowing electronic distribution (if such use is not permitted by the fair use doctrine) which will be submitted to UKnowledge as Additional File.

I hereby grant to The University of Kentucky and its agents the irrevocable, non-exclusive, and royalty-free license to archive and make accessible my work in whole or in part in all forms of media, now or hereafter known. I agree that the document mentioned above may be made available immediately for worldwide access unless an embargo applies.

I retain all other ownership rights to the copyright of my work. I also retain the right to use in future works (such as articles or books) all or part of my work. I understand that I am free to register the copyright to my work.

REVIEW, APPROVAL AND ACCEPTANCE

The document mentioned above has been reviewed and accepted by the student's advisor, on behalf of the advisory committee, and by the Director of Graduate Studies (DGS), on behalf of the program; we verify that this is the final, approved version of the student's thesis including all changes required by the advisory committee. The undersigned agree to abide by the statements above.

Xinshuai Yan, Student

Dr. Susan Gardner, Major Professor

Dr. Christopher Crawford, Director of Graduate Studies

NEUTRON-ANTINEUTRON TRANSITIONS: EXPLORING $B - L$ VIOLATION WITH QUARKS

DISSERTATION

A dissertation submitted in partial fulfillment of the
requirements for the degree of Doctor of Philosophy in the
College of Arts and Sciences
at the University of Kentucky

By
Xinshuai Yan
Lexington, Kentucky

Director: Dr. Susan Gardner, Professor of Physics
Lexington, Kentucky 2017

ABSTRACT OF DISSERTATION

NEUTRON-ANTINEUTRON TRANSITIONS: EXPLORING $B-L$ VIOLATION WITH QUARKS

In the Standard Model (SM), the quantity baryon number (B) − lepton number (L), $B-L$, is perfectly conserved. Therefore, the observation of $B-L$ violation would reveal the existence of physics beyond the SM. Traditionally, given the severe experimental constraints on $|\Delta B| = 1$ processes, $B-L$ violation with baryons is probed via neutron-antineutron ($n-\bar{n}$) oscillations, although this process suffers from quenching in the presence of external fields or matter.

In this dissertation, we discuss another possibility, $n-\bar{n}$ conversion, in which the $|\Delta B| = 2$ process appears with an external source. We start with the Lorentz invariant $B-L$ violating operators of lowest mass dimension and show how the appearance of constraints on the "arbitrary" phases in the discrete symmetry transformations help restrict the possible low energy $n-\bar{n}$ transformation operators. To explain the appearance of CPT odd $n-\bar{n}$ transition operators (although they eventually vanish due to the fermion anticommutation relations), we connect it to theories of self-conjugate isofermions and show that the appearance of $n-\bar{n}$ oscillations cannot occur in pure Quantum Chromodynamics (QCD) in the chiral limit. We then show how $n-\bar{n}$ conversion can be free from quenching and demonstrate one way how it can be connected to $n-\bar{n}$ oscillations since the quarks carry electromagnetic charge. Effective field theory is utilized to find the quark-level conversion operators and to determine the coupling parameter associated with the nuclear-level conversion operators. Finally, we argue how $n-\bar{n}$ conversion can provide a complementary probe to oscillation experiments. We discuss possible $n-\bar{n}$ conversion proposals and explicitly show how $n-\bar{n}$ conversion experiments can set limits on the scale of $B-L$ violation.

KEYWORDS: $n-\bar{n}$ oscillation, discrete symmetries, $n-\bar{n}$ conversion, CP violation

Author's signature: Xinshuai Yan

Date: July 28, 2017

NEUTRON-ANTINEUTRON TRANSITIONS: EXPLORING $B - L$ VIOLATION WITH QUARKS

By
Xinshuai Yan

Director of Dissertation: Dr. Susan Gardner

Director of Graduate Studies: Dr. Christopher Crawford

Date: July 28, 2017

ACKNOWLEDGMENTS

First of all, I would like to express my great gratitude to my advisor Dr. Susan Gardner. She is an amazing physicist and a wonderful mentor. Her broad research interest leads me to work on different research projects and inspires my interest in various topics of physics. Her continuous encouragement in attending various summer schools and in giving presentations not only helps to broaden my research horizon but also to improve my social skills. Working under her guidance has been a great experience that I will always cherish.

Besides my advisor, I would like to thank the rest of my committee members: Dr. Sumit Das, Dr. Keh-Fei Liu, and Dr. Peter Perry for their kind guidance. I also really appreciate the help I received from Dr. Brad Plaster and Dr. Michael Eides.

Last but not least, I am very grateful to my parents and my younger brother and sister for their unconditional love and support.

TABLE OF CONTENTS

LIST OF FIGURES

LIST OF TABLES

CHAPTER 1

INTRODUCTION

Electrically neutral particle oscillations are no longer a surprising phenomenon in particle physics and have been playing an important role in revealing the nature of matter and forces participating in them. Neutral meson oscillations, such as $K^0 - \bar{K}^0$ and $B^0 - \bar{B}^0$, and neutrino oscillations are two excellent examples. The nature of CP[1] violation in the Standard Model (SM) was first observed through the decay of the CP-odd kaon (K_L) into two charged pions[1]. Although it appears in a decay process, later Wolfenstein pointed out that it actually arises from the $K^0 - \bar{K}^0$ mixing[2]. That CP violation can arise with the help of neutral meson oscillations was later confirmed by studies of the $B\bar{B}$ system, which also help in realization of the first true test of time reversal (T) violation in the SM [3]. Neutrinos have been treated as massless particles in the SM, and experimental observation of neutrino oscillations is the first clear evidence of existence of new physics, i.e., physics beyond the SM (BSM), because this can only occur if the neutrinos have mass. Since the neutron and antineutron are electrically neutral, the only thing forbidding a neutron from transforming into an antineutron is the baryon number (B) conservation.

There are many compelling reasons to believe that fundamental particle interactions should not respect baryon number symmetry. Possibly the most powerful one is that to generate the observed matter-antimatter asymmetry (or baryon asymmetry) in the universe (BAU) baryon number violation is necessary [4].

In fact, even the SM allows for baryon number violation. In the SM, the Lagrangian possesses an accidental[2] global baryon number symmetry. Because of the conserved baryon number current, $\partial_\mu j^\mu_B = 0$, it is impossible to violate baryon number at the classical level. However, Hooft [5] pointed out that loop-level effects can cause the violation of both B and L, but their cancellation leaves the combination $B - L$ intact. Although the probability of such processes occurring today is exponentially suppressed, in special situations, such as the primordial universe at very high temperatures [6, 7, 8, 9], B and L violations can play a significant role in baryogenesis.

[1] C and P denote charge conjugation and parity respectively.

[2] The most general renormalizable Lagrangian, which is invariant under the SM gauge groups and contains only color singlet Higgs fields, is automatically invariant under global Abelian symmetries, hence the name "accidental".

Nevertheless, neither B nor L is strictly conserved, and only $B-L$ is truly conserved in the SM. Therefore, any observation of $B-L$ violation would reveal the existence of new physics.

$B-L$ violation can appear in theories of leptons only. The most intriguing possibility is that of Majorana neutrinos, i.e., neutrinos that are their own antiparticles. Since the establishment of massive neutrinos, two theoretical descriptions of a massive neutrino become available: it can be either a Dirac or a Majorana particle, which corresponds to its mass emerging from either Dirac or Majorana mass terms. In fact, it can also emerge from mass of both types [10], though the mass eigenstates are still Majorana [11, 12]. A nonzero signal in searches for neutrinoless double beta decay ($\beta\beta_{0\nu}$) [13, 14, 15] would establish the Majorana character of neutrino, because $B-L$ violation would always generate an effective Majorana mass term even if such a mass term were not explicitly present [16]. However, observing the $\beta\beta_{0\nu}$ process is challenging. Refs.[17, 18, 19] point out that the contributions to the $\beta\beta_{0\nu}$ amplitude from the various neutrino mass can interfere destructively and partially cancel each other. Moreover, even a total cancellation is possible in a certain gauge model [20]. Consequently, it is possible that we may never observe such a process. To date no definite signal has been observed. Therefore, exploring $B-L$ violation in other sectors is necessary.

$B-L$ violation can also appear in theories with quarks because quarks carry a baryon number of 1/3. One example would be neutron - antineutron ($n-\bar{n}$) oscillation. There are several motivations to carry out $n-\bar{n}$ oscillation searches.

First of all, $n-\bar{n}$ oscillation searches may aid in the understanding of neutrino oscillations. It has been noted that well motivated quark-lepton unified theories which implement the seesaw mechanism[3] for neutrino masses can lead to observable amplitude of $n-\bar{n}$ oscillation [24, 25, 26, 27, 28, 29, 30, 31, 32]. Moreover, recently it has been shown that observing $n-\bar{n}$ oscillations in addition to another B violating mode (not necessarily breaking $B-L$), such as $p\to e^+\pi^0$ or $n\to e^-\pi^+$, can reveal the Majorana nature of neutrino [33]. This discussion utilizes a model-independent effective operator approach. It is showed that a Feynman diagram for $\beta\beta_{0\nu}$ can always be constructed by combining the responsible diagrams for $n-\bar{n}$ oscillations and any other B violating mode. For example, the Feynman diagrams responsible for $p\to e^+\pi^0$, $n\to e^-\pi^+$, and $n-\bar{n}$ oscillations are shown in Fig. 1.1. Then one can construct $\beta\beta_{0\nu}$ diagrams in Fig. 1.2 from the diagrams responsible for $n-\bar{n}$ oscillation

[3]The seesaw mechanism consists of making one particle light at the expense of making another heavy [21, 22, 23].

and the other B violating modes, and thus demonstrates the Majorana character of neutrino without an observation of $\beta\beta_{0\nu}$.

Secondly, the interactions that generate $n-\bar{n}$ oscillations may also be responsible for the generation of the BAU [34]. It is argued in Ref. [34] that the primordial baryon asymmetry induced by interactions causing such oscillations would survive non-perturbative weak interaction effects, unlike the one responsible for the leading proton decay modes, $p \to e^+\pi^0$ and $p \to \bar{\nu}K^+$, which violate B and L, but preserve $B-L$. Therefore, there may be an intimate connection between $n-\bar{n}$ oscillation and the observed BAU [24].

Finally, the lowest mass dimension operators that can mediate proton (or B violating neutron) decay with SM fields and symmetries has dimension 6. For example, the $p \to e^+\pi^0$ decay can be characterized by the dimension-six effective Lagrangian suppressed by two powers of a new physics cutoff Λ_p [35, 36]. The current limit on its inverse decay rate from the SuperKamiokande (SuperK) experiment is $\tau(p \to e^+\pi^0) > 1.4 \times 10^{34}$ yrs [37]. Applying the most recent lattice evaluation of the nucleon matrix element leads to a lower limit of $\Lambda_p > 4.9 \times 10^{15}$ GeV. Since $n-\bar{n}$ oscillations arise from the dimension-nine effective Lagrangian, they are suppressed by five powers of a cutoff $\Lambda_{n\bar{n}}$ [38]. The best limit on the $n-\bar{n}$ oscillation time for free neutrons is $\tau(n-\bar{n}) > 0.86 \times 10^8$ s, which comes from an experiment performed at the Institut Laue-Langevin (ILL) [39]. It yields a much lower limit $\Lambda_{n\bar{n}} > 10^5$ GeV. A comparable limit is also obtained by the SuperK [40] for bound neutrons inside nuclear matter. Consequently, an observation of $n-\bar{n}$ oscillation near current levels of sensitivity would suggest a relatively low scale of new physics.

$B-L$ violation can appear in theories of both quarks and leptons. The $n \to e^-\pi^+$ decay is a typical example. It obeys $\Delta(B-L) = -2$, and its effective Lagrangian has dimension-seven [41, 42, 43, 44]. The current best limit on the lifetime of this decay is $\tau(n \to e^-\pi^+) > 6.5 \times 10^{31}$ yrs from the IMB experiment [45], which yields a limit $\Lambda_n > 6.6 \times 10^{10}$ GeV. Compared with $\Lambda_{n\bar{n}}$, Λ_n is still 5 orders of magnitude larger.

The possible mechanisms of generating $n-\bar{n}$ oscillations have been explored in various models. Some early works on the subject can be found in Refs. [46, 47, 48], and some latest models can be found, e.g., in Refs. [49, 32]. An effective $|\Delta B| = 2$ operator arises from the diquark couplings to a particle "X" in Fig. 1.3. These $X_{1,2}$ particles carry baryon number, and generally they obtain their masses through a spontaneous breaking of a big symmetry in a grand unified theory (GUT) model to a relatively smaller symmetry, e.g., from SU(5) to the SM symmetry. These masses usually are very heavy. Note that they are not necessarily scalar particles, though in

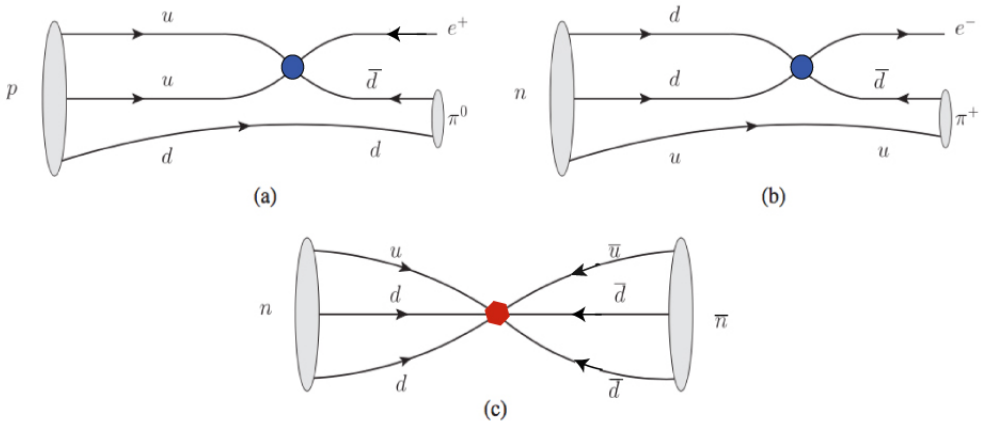

Figure 1.1: Diagrams responsible for (a) proton decay; (b) neutron decay; and (c) $n-\bar{n}$ oscillations. Note that we have revised these diagrams from Ref. [33] to make them more transparent. The blue circle denotes the vertex associated with the dimension 6 operator, and the red polygon is the vertex associated with the dimension 9 operator. It is easy to check that processes (b) and (c) break the $B-L$, while (a) does not though both B and L are violated.

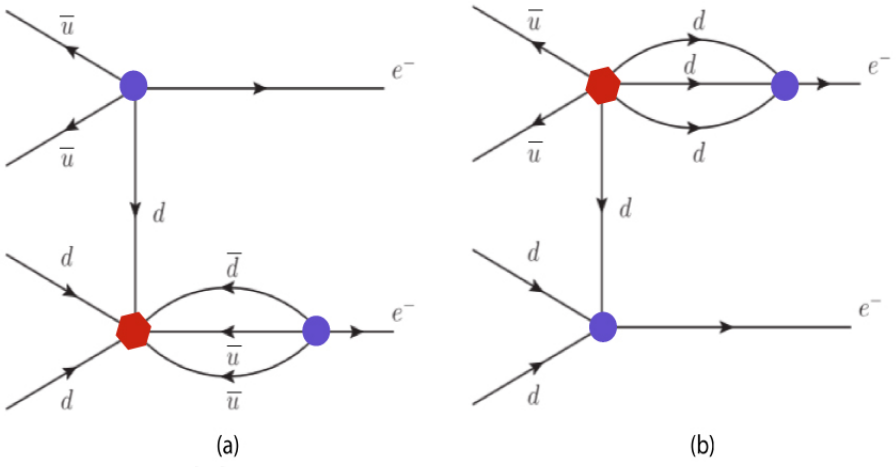

Figure 1.2: Neutrinoless double β decay diagrams determined by (a) $p \to e^+\pi^0$ decay and $n-\bar{n}$ oscillations; and (b) $n \to e^-\pi^+$ decay and $n-\bar{n}$ oscillations [33].

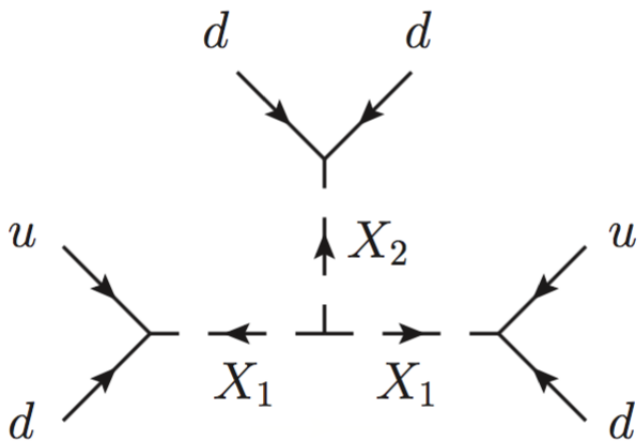

Figure 1.3: Feynman diagram contributing to neutron-antineutron oscillations [32].

most of cases they are. For example, a super-heavy vector boson is used in Ref. [47]. Interestingly, Ref. [46] showed that the mechanism that produces Majorana neutrinos also yields $n-\bar{n}$ oscillations. The effective $|\Delta B| = 2$ operator is a six-fermion operator and is suppressed by the masses of X particles. We will explicitly discuss the six-fermion $n - \bar{n}$ oscillation operators with certain symmetries in a later chapter.

Generally one can search for $n - \bar{n}$ oscillations with free neutrons or bound neutrons in nuclei. However, it is well-known that $n - \bar{n}$ oscillation is very sensitive to the environment [50, 51]. In the presence of magnetic field or matter, its transition probability suffers from quenching problems. Due to the atmospheric neutrino induced background [51], the search for $n - \bar{n}$ oscillations in nuclear decay experiments becomes less efficient than the one with free neutrons. However, it has been pointed out recently that $n - \bar{n}$ oscillation search with free neutrons requires more stringent experimental conditions [52], so that it would not have been possible to observe $n-\bar{n}$ oscillations in existing searches. There is another $|\Delta B| = 2$ and $|\Delta L| = 0$ process, dinucleon decay, which can also be related to $n - \bar{n}$ oscillations. However, the dinucleon decay rate depends on how close the nucleons in the nuclei can be found to be. This, in turn, depends on the detailed structure of the nuclear state in way that it is difficult to test. Moreover, the dinucleon decay experiments involve large detecting setups, for which the atmospheric neutrino induced background can be a problem.

In this thesis, we seek alternative ways to explore $B - L$ violations with $|\Delta B| = 2$ and $|\Delta L| = 0$ processes without such disadvantages. In particular, we discuss a new possibility, $n-\bar{n}$ conversion, with which can achieve our goal. This thesis incorporates

two published papers: [53], [54], and one ongoing work, which constitutes Chapters 3 - 4, 8, and 5 - 7, respectively. The outline of the thesis is arranged as below.

In Chap. 2, the phenomenology of $n-\bar{n}$ oscillations is discussed. The disadvantages we have mentioned are also explicitly discussed. In Chap. 3, we consider the Lorentz invariant $B-L$ violating operators with lowest mass dimension, and check their CPT transformation properties to make sure they are CPT invariant. We find that there exist intrinsic phase constraints associated with discrete symmetry transformations of fermion fields. Moreover, one interesting operator we call a $n-\bar{n}$ conversion operator is proposed. Unlike $n-\bar{n}$ oscillations that suffer from a quenching problem due to the energy difference between the neutron and antineutron in the presence of magnetic fields, $n-\bar{n}$ conversions can flip the spin, so that the neutron and antineutron have the same energy in the presence of magnetic fields and the quenching problem is solved. In Chap. 4, the relation between $B-L$ violation and theories of self-conjugate fermions is discussed. We find that it is impossible to study $n-\bar{n}$ oscillations in QCD in the chiral limit [4]. To serve the purpose of later discussions, a brief but necessary discussion about the MIT bag model and the matrix elements calculations of quark-level $n-\bar{n}$ oscillations is given in Chap. 5. The $n-\bar{n}$ conversion operator is studied in Chap. 6. Noting the charged quarks inside neutrons, we manage to determine the associated coupling coefficient through an electromagnetic connection between $n-\bar{n}$ oscillation and conversion operators in the MIT bag model. In Chap. 7, possible experimental realizations of $n-\bar{n}$ conversion are considered. Other possible theoretical processes with $|\Delta B|=2$ and $|\Delta L|=0$ are also discussed. Chapter 8 gives a brief summary of CP violation in the neutral B meson oscillation ($B\bar{B}$) system. A generalized "T" violating method proposed to give a better determination of small effects, such as penguin contributions, is discussed. We argue that it can greatly enable precision studies of CP violation in future experiments. CP violation in $n-\bar{n}$ oscillations is also discussed. There is no CP violating observable associated with $n-\bar{n}$ oscillation operators alone, hence observing $n-\bar{n}$ oscillation cannot imply the existence of CP violation. One can probe CPV in $n-\bar{n}$ oscillations through the failure of detailed balance, i.e., the probability for $n\to\bar{n}$ is not equal to that for $\bar{n}\to n$. We consider a particular model mechanism in which such an effect can occur. Finally, a summary of the whole thesis is given in Chap. 9.

[4]The Lagrangian contains only the SU(3) color gauge fields and the quark fields, and in the chiral limit quarks belonging to the same isospin doublet are indistinguishable.

CHAPTER 2

PHENOMENOLOGY OF $n - \bar{n}$ OSCILLATIONS

2.1 $n - \bar{n}$ oscillations in the 2×2 framework

Neutron-antineutron oscillations have been studied in the context of a 2×2 effective Hamiltonian framework some time ago [55, 56]. Here I will give a brief summary of the general formalism for the analysis of $n-\bar{n}$ oscillations. A more detailed discussion about $n-\bar{n}$ oscillations both in theory and experiment can be found in Refs. [50, 51].

Given CPT symmetry is assumed a priori, the effective Hamiltonian (H) in the basis ($|n\rangle$, $|\bar{n}\rangle$) has the general form

$$\mathcal{M} = \begin{pmatrix} E_n & \delta \\ \delta & E_{\bar{n}} \end{pmatrix}, \tag{2.1}$$

where the off-diagonal elements δ are the matrix elements of $|\Delta B| = 2$ operators. They are taken to be real and are denoted as

$$\langle n|H|\bar{n}\rangle = \langle \bar{n}|H|n\rangle \equiv \delta. \tag{2.2}$$

The $n - \bar{n}$ oscillation time is defined as

$$\tau_{n\bar{n}} = \frac{1}{\delta}. \tag{2.3}$$

The diagonal matrix elements of H are labeled as

$$\langle n|H|n\rangle = E_n, \ \langle \bar{n}|H|\bar{n}\rangle = E_{\bar{n}}, \tag{2.4}$$

with $\Im(E_n) = \Im(E_{\bar{n}}) = -i\lambda/2$, where $\lambda^{-1} = \tau_n = 880\text{s}$ [57] is the mean lifetime of a free neutron.

The diagonalization of $\mathcal{M}$ yields the mass eigenstates, namely,

$$\begin{pmatrix} |n_1\rangle \\ |n_2\rangle \end{pmatrix} = \begin{pmatrix} \cos\theta & \sin\theta \\ -\sin\theta & \cos\theta \end{pmatrix} \begin{pmatrix} |n\rangle \\ |\bar{n}\rangle \end{pmatrix} \tag{2.5}$$

with $\tan(2\theta) = 2\delta/\Delta E$, and the respective energy eigenvalues

$$E_{1,2} = \frac{1}{2}\Big[E_n + E_{\bar{n}} \pm \sqrt{(\Delta E)^2 + 4\delta^2}\Big], \tag{2.6}$$

where $\Delta E = E_n - E_{\bar{n}}$, which incorporates any interaction effects with the external environment that are different for the neutron and the antineutron.

If we start with a pure neutron state $|n\rangle$ at $t = 0$, then the probability of finding an antineutron after a finite time t is given by

$$P_{\bar{n}}(t) = |\langle \bar{n}|n(t)\rangle|^2 = \frac{\delta^2}{(\Delta E/2)^2 + \delta^2} \sin^2[\sqrt{(\Delta E/2)^2 + \delta^2}t]e^{-\lambda t}. \tag{2.7}$$

Note that only the imaginary part of E_n and $E_{\bar{n}}$ can contribute to the exponential. Since t is usually much smaller than τ_n, the exponential term can also be dropped. We see that when $\Delta E = 0$, the transition probability $P_{\bar{n}} = \sin^2(\delta t)$, which is the case for $n - \bar{n}$ oscillations in the absence of magnetic fields and matter. It appears that the transition probability for $n \to \bar{n}$ is always quenched by the energy difference ΔE. This can be easily explained from the point of view of physics conservation laws. In order to obtain $n-\bar{n}$ oscillations, certain physics conservation laws must be respected. The most crucial one is the energy-momentum conservation law, which demands that initial and final particles must share the same total energy and momentum. In this case, the initial and final particles are only a neutron (antineutron) and an antineutron (neutron) respectively. If there exists an energy difference ΔE between them, it would be very hard to perform $n - \bar{n}$ oscillation without breaking energy-momentum conservation law, and thus it is not surprising that such transition probability is always smaller than $\sin^2(\delta t)$.

There are various factors that can cause an energy difference between neutrons and antineutrons. For example, since neutrons and antineutrons are spin 1/2 fermion particles, an external magnetic field can result in an ΔE. Experiencing different optical potentials inside nuclei, neutrons and antineutrons also have different energies. All these effects result in a quenched transition probability of $n - \bar{n}$, and they will be explicitly discussed in later subsections.

It may be worthy having a general idea about the energy scale of δ from the beginning. The existing upper bound on $|\delta|$ from existing experiments, e.g., in Refs. [39, 40], is approximately less than 10^{-32} GeV, which is 32 orders of magnitude smaller than the mass of the neutron. This constraint poses a challenge for any conceivable experimental environment since $|\Delta E|$ is generally orders of magnitude larger than $|\delta|$. For example, consider the $|\Delta E|$ generated by a magnetic field. Since the signs of magnetic moments of the neutron (μ_n) and antineutron are opposite, in presence of a magnetic field $\mathbf{B}$, neutron and antineutron energies will be different by

$$|\Delta E| = 2|\mu_{\mathbf{n}} \cdot \mathbf{B}| = (1.206 \times 10^{-22}\text{MeV})\Big(\frac{B}{10^{-9}\text{T}}\Big), \tag{2.8}$$

where $B = |\mathbf{B}|$. Note that the value of $|\Delta E| \simeq 10^{-22}$ MeV, though resulting from a very small magnetic field 1 nT, is still much larger than $|\delta|$, in fact $|\Delta E/\delta| \simeq 10^7$.

Apparently the transition probability of $n-\bar{n}$ always suffers from a severe quenching problem. Then one would wonder if we could really ever detect $n-\bar{n}$ oscillations. It turns out that one can work in the so-called "quasi-free" limit, i.e., $|\Delta E|t \ll 1$. Note that in this limit, taking the argument of the sine function to be small results in a unquenched transition probability

$$P_{\bar{n}}(t) = (\delta t)^2 e^{-\lambda t} = \Big(\frac{t}{\tau_{n-\bar{n}}}\Big)^2 e^{-\lambda t}, \tag{2.9}$$

where $\tau_{n-\bar{n}}$ is the oscillation time defined as

$$\tau_{n-\bar{n}} = \frac{1}{|\delta|}. \tag{2.10}$$

Now let us turn to explicit cases.

2.1.1 $n-\bar{n}$ oscillations in vacuum

Neutron-antineutron oscillations in vacuum is the simplest case, in which a neutron (antineutron) spontaneously transforms into an antineutron (neutron). Due to the angular momentum conservation law the initial and final particles share the same spin projections. Moreover, since nothing disturbs the energy and momentum of initial neutrons (antineutrons), the energy-momentum conservation law ensures final antineutrons (neutrons) have the same energy and momentum. If CPT symmetry is not broken, which guarantees that particle and its antiparticle have the same mass, then we can expect an unquenched transition probability.

Let us demonstrate that explicitly. In the rest frame of neutron (antineutron), the diagonal matrix elements of H now can be simply written as

$$\langle n|H|n\rangle = \langle \bar{n}|H|\bar{n}\rangle = m_n - \frac{i\lambda}{2}, \tag{2.11}$$

where m_n is the mass of neutron and $\lambda^{-1} = \tau_n$ is the mean lifetime of a free neutron. Then the matrix H in the basis $(|n\rangle, |\bar{n}\rangle)$ takes the form

$$\mathcal{M} = \begin{pmatrix} m_n - i\lambda/2 & \delta \\ \delta & m_n - i\lambda/2 \end{pmatrix}. \tag{2.12}$$

Diagonalizing $\mathcal{M}$ yields the mass eigenstates

$$|n_\pm\rangle = \frac{1}{\sqrt{2}}(|n\rangle \pm |\bar{n}\rangle), \tag{2.13}$$

and the respective eigenvalues

$$m_{\pm} = m_n - \frac{i\lambda}{2} \pm \delta. \tag{2.14}$$

Now the transition probability is simply

$$P_{\bar{n}}(t) = \sin^2(\delta t)e^{-\lambda t} = \sin^2(t/\tau_n)e^{-\lambda t}, \tag{2.15}$$

and it is indeed not quenched.

2.1.2 $n - \bar{n}$ oscillations in a static magnetic field B

Now we turn to the discussion of $n - \bar{n}$ oscillations in a static magnetic field. As mentioned before, neutron and antineutron interact with the external magnetic field $\mathbf{B}$ via their magnetic dipole moments, $\boldsymbol{\mu}_{n,\bar{n}} = \mu_{n,\bar{n}}\boldsymbol{\sigma}$, where $\mu_n = -\mu_{\bar{n}}$ and $\boldsymbol{\sigma}$ is the Pauli matrix vector, which is related to spin by the relation $\boldsymbol{S} = \hbar\boldsymbol{\sigma}/2$.

Now the matrix $\mathcal{M}$ takes the form

$$\mathcal{M} = \begin{pmatrix} m_n - i\lambda/2 - \boldsymbol{\mu}_n \cdot \boldsymbol{B} & \delta \\ \delta & m_n - i\lambda/2 + \boldsymbol{\mu}_n \cdot \boldsymbol{B} \end{pmatrix}. \tag{2.16}$$

The mass eigenstates $|n_1\rangle$ and $|n_2\rangle$ are given by Eq. 2.5 with

$$\tan(2\theta) = -\frac{\delta}{\boldsymbol{\mu}_n \cdot \boldsymbol{B}}. \tag{2.17}$$

The eigenvalues of $\mathcal{M}$ can also be easily obtained through Eq. 2.6

$$E_{1,2} = m_n \pm \sqrt{(\boldsymbol{\mu}_n \cdot \boldsymbol{B})^2 + \delta^2} - \frac{i\lambda}{2}. \tag{2.18}$$

As discussed before, the energy scale $|\boldsymbol{\mu}_n \cdot \boldsymbol{B}|$ naturally dwarfs that of δ, we can simplify the formula of the transition probability by taking

$$\sqrt{(\Delta E/2)^2 + \delta^2} \simeq |\boldsymbol{\mu}_n \cdot \boldsymbol{B}|, \tag{2.19}$$

and eventually obtain

$$P_{\bar{n}}(t) = \left(\frac{\delta}{\boldsymbol{\mu}_n \cdot \boldsymbol{B}}\right)^2 \sin^2(|\boldsymbol{\mu}_n \cdot \boldsymbol{B}|t)e^{-\lambda t}. \tag{2.20}$$

We see that unless we work in the "quasi-free" limit, the energy splitting of the neutron and antineutron in a magnetic field always quenches the appearance of $n - \bar{n}$ oscillations. Thus the strategy in past and proposed searches for $n - \bar{n}$ oscillations for free neutrons has been to minimize the magnetic field [39, 58].

Note that such energy splitting results from two factors: one is the relation $\mu_n = -\mu_{\bar{n}}$ and the other one is the consideration of same spin projections for both neutrons and antineutrons. There is nothing we can do about the first factor without breaking CPT symmetry. However, one can alter the second condition by introducing an external current into the $n - \bar{n}$ oscillation system. Because of the additional angular momentum contribution from the current, the total angular momenta can be still conserved while the spin projections of the neutrons and antineutrons become opposite. Although it will no longer be a $n - \bar{n}$ oscillation process, it does result in a transition that would be free from a quenching problem. This motivates us to form the $n - \bar{n}$ conversion idea that will be discussed in later chapters.

2.1.3 $n - \bar{n}$ oscillations in matter

The matrix $\mathcal{M}$ in matter takes the form [47]

$$\mathcal{M} = \begin{pmatrix} m_{n,eff} & \delta \\ \delta & m_{\bar{n},eff} \end{pmatrix}, \tag{2.21}$$

with

$$m_{n,eff} = m_n + U_n, \quad m_{\bar{n},eff} = m_n + U_{\bar{n}}, \tag{2.22}$$

where U_n and $U_{\bar{n}}$ are nuclear potentials that neutron and antineutron experience respectively inside matter (i.e., a nucleus). The nuclear potential U_n is practically real, $U_n = U_{nR}$, while because of the annihilation of an antineutron with another nucleon, $U_{\bar{n}}$ has a large imaginary part,

$$U_{\bar{n}} = U_{\bar{n}R} + iU_{\bar{n}I}. \tag{2.23}$$

Moreover, U_{nR}, $U_{\bar{n}R}$, and $U_{\bar{n}I}$ are all in the order of 100 MeV [59, 60, 61, 62]. In fact the difference $m_{n,eff} - m_{\bar{n},eff} \sim 100$ MeV, therefore the $n - \bar{n}$ transition probability is severely suppressed in matter. The eigenvalues of $\mathcal{M}$ are

$$E_{1,2} = \frac{1}{2}\Big[m_{n,eff} + m_{\bar{n},eff} \pm \sqrt{(m_{n,eff} - m_{\bar{n},eff})^2 + 4\delta^2}\Big]. \tag{2.24}$$

Expanding E_1, we have

$$E_1 \simeq m_n + U_n - i\frac{\delta^2 U_{\bar{n}I}}{(U_{nR} - U_{\bar{n}R})^2 + U_{\bar{n}I}^2}. \tag{2.25}$$

The imaginary part leads to matter (nucleus) instability via the annihilation of the $\bar{n}$ with one of the other nucleons, producing mainly pions. The corresponding rate,

or so-called nuclear disappearance width, is

$$\Gamma_d = \frac{1}{\tau_d} = \frac{2\delta^2 |U_{\bar{n}I}|}{(U_{nR} - U_{\bar{n}R})^2 + U_{\bar{n}I}^2}. \tag{2.26}$$

Thus, $\tau_d \propto \delta^{-2}$ and typically it is written as

$$\tau_d = R\tau_{n\bar{n}}^2, \tag{2.27}$$

where the value of the reduced lifetime R depends on the nucleus and can be obtained from nuclear structure calculations. Theoretical estimates for various R can be found in Ref. [62]. The reduced lifetime R is calculated by solving the coupled $n - \bar{n}$ radial wave equations, which involve the nuclear potentials both for neutrons and antineutrons. A large uncertainty arises because of the uncertainty in the strength of the absorptive (imaginary) $\bar{n}$-nuclear potential [62]. Ref. [62] claims that the overall theoretical uncertainty is about 10% - 15%, but this is difficult to validate.

Table 1.1 shows the effective limit on the $n - \bar{n}$ oscillation time $\tau_{n\bar{n}}$ from experimental limits on nuclear stability. The best limit comes from the Super-Kamiokande (Super-K) nuclear decay experiment: $\tau_{n\bar{n}} > 2.7 \times 10^8$ s.

Experiment (year)	Type	Effective limit on $\tau_{n\bar{n}}$(sec)
SNO (2017)	nuclear decay in ^{2}H	$> 1.23 \times 10^8$ [63]
Super-K (2015)	nuclear decay in ^{16}O	$> 2.7 \times 10^8$ [40]
Soudan (2002)	nuclear decay in ^{56}Fe	$> 1.2 \times 10^8$ [64]
ILL (1994)	free neutron	$> 0.86 \times 10^8$ [39]
ESS (2023-2025)	free neutron	$\geq 1.0 \times 10^{11}$ [58]

Table 2.1: Best limits on the neutron-antineutron oscillation time from experiments of different types. Note that ESS is a projection for a future experiment, therefore its limit on $\tau_{n\bar{n}}$ is not a real limit.

As the experiments push the limits on $\tau_{n\bar{n}}$ to much higher precision, the nuclear decay searches, such as SNO [63], Super-K [40], and Soudan [64], become less efficient because of the background induced by atmospheric neutrinos. Therefore it appears a good idea to focus on the free neutron oscillation experiment rather than a failure of nuclear stability or a dinucleon decay search. The European Spallation Source (ESS) experiment [58] is exactly such an experiment. By improving the removal of magnetic

fields and matter, the ESS experiment expects to measure $n - \bar{n}$ oscillations in free neutron beams with a sensitivity of three orders of magnitude better than the ILL experiment [39].

2.2 Quantum damping of $n - \bar{n}$ oscillations

In the previous section, our discussion of $n - \bar{n}$ oscillations, with or without the presence of environmental effects, are based on the transition probability obtained by solving the time-dependent Schrödinger equations. Recently a new approach based on the density matrix formalism and Bloch equation has been proposed to the problems of both neutron-antineutron and neutron-mirror-neutron oscillations [65, 52]. It takes the advantage of the density matrix formalism in describing the quantum system in contact with the environment.

The system these authors consider is still a two-state system, $|n_1\rangle$ and $|n_2\rangle$, in which n_1 and n_2 can represent a neutron and an antineutron or a neutron and a mirror-neutron. A state of a system in vacuum is a pure state and can be written as

$$|\psi\rangle = \phi_1(t)|n_1\rangle + \phi_2(t)|n_2\rangle, \tag{2.28}$$

where ϕ_1 and ϕ_2 are complex coefficients. The density matrix of such system is given by

$$\hat{\rho}(t) = \begin{pmatrix} \phi_1\phi_1^* & \phi_1\phi_2^* \\ \phi_2\phi_1^* & \phi_2\phi_2^* \end{pmatrix} \equiv \begin{pmatrix} \rho_{11} & \rho_{12} \\ \rho_{21} & \rho_{22} \end{pmatrix}. \tag{2.29}$$

The Hamiltonian of this system has the same formula as the 2×2 effective Hamiltonian, with ΔE representing the energy splitting caused by the environmental effects, such as magnetic field or surrounding gas particles. Due to the interactions with the environment, the time evolution of the effective density matrix is described by the Lindblad [66, 67] equations,

$$\dot{\hat{\rho}}(t) = \frac{d\hat{\rho}(t)}{dt} = -i[H, \hat{\rho}(t)] + \sum_n [L_n\hat{\rho}(t)L_n^\dagger - \frac{1}{2}L_n^\dagger L_n\hat{\rho}(t) - \frac{1}{2}\hat{\rho}(t)L_n^\dagger L_n], \tag{2.30}$$

where L_i are Lindblad operators.

Theoretically Eq. 2.30 can be solved in a straightforward way. Refs. [66, 67] utilize a different method. They introduce a real Bloch 3-vector $\mathbf{R}$ [68], so that the density matrix can be expanded over Pauli matrices

$$\hat{\rho} = \frac{1}{2}(1 + \mathbf{R}\sigma), \tag{2.31}$$

where

$$\mathbf{R} = \begin{pmatrix} \rho_{12} + \rho_{21} \\ -i(\rho_{21} - \rho_{12}) \\ \rho_{11} - \rho_{22} \end{pmatrix}. \tag{2.32}$$

Now Eq. 2.30 can be replaced by an equation of motion for the Bloch vector $\mathbf{R}$. Giving an initial condition, e.g., $\mathbf{R}$(t=0)=(0, 0, 1) denoting the system is initially in the $|n_1\rangle$ state, one can find the solution of R_z. Then combining with the normalization condition $\rho_{11} + \rho_{22} = 1$, yields ρ_{22}, the probability of the system finally in the $|n_2\rangle$ state.

Under certain simplifying assumptions, Ref. [52] finds that such a Bloch equation is actually an equation for a damped oscillator and the damping parameter that incorporates the interaction information of the system with the environment controls the rate at which coherence will be destroyed by the environment. An explicit application of such an analysis to the $n-\bar{n}$ oscillation experiment performed at the ILL[39] with free neutrons is presented, and it is claimed that much higher vacuum than the one used in the ILL experiment is required, otherwise there is no hope to realize oscillations with free neutrons for the neutron free-flight time used in the experiment. Therefore, it appears that even the efficient searches, $n - \bar{n}$ oscillation searches with free neutrons, are very challenging. Thus, exploring other possibilities is important.

2.3 Dinucleon decay

There is another experimentally accessible process for baryon number violation by two units, dinucleon decay. The name "dinucleon decay" is because the quarks of the two bound nucleons interact to produce a decay final state in which the nucleons are absent. This process is usually mediated by the exchange of a non-standard model particle, which can appear in various B violating models. An example of a dinucleon decay tree diagram from one of the models is shown in Fig. 2.1.

Just as in the case of $n - \bar{n}$ oscillation in matter, the dinucleon decay lifetimes τ_{NN} can be related to the $n-\bar{n}$ oscillation time $\tau_{n\bar{n}}$. Note that as the relevant energy scale of such processes drop, the effects of scalar particles X_1 and X_2, because of their heavy masses, do not explicitly appear in the operators, and thus the Feynman diagram in Fig. 2.1 without the spectator quarks generates an effective six-quarks operator, which, according to the crossing symmetry, should be able to mediate both

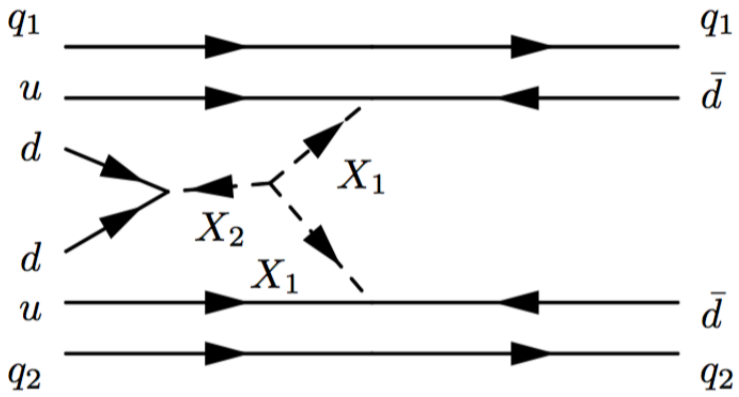

Figure 2.1: Feynman diagram for dinucleon decay to pions from model [32]. Spectator quarks q_1 and q_2 can be either u or d. The X_1 and X_2 are scalar particles belong to $(\bar{6}, 1, -1/3)$ and $(\bar{6}, 1, 2/3)$ representations of the SM $SU(3) \bigotimes SU(2) \bigotimes U(1)$ gauge group.

$n - \bar{n}$ oscillation and dinucleon decay. In Ref. [69], both $n - \bar{n}$ and dinucleon decay with the same operator is discussed. The operator takes the general form:

$$\mathcal{O}_{\Delta B=2} = \frac{1}{\Lambda_{sup}^5} \mathcal{O}_{6q}, \tag{2.33}$$

where $\mathcal{O}_{6q}$ denotes a six-quark operator, and Λ_{sup} is a supersymmetry (or, more generally a new physics) energy scale. Since $\mathcal{O}_{6q}$ has mass dimension nine, dimensional analysis show that a fifth power of Λ_{sup} is necessary. If all the participating quarks come from the first generation, this operator can generate both $n - \bar{n}$ oscillation and dinucleon decay. The $n - \bar{n}$ oscillation time for free neutrons is given by

$$\tau_{n\bar{n}} \approx \frac{\Lambda_{sup}^5}{\Lambda_{QCD}^6}, \tag{2.34}$$

where Λ_{QCD} is the QCD scale. The dinucleon decay time τ_{NN} is given by [69, 70]

$$\tau_{NN} \approx \frac{\pi M_N^2}{8\rho_N} \frac{\Lambda_{sup}^{10}}{\Lambda_{QCD}^{10}}, \tag{2.35}$$

where ρ_N is the average nuclear density and M_N denotes the nucleon mass. From Eqs. 2.34 and 2.35, we obtain a relation

$$\tau_{NN} \approx \frac{\pi M_N^2}{8\rho_N} \Lambda_{QCD}^2 \tau_{n\bar{n}}^2 = T_{nuc} \tau_{n\bar{n}}^2. \tag{2.36}$$

Although this equation is very similar to the formula of Eq. 2.27, the relevant physics is different. Taking $\Lambda_{QCD} = 200$ MeV, $M_N = 1$ GeV, $\rho_N \approx 0.25$ fm^{-3}, we have

$T_{nuc} \approx 1.1 \times 10^{25}$ s^{-1}. For $n - \bar{n}$ oscillation, R is related to the difference in neutron and antineutron nuclear potentials. It is calculated to be 0.517×10^{23} s^{-1} [62], which is 2 orders of magnitude smaller.

There have been at least three dinucleon decay searches performed previously [71, 72, 73]. The best limit on τ_{NN} is $\tau(^{16}O(nn) \rightarrow^{14} O\pi^0\pi^0) > 4.04 \times 10^{32}$ years obtained by Super-K [73]. However, translated into the limit on $\tau_{n\bar{n}}$, it is still two orders of magnitude smaller than the limit from nuclear stability tests [40]. Moreover, the neutron-antineutron oscillation time obtained in both cases is connected to a big suppression factor T_{NN} and R that are obtained through model calculations. We discussed in the T_{NN} case, theoretical uncertainties appear due to the various approximations used. In addition to theoretical uncertainties, dinucleon decay searches are also sensitive to the background induced by atmospheric neutrinos, which consequently makes these two methods less efficient than $n - \bar{n}$ oscillation searches with free neutrons.

2.4 Motivation for $n - \bar{n}$ conversion

In this chapter, we have explicitly discussed the three known methods of $B - L$ violation searches in the quark sector. We have seen that $n - \bar{n}$ oscillations always suffer from quenching problems. For a $n - \bar{n}$ oscillation search with free neutrons, the transition probability is very sensitive to the environment. The presence of external magnetic fields or matter can easily reduce the chance of observing a $n - \bar{n}$ oscillation. Ref. [52] claims that there is little hope to observe oscillations with free neutrons for the parameters of the ILL experiment, because the ILL limit on $n - \bar{n}$ oscillation time would be at least four orders of magnitude worse if the constraints in Ref.[52] are satisfied. Although $n - \bar{n}$ oscillation is severely suppressed in nuclei, the experiments can take advantage of the enormous size of underground detectors for neutrino experiments and thus can potentially set sensitive limits. However, due to the uncertainties coming from the $\bar{n}$-nuclear potential and from the background induced by atmospheric neutrinos, $n-\bar{n}$ oscillation searches through nuclear stability tests will be difficult to improve. Finally, a dinucleon decay method is also discussed. However, just like the second case, a model dependent parameter is involved, which also results in additional theoretical uncertainties.

When we discussed $n-\bar{n}$ oscillations in a magnetic field, we argued that a spin-flip between the neutron and antineutron could keep the energies of neutron and antineutron the same and potentially evade quenching. This motivates us to seek alternative

methods and eventually to propose a new mechanism called $n - \bar{n}$ conversion.

CHAPTER 3

PHASE CONSTRAINTS ON DISCRETE-SYMMETRY TRANSFORMATIONS OF FERMIONS IN $B - L$ VIOLATING THEORIES

"A thing is ***symmetrical*** if there is something that you can do to it so that after you have finished doing it it looks the same as it did before." —Hermann Weyl [74]

In nature there are two kinds of symmetries: continuous and discrete. A typical example of a continuous symmetry is a rotation. Consider a perfect sphere painted in one color (say blue). It always looks the same no matter which axes that we pick to rotate it about and by what angles. Traditionally it is called the identity (**I**) or doing nothing if the rotated angle is zero. It is also easy to notice that a rotation by a large angle can be achieved by a consecutive set of rotations by small angles, no matter how small. In other words, all rotations are continuous linked to the identity **I**. This property applies for all continuously symmetries, whereas it does not work for discrete symmetries.

There are three fundamental discrete symmetry transformations: parity (P), charge-conjugation (C), and time-reversal (T). Classically under P, the direction of a vector reverses its sign, e.g. $\mathbf{x} \to -\mathbf{x}$; under C, the charge flips sign; under T, the sign of the time label flips, which is like playing a movie backward. More detailed introduction of these discrete symmetry transformations in classical mechanics, quantum mechanics, and quantum field theory can be found, e.g., in Bigi and Sanda [75]. Here we want to focus on the discrete-symmetry transformation properties of a fermion field.

Generally there is an unimodular phase factor associated with each discrete symmetry. These phase factors are considered to be arbitrary and have no physical consequence. This is not surprising since the "normal" Lagrangian involving fermion fields takes bilinear forms, e.g., $\bar{\psi}\Gamma\psi$, in which Γ is some product of gamma matrices, and under any discrete symmetry transformations, if ψ accrues a additional phase factor λ, then $\overline{\psi}$ will accrue a λ^*, then consequently this phase factor does not contribute to the bilinear form. However, this is no longer true when Majorana fields are involved. Since the antiparticle of a Majorana particle is itself, and there is no

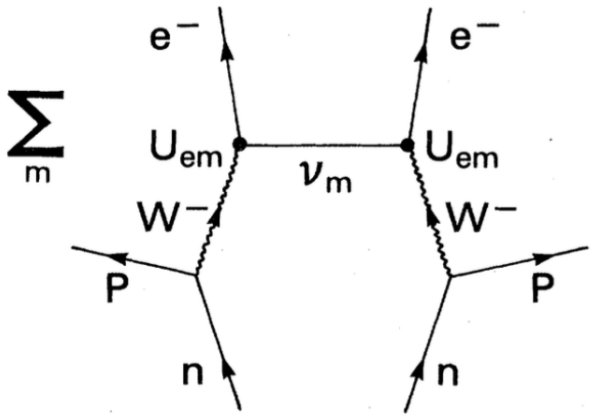

Figure 3.1: Neutrinoless double-β decay. The ν_m are the various neutrino mass eigenstates which couple to an electron, each with a factor U_{em} [19]

evidence indicating that electric charge conservation law is broken, possible Majorana candidates should be electric neutral. Among all the fundamental particles in SM, the neutrino certainly is a possible candidate. It is well known that observation of $\beta\beta_{0\nu}$ would establish the Majorana character of neutrinos [14]. However, the inability to detect such a reaction does not prove that they are not, because the contributions of different ν_m to $\beta\beta_{0\nu}$ in Fig. 3.1 can interact destructively and cancel each other [19]. (Note that in Fig. 3.1, m runs over the neutrino mass eigenstates and U is the neutrino mixing matrix). Doi *et al.* claimed that the interference could be destructive if CP is broken [17]. However, this claim was disproved by Wolfenstein who asserted that even when CP was conserved, because of the opposite CP parities of the interfering neutrinos, destructive interference could still occur [18]. This assertion was later confirmed by Halprin, Petcov, and Rosen [76]. By studying the field-theoretic treatment of Majorana particles, Kayser found the phase constraints associated with discrete-symmetry transformations of Majorana fields [77, 19]. He pointed out that when CP is conserved the amplitude for $\beta\beta_{0\nu}$ depends on a phase factor of the CP transformation of Majorana neutrinos[1] that must be imaginary. Therefore, neutrinos with opposite CP parities do interfere destructively, just as Wolfenstein asserted.

It should be pointed out that the existence of phase constraints associated with discrete symmetries was already noted by Feinberg and Weinberg [78], as well as by Carruthers [79]. They determined the existence of phase restrictions in the P and TC transformations. Haxton and Stephenson [80] found the phase constraint of C

[1]The phase factor of the CP transformation of a Majorana particle is different from the one of a Majorana field, because there a "creation phase factor" associated with the Majorana creation operator, but there is no such phase associated with the field [19].

by using a similar method to ours. However, they did not find the phase constraints associated with other discrete symmetries, nor fully recognize their consequences.

In this chapter, we will explicitly demonstrate the existence of phase restrictions associated with the discrete-symmetry transformations of a Majorana field first and then generalize them to those of a general fermion field. After obtaining these constraints, we will apply them to check the CPT transformation properties of the $B-L$ violating operators with lowest mass dimension.

3.1 Discrete-symmetry transformations of fermion fields

The discrete-symmetry transformations of a four-component fermion field $\psi(x)$ are given by [81]

$$\mathbf{C}\psi(x)\mathbf{C}^{-1} = \eta_c C\gamma^0\psi^*(x) \equiv \eta_c i\gamma^2\psi^*(x) \equiv \eta_c\psi^c(x)\,, \tag{3.1}$$

$$\mathbf{P}\psi(t,\mathbf{x})\mathbf{P}^{-1} = \eta_p\gamma^0\psi(t,-\mathbf{x})\,, \tag{3.2}$$

$$\mathbf{T}\psi(t,\mathbf{x})\mathbf{T}^{-1} = \eta_t\gamma^1\gamma^3\psi(-t,\mathbf{x})\,, \tag{3.3}$$

where η_c, η_p, and η_t are unimodular phase factors of the C, P, and T transformations, respectively. Note that $\psi^c(x)$ is the conjugate field and that $\mathbf{C}^2\psi(x)\mathbf{C}^{-2} = \psi(x)$ and $\mathbf{T}^2\psi(x)\mathbf{T}^{-2} = -\psi(x)$, irrespective of arbitrary phases, but that $\mathbf{P}^2\psi(x)\mathbf{P}^{-2} = \eta_p^2\psi(x)$.

We have chosen the Dirac-Pauli representation in which the gamma matrices take the form

$$\gamma^0 = \begin{pmatrix} I & 0 \\ 0 & -I \end{pmatrix},\ \gamma^i = \begin{pmatrix} 0 & \sigma^i \\ -\sigma^i & 0 \end{pmatrix}, \tag{3.4}$$

where I is the 2×2 unit matrix and σ^i (i=1,2,3) refers to the Pauli matrices

$$\sigma^1 = \begin{pmatrix} 0 & 1 \\ 1 & 0 \end{pmatrix},\ \sigma^2 = \begin{pmatrix} 0 & -i \\ i & 0 \end{pmatrix},\ \sigma^3 = \begin{pmatrix} 1 & 0 \\ 0 & -1 \end{pmatrix}. \tag{3.5}$$

There are two other gamma matrices that are pertinent to our discussion, the charge conjugation matrix $C = i\gamma^2\gamma^0$ and the matrix $\gamma^5 \equiv i\gamma^0\gamma^1\gamma^2\gamma^3$.

The plane-wave expansion of a Dirac field $\psi(x)$ is given by

$$\psi(x) = \int \frac{d^3\mathbf{p}}{(2\pi)^{3/2}\sqrt{2E}} \sum_{s=\pm} \left\{ b(\mathbf{p},s)u(\mathbf{p},s)e^{-ip\cdot x} + d^\dagger(\mathbf{p},s)v(\mathbf{p},s)e^{ip\cdot x} \right\}, \tag{3.6}$$

with spinors defined as

$$u(\mathbf{p},s)=\mathcal{N}\begin{pmatrix}\chi^{(s)}\\ \frac{\sigma\cdot\mathbf{p}}{E+M}\chi^{(s)}\end{pmatrix}\quad;\quad v(\mathbf{p},s)=\mathcal{N}\begin{pmatrix}\frac{\sigma\cdot\mathbf{p}}{E+M}\chi'^{(s)}\\ \chi'^{(s)}\end{pmatrix}, \tag{3.7}$$

noting $\chi'^{(s)}=-i\sigma^2\chi^{(s)}$, $\chi^+=\binom{1}{0}$, $\chi^-=\binom{0}{1}$, $\mathcal{N}=\sqrt{E+M}$, and $b(d)$ annihilates a particle (antiparticle). To study the transformation properties of $b(d)$ and $b^\dagger(d^\dagger)$ under C, P, and T , the following relations are very helpful.

$$\begin{aligned}
\gamma^0u(\mathbf{p},s) &= u(-\mathbf{p},s), &(3.8)\\
\gamma^0v(\mathbf{p},s) &= -v(-\mathbf{p},s)\,, &(3.9)\\
u(\mathbf{p},s) &= i\gamma^2v^*(\mathbf{p},s)\,, &(3.10)\\
u^*(\mathbf{p},s) &= s\gamma^1\gamma^3u(-\mathbf{p},-s), &(3.11)\\
v^*(\mathbf{p},s) &= s\gamma^1\gamma^3v(-\mathbf{p},-s)\,, &(3.12)\\
\gamma^5u(\mathbf{p},s) &= -sv(\mathbf{p},-s)\,. &(3.13)
\end{aligned}$$

After applying these relations to Eq. (3.1)-(3.3), we find the following transformation properties:

$$\begin{aligned}
\mathbf{C}b(\mathbf{p},s)\mathbf{C}^\dagger &= \eta_c d(\mathbf{p},s)\ ;\ \mathbf{C}d^\dagger(\mathbf{p},s)\mathbf{C}^\dagger=\eta_c b^\dagger(\mathbf{p},s)\,,\\
\mathbf{C}b^\dagger(\mathbf{p},s)\mathbf{C}^\dagger &= \eta_c^* d^\dagger(\mathbf{p},s)\ ;\ \mathbf{C}d(\mathbf{p},s)\mathbf{C}^\dagger=\eta_c^* b(\mathbf{p},s)\,, &(3.14)\\
\mathbf{P}b(\mathbf{p},s)\mathbf{P}^\dagger &= \eta_p b(-\mathbf{p},s)\ ;\ \mathbf{P}d^\dagger(\mathbf{p},s)\mathbf{P}^\dagger=-\eta_p d^\dagger(-\mathbf{p},s)\,,\\
\mathbf{P}b^\dagger(\mathbf{p},s)\mathbf{P}^\dagger &= \eta_p^* b^\dagger(-\mathbf{p},s)\ ;\ \mathbf{P}d(\mathbf{p},s)\mathbf{P}^\dagger=-\eta_p^* d(-\mathbf{p},s)\,, &(3.15)\\
\mathbf{T}b(\mathbf{p},s)\mathbf{T}^{-1} &= s\eta_t b(-\mathbf{p},-s)\ ;\ \mathbf{T}d^\dagger(\mathbf{p},s)\mathbf{T}^{-1}=s\eta_t d^\dagger(-\mathbf{p},-s)\,,\\
\mathbf{T}b^\dagger(\mathbf{p},s)\mathbf{T}^{-1} &= s\eta_t^* b^\dagger(-\mathbf{p},-s)\ ;\ \mathbf{T}d(\mathbf{p},s)\mathbf{T}^{-1}=s\eta_t^* d(-\mathbf{p},-s). &(3.16)
\end{aligned}$$

3.2 Discrete-symmetry phase constraints on Majorana fields

The plane-wave expansion of a general Majorana field ψ_m is written as

$$\psi_m(x)=\int\frac{d^3\mathbf{p}}{(2\pi)^{3/2}\sqrt{2E}}\sum_s\left\{f(\mathbf{p},s)u(\mathbf{p},s)e^{-ip\cdot x}+\lambda f^\dagger(\mathbf{p},s)v(\mathbf{p},s)e^{ip\cdot x}\right\}, \tag{3.17}$$

where $f^\dagger$ and f denote the creation and annihilation operators for the Majorana particle. Unlike the Dirac field, there is a unimodular parameter λ called a creation phase factor. It can be chosen arbitrarily.

Under **C** transformation,

$$\mathbf{C}\psi_m(x)\mathbf{C}^{-1} = i\eta_c\gamma^2\psi_m^*(x) \tag{3.18}$$

Since a Majorana particle is a fermion that is its own antiparticle, there exists a Majorana relation

$$\psi_m(x) = \lambda\psi_m^c(x), \tag{3.19}$$

or

$$i\gamma^2\psi_m^*(x) = \lambda^*\psi_m(x). \tag{3.20}$$

Eq. (3.18) and Eq. (3.20) yield

$$\mathbf{C}\psi_m(x)\mathbf{C}^{-1} = \eta_c\lambda^*\psi_m(x). \tag{3.21}$$

Now the left hand of the equation above can be explicitly written as

$$\begin{aligned}&\mathbf{C}\psi_m(x)\mathbf{C}^{-1}\\ =\ &\int \widetilde{d^3\mathbf{p}}\sum_s \left\{\mathbf{C}f(\mathbf{p},s)\mathbf{C}^{-1}u(\mathbf{p},s)e^{-ip\cdot x} + \lambda\mathbf{C}f^\dagger(\mathbf{p},s)\mathbf{C}^{-1}v(\mathbf{p},s)e^{ip\cdot x}\right\},\end{aligned} \tag{3.22}$$

where we define $\widetilde{d^3\mathbf{p}} \equiv \frac{d^3\mathbf{p}}{(2\pi)^{3/2}\sqrt{2E}}$. In the mean time, the right hand of this equation takes the form

$$\eta_c\lambda^*\psi_m(x) = \eta_c\lambda^*\int \widetilde{d^3\mathbf{p}}\sum_s \left\{f(\mathbf{p},s)u(\mathbf{p},s)e^{-ip\cdot x} + \lambda f^\dagger(\mathbf{p},s)v(\mathbf{p},s)e^{ip\cdot x}\right\}. \tag{3.23}$$

Comparing Eq. (3.22) with (3.23) give us the relations below

$$\mathbf{C}f(\mathbf{p},s)\mathbf{C}^{-1} = \eta_c\lambda^* f(\mathbf{p},s), \tag{3.24}$$

$$\mathbf{C}f^\dagger(\mathbf{p},s)\mathbf{C}^{-1} = \eta_c\lambda^* f^\dagger(\mathbf{p},s). \tag{3.25}$$

Since **C** is a unitary operator, taking the Hermitian conjugate of either relation reveals that $\eta_c^*\lambda$ is real.

Note that under the **CP** transformation

$$\mathbf{CP}\psi_m(t,\mathbf{x})(\mathbf{CP})^{-1} = i\eta_p\eta_c\gamma^0\gamma^2\psi_m^*(t,-\mathbf{x}). \tag{3.26}$$

Then Eq. (3.20) yields

$$\mathbf{CP}\psi_m(t,\mathbf{x})(\mathbf{CP})^{-1} = \eta_p\eta_c\lambda^*\gamma^0\psi_m(t,-\mathbf{x}). \tag{3.27}$$

Following the same procedure as above, we can obtain another set of relations

$$\mathbf{CP} f(\mathbf{p},s)(\mathbf{CP})^{-1} = \eta_c\eta_p\lambda^* f(-\mathbf{p},s)\,, \tag{3.28}$$
$$\mathbf{CP} f^\dagger(\mathbf{p},s)(\mathbf{CP})^{-1} = -\eta_c\eta_p\lambda^* f^\dagger(-\mathbf{p},s)\,. \tag{3.29}$$

Since **CP** is a unitary operator, taking the Hermitian conjugate of either relation shows that $\eta_p^*\eta_c^*\lambda$ must be imaginary. Note that we have already established that $\eta_c^*\lambda$ is real, so that η_p^* itself must be imaginary.

Now under **T** we have

$$\mathbf{T}\psi_m(t,\mathbf{x})(\mathbf{T})^{-1} = \eta_t\gamma^1\gamma^3\psi_m(-t,\mathbf{x}), \tag{3.30}$$

which yields

$$\mathbf{T} f(\mathbf{p},s)(\mathbf{T})^{-1} = s\eta_t f(-\mathbf{p},-s), \tag{3.31}$$
$$\mathbf{T} f^\dagger(\mathbf{p},s)(\mathbf{T})^{-1} = s\eta_t\lambda^2 f^\dagger(-\mathbf{p},-s). \tag{3.32}$$

Since **T** is an antiunitary operator, we write $\mathbf{T} = KU_t$, where U_t is a unitarity operator and K denotes conjugation. Then taking the Hermitian conjugate of either relation shows that $\eta_t\lambda$ must be real.

Finally we note the CPT transformation of ψ_m

$$\mathbf{CPT}\psi_m(x)(\mathbf{CPT})^{-1} = -\eta_c\eta_p\eta_t\gamma^5\psi_m^*(-x)\,, \tag{3.33}$$

which yields

$$\xi f(\mathbf{p},s)\xi^{-1} = s\lambda^*\eta_c\eta_p\eta_t f(\mathbf{p},-s)\,, \tag{3.34}$$
$$\xi f^\dagger(\mathbf{p},s)\xi^{-1} = -s\lambda\eta_c\eta_p\eta_t f^\dagger(\mathbf{p},-s)\,, \tag{3.35}$$

where we employ $\mathbf{CPT} \equiv \xi$. Since ξ is also an antiunitary operator, we define $\xi = KU_{cpt}$, where U_{cpt} denotes a unitarity operator. As we have done before, taking the Hermitian conjugate of either relation reveals that $\eta_c\eta_p\eta_t$ is pure imaginary. Since we have already established that η_p is imaginary, we find that $\eta_c\eta_t$ must also be real. The same conclusion can be drawn through the analysis of the **TC** transformation as well. In contrast to $\eta_c\eta_t$, the combination $\eta_c\eta_p$ itself is unconstrained. In summary, we have found all the restrictions on the phases that appear in **C**, **P**, **T**, and combinations thereof.

3.3 Discrete-symmetry phase constraints on Dirac fields in $B-L$ violating theories

In this section, we consider the discrete-symmetry transformation properties of a Dirac field in a $B-L$ violating theory and check if the same phase constraints also hold. We start with a special Majorana field that is constructed from Dirac fields, i.e., $\psi_m = a\psi + b\mathbf{C}\psi\mathbf{C}^\dagger$, in which a and b are complex numbers to be determined. Under $\mathbf{C}$, ψ_m becomes

$$\mathbf{C}\psi_m\mathbf{C}^\dagger = \frac{b}{a}(a\psi + \frac{a^2}{b}\mathbf{C}\psi\mathbf{C}^\dagger)\,.$$

Since ψ_m is a Majorana field, $\mathbf{C}\psi_m\mathbf{C}^\dagger \propto \psi_m$, yielding the condition $a^2 = b^2$, i.e., $a = \pm b$. After imposing a normalization condition on ψ_m, we find

$$\psi_{m\pm}(x) = \frac{1}{\sqrt{2}}(\psi(x) \pm \mathbf{C}\psi(x)\mathbf{C}^\dagger). \tag{3.36}$$

Its plane-wave expansion can be written as

$$\begin{aligned}\psi_{m\pm} = \int \widetilde{d^3\mathbf{p}} \sum_s \{&\frac{1}{\sqrt{2}}[b(\mathbf{p},s) \pm \eta_c d(\mathbf{p},s)]u(\mathbf{p},s)e^{-ip\cdot x} \\ &+\frac{1}{\sqrt{2}}[d^\dagger(\mathbf{p},s) \pm \eta_c b^\dagger(\mathbf{p},s)]v(\mathbf{p},s)e^{ip\cdot x}\}.\end{aligned} \tag{3.37}$$

Comparing with Eq. (3.17), we define

$$w_{m\pm}(\mathbf{p},s) \equiv \frac{1}{\sqrt{2}}[b(\mathbf{p},s) \pm \eta_c d(\mathbf{p},s)]. \tag{3.38}$$

Note that the second term of Eq. (3.37) can be written as

$$\frac{1}{\sqrt{2}}(d_s^\dagger(\mathbf{p}) \pm \eta_c b_s^\dagger(\mathbf{p})) = \pm\eta_c w_{m\pm}^\dagger(s,\mathbf{p}). \tag{3.39}$$

Therefore, we can rewrite ψ_m in a simple way:

$$\psi_{m\pm}(x) = \int \widetilde{d^3\mathbf{p}} \sum_s \left\{w_\pm(\mathbf{p},s)u(\mathbf{p},s)e^{-ip\cdot x} \pm \eta_c w_\pm^\dagger(\mathbf{p},s)v(\mathbf{p},s)e^{ip\cdot x}\right\}. \tag{3.40}$$

A comparison with Eq. (3.17) shows that the creation phase λ is no longer arbitrary; rather, $\lambda = \pm\eta_c$.

Since $\psi_{m\pm}$ is a Majorana field, our original procedures, as well as our conclusions, should still apply. For example, applying the $\mathbf{C}$ transformation to $\psi_{m\pm}$ yields

$$\mathbf{C}\psi_{m\pm}(x)\mathbf{C}^{-1} = \frac{1}{\sqrt{2}}[(\eta_c i\gamma^2)\psi^*(x) \pm \psi(x)] = \pm\psi_{m\pm}\,, \tag{3.41}$$

which is automatically consistent with our earlier conclusion that $\eta_c^*\lambda$ is real, since $\lambda = \pm\eta_c$. Recall we found that $\eta_c^*\eta_p^*\lambda$ must be imaginary in the last section. Now substituting λ by $\pm\eta_c$ yields that η_p has to be imaginary. Applying the same trick to the CPT transformation to $\psi_\pm$ results in the same conclusion for $\eta_c\eta_p\eta_t$.

Under T, $\psi_{m\pm}$ becomes

$$\mathbf{T}\psi_{m\pm}(t,\mathbf{x})\mathbf{T}^{-1} = \frac{1}{\sqrt{2}}\{\eta_t\gamma^1\gamma^3\psi(-t,\mathbf{x}) \pm (\eta_c\eta_t)^*(i\gamma^2)^*\gamma^1\gamma^3\psi^*(-t,\mathbf{x})\}\,, \quad (3.42)$$

but noting Eq. (3.3) this should be equivalent to

$$\eta_t\gamma^1\gamma^3\psi_{m\pm}(-t,\mathbf{x}) = \frac{1}{\sqrt{2}}\{\eta_t\gamma^1\gamma^3\psi(-t,\mathbf{x}) \pm i\eta_t\eta_c\gamma^1\gamma^3\gamma^2\psi^*(-t,\mathbf{x})\}\,; \quad (3.43)$$

and we conclude that $\eta_c\eta_t$ is real. Upon applying CT (or TC) to $\psi_{m\pm}$ we find just the same constraint: that $\eta_c\eta_t$ must be real.

In summary, we have found that in order to preserve the phase restrictions found in the Majorana case, the phases in the discrete symmetry transformations of fermion fields must themselves be restricted. Specifically we have found that η_p must be imaginary and that the combination $\eta_c\eta_t$ must be real. As a result, we find that $\mathbf{P}^2\psi(x)\mathbf{P}^{-2} = -\psi(x)$. Furthermore, we find that although $\eta_c\eta_p\eta_t$ is pure imaginary the combination $\eta_c\eta_p$ is unconstrained.

Although the phase restrictions we have found are worked out in a particular gamma matrix representation, our conclusions do not depend on this choice. The only key relation is $(\gamma^\mu)^\dagger = \gamma^0\gamma^\mu\gamma^0$, which is satisfied in most of commonly used representations, such as the Dirac, Weyl, and Majorana representations. In addition, unitary transformations exist that connect all the representations for which Eq. (3.1) holds[2]. Therefore, we believe the phase restrictions we have found to be an intrinsic property of the discrete symmetries. Moreover, our conclusions apply to the transformations of two-component (Majorana) fields as well. For completeness, we present the particular phase restrictions associated with the discrete-symmetry transformations of two-component Majorana fields in Appendix A.

3.4 Lorentz invariant $B-L$ violating operators and their CPT transformation properties

We work at energies far below the scale of $B-L$ breaking. In fact, we work at sufficiently low-energy scales that the Dirac field ψ can be regarded as elementary. Under

[2]A similar argument can also be found in Ref. [82].

this assumption we can enumerate all the Lorentz invariant $B-L$ violating operators with lowest mass dimension. Following the standard classification of fermion bilinears, we consider the operators

$$\mathcal{O}_1 = \psi^T C\psi + \text{h.}c., \tag{3.44}$$

$$\mathcal{O}_2 = \psi^T C\gamma_5\psi + \text{h.}c.\,, \tag{3.45}$$

$$\mathcal{O}_3 = \psi^T C\gamma^\mu\psi\,\partial^\nu F_{\mu\nu} + \text{h.}c.\,, \tag{3.46}$$

$$\mathcal{O}_4 = \psi^T C\gamma^\mu\gamma_5\psi\,\partial^\nu F_{\mu\nu} + \text{h.}c.\,, \tag{3.47}$$

$$\mathcal{O}_5 = \psi^T C\sigma_{\mu\nu}\psi\,F^{\mu\nu} + \text{h.}c.\,, \tag{3.48}$$

$$\mathcal{O}_6 = \psi^T C\sigma_{\mu\nu}\gamma_5\psi\,F^{\mu\nu} + \text{h.}c.\,, \tag{3.49}$$

where we have included the axial tensor operator $\mathcal{O}_6$ even though it is not necessary. Note that we do not include operators with derivatives on the fermion field operators because this generally results in an operator with a higher mass dimension. For example, compared with operator $\mathcal{O}_3$, operator $\psi^T C\partial_\mu\psi\partial_\nu F^{\mu\nu} + h.c.$ has one more mass dimension. We have also included the electromagnetic (EM) field strength tensor $F^{\mu\nu}$ because we want to realize a $B-L$ violating process through electromagnetic interactions, although technically $\partial^\nu F_{\mu\nu}$ is an EM current and can be replaced by any other kinds of gauge-invariant current.

We should check that these operators are indeed Lorentz invariant. Under the Lorentz transformation Λ, a fermion field $\psi(x)$ transforms into $\psi'(x)$ [83]

$$\psi'(x) = \Lambda_{\frac{1}{2}}\psi(\Lambda^{-1}x), \tag{3.50}$$

where

$$\Lambda_{\frac{1}{2}} = \exp(-\frac{i}{4}\omega_{\mu\nu}\sigma^{\mu\nu}) \tag{3.51}$$

is the spinor representation of Λ, and $\omega_{\mu\nu}$, an antisymmetric tensor, gives the infinitesimal angles. Noting the relation between the tensor matrix, $\sigma^{\mu\nu} = i[\gamma^\mu,\gamma^\nu]/2$, and the charge conjugation matrix C,

$$(\sigma^{\mu\nu})^{\mathrm{T}}C = -C\sigma^{\mu\nu}, \tag{3.52}$$

one can obtain another relation

$$\Lambda_{\frac{1}{2}}^T C = C\Lambda_{\frac{1}{2}}^{-1}, \tag{3.53}$$

so that under the Lorentz transformation,

$$\psi^T(x)C \overset{\mathbf{LT}}{\Longrightarrow} \psi^T(\Lambda^{-1}x)C\Lambda_{\frac{1}{2}}^{-1}. \tag{3.54}$$

Given the γ matrices transform just like a Lorentz vector, i.e.,

$$\Lambda_{\frac{1}{2}}^{-1}\gamma^{\mu}\Lambda_{\frac{1}{2}} = \Lambda^{\mu}_{\nu}\gamma^{\nu}, \tag{3.55}$$

We can see that these operators are indeed Lorentz invariant.

Before applying these operators to various physical problems, there is anther theorem we need to consider, namely, the CPT theorem. It says that any Lorentz invariant local quantum field theory (QFT) with a Hermitian Hamiltonian must have CPT symmetry [3]. Therefore, we should check the CPT transformation properties of these operators and list the results below

$$\mathcal{O}_1(x) \quad \overset{\mathbf{CPT}}{\Longrightarrow} -(\eta_c\eta_p\eta_t)^2\,\mathcal{O}_1(-x)\,, \tag{3.56}$$
$$\mathcal{O}_2(x) \quad \overset{\mathbf{CPT}}{\Longrightarrow} -(\eta_c\eta_p\eta_t)^2\,\mathcal{O}_2(-x)\,, \tag{3.57}$$
$$\mathcal{O}_3(x) \quad \overset{\mathbf{CPT}}{\Longrightarrow} \ (\eta_c\eta_p\eta_t)^2\,\mathcal{O}_3(-x)\,, \tag{3.58}$$
$$\mathcal{O}_4(x) \quad \overset{\mathbf{CPT}}{\Longrightarrow} -(\eta_c\eta_p\eta_t)^2\,\mathcal{O}_4(-x)\,, \tag{3.59}$$
$$\mathcal{O}_5(x) \quad \overset{\mathbf{CPT}}{\Longrightarrow} \ (\eta_c\eta_p\eta_t)^2\,\mathcal{O}_5(-x)\,, \tag{3.60}$$
$$\mathcal{O}_6(x) \quad \overset{\mathbf{CPT}}{\Longrightarrow} \ (\eta_c\eta_p\eta_t)^2\,\mathcal{O}_6(-x)\,. \tag{3.61}$$

Remarkably, the set of operators $\mathcal{O}_i$ do not transform under CPT with a definite sign, and the phase constraints we have derived before, that $(\eta_c\eta_p\eta_t)^2 = -1$, only serves to flip the sign of each eigenvalue.

3.5 CPT-odd "problem"

The apparent existence of CPT-odd operators that are Lorentz scalar is inconsistent with Greenberg's CPT theorem[4] [85], which asserts that for local theory, CPT breaking implies the Lorentz symmetry is also broken. We call it the CPT-odd "problem", but we will show that it is not a real problem. We will apply the correct phase factor of CPT transformation, appreciate the fact that half of these operators vanish due to fermion antisymmetry, and demonstrate that all the surviving operators are CPT even so that the CPT-odd "problems" is solved automatically as well.

3.5.1 CPT-odd operators with Majorana fields

In the case of Majorana fields, for which Eq. (3.20) holds, we can immediately show that the operators of Eqs. (3.46, 3.48, 3.49) — and only these of our list — vanish

[3] For a rigorous and general proof, we refer to Ref. [84].

[4] Note that this theorem is not the same CPT theorem discussed in Sec. 3.4.

identically, and that this follows from the anticommuting nature of fermion fields. Note that Eq. (3.20) can be rewritten as any of

$$\psi_m^T C = \lambda \bar{\psi}_m \,,\; C^\dagger \psi_m^* = \lambda^* \gamma^0 \psi_m \,,\; \psi_m^\dagger C^\dagger = -\lambda^* \psi_m^T \gamma^0 \,,\; C\psi_m = -\lambda \gamma^0 \psi_m^* \,. \tag{3.62}$$

Thus $\mathcal{O}_1$, e.g., can be rewritten as

$$\mathcal{O}_1 = \psi_m^T C \psi_m + \text{h.}c. = (\lambda + \lambda^*) \bar{\psi}_m \psi_m \,, \tag{3.63}$$

also

$$\mathcal{O}_1 = \psi_m^T C \psi_m + \text{h.}c. = -(\lambda + \lambda^*) \psi_m^T \bar{\psi}_m^T \,. \tag{3.64}$$

Since $\bar{\psi}_m \psi_m = -\psi_m^T \bar{\psi}_m^T$, Eq. (3.63) and (3.64) are identical and hence $\mathcal{O}_1$ needs not vanish.

Similarly for $\mathcal{O}_2$ we have $(\lambda - \lambda^*) \bar{\psi}_m \gamma_5 \psi_m$, or $-(\lambda - \lambda^*) \psi_m^T \gamma_5 \bar{\psi}_m^T$, and thus $\mathcal{O}_2$ also need not vanish. Noting that $C\gamma^\mu = -\gamma^{\mu\,T} C$ we see, however, that $\mathcal{O}_3 = (\lambda + \lambda^*) \bar{\psi}_m \gamma^\mu \psi_m j_\mu = (\lambda + \lambda^*) \psi_m^T \gamma^{\mu\,T} \bar{\psi}_m^T j_\mu$, with $j_\mu \equiv \partial^\nu F_{\mu\nu}$, and thus $\mathcal{O}_3$ vanishes. In contrast, we have that $\mathcal{O}_4 = (\lambda - \lambda^*) \bar{\psi}_m \gamma^\mu \gamma_5 \psi_m j_\mu = -(\lambda - \lambda^*) \psi_m^T \gamma_5 \gamma^{\mu\,T} \bar{\psi}_m^T j_\mu$, and we conclude that $\mathcal{O}_4$ can be nonzero. Finally, since $(\sigma^{\mu\nu})^T C \gamma^\mu = -C\sigma^{\mu\nu}$, we have that $\mathcal{O}_5 = (\lambda + \lambda^*) \bar{\psi}_m \sigma^{\mu\nu} \psi_m F_{\mu\nu} = (\lambda + \lambda^*) \psi_m^T (\sigma^{\mu\nu})^T \bar{\psi}_m^T F_{\mu\nu}$, as well as $\mathcal{O}_6 = (\lambda - \lambda^*) \bar{\psi}_m \sigma^{\mu\nu} \gamma_5 \psi_m F_{\mu\nu} = (\lambda - \lambda^*) \psi_m^T \gamma_5 (\sigma^{\mu\nu})^T \bar{\psi}_m^T F_{\mu\nu}$. We see that both $\mathcal{O}_5$ and $\mathcal{O}_6$ vanish as well.

3.5.2 CPT-odd operators with Dirac fields

In the case of Dirac fields, for which Eq. (3.20) does not hold, a similarly ready proof that the operators of Eqs. (3.46, 3.48, 3.49) vanish is not available. In this case we evaluate the operators explicitly by postulating that the field operators satisfy equal-time anticommutation relations and expanding them in the free-particle, plane-wave expansion of Eq. (3.6). We then immediately find that $\mathcal{O}_5$ and $\mathcal{O}_6$, as well as $\mathcal{O}_3$, vanish due to the anticommuting nature of fermion fields. Since our demonstration assumes that the fermion is both free and point-like, we now turn to ways in which we can make it more general, considering the conditions under which we can extend it to the case of bound particles, as well as to that of strongly bound composite particles. We would like our conclusions to be pertinent to $n - \bar{n}$ oscillations, for both free and bound neutrons.

In the case that the particle is loosely bound, e.g., the effect of the "wrong CPT" operators is still zero because the loosely bound state can be regarded as a linear

superposition of free states of momentum $\mathbf{k}$, weighted by its wave function [83]. Since the wrong CPT operators vanish for free states, then the operators involving such loosely bound particles will also. We note that since the binding energies of neutrons in large nuclei are no more than $\sim$ 8 MeV per particle, our argument should be sufficient to conclude that Eqs. (3.46, 3.48, 3.49) do not operate for bound neutrons.

An interesting question may be what happens if the fermion is actually a strongly bound composite particle, such as the neutron itself. We have explored this in the particular case of $n-\bar{n}$ oscillations using the MIT bag model [86, 87], following the analysis of Ref. [38]. A detailed description of the MIT bag model will be presented in a later section.

In the MIT bag model, since the quarks within the bag are free, an expansion of the quark fields in single-particle modes analogous to Eq. (3.6) exists [87], suggesting that the results of our earlier analysis at the nucleon level should be pertinent here as well. Indeed an explicit calculation of the transition matrix element $\langle\bar{n}|\mathcal{O}_1|n\rangle$ using the $\mathcal{O}_1$ operator of Ref. [38] with the substitution of $u^{T\alpha}_{\chi 1}C\sigma^{\mu\nu}u^{\beta}_{\chi 1}F_{\mu\nu}$ for $u^{T\alpha}_{\chi 1}Cu^{\beta}_{\chi 1}$ yields zero. In what follows we thus assume that the operators of Eqs. (3.46, 3.48, 3.49) do indeed vanish if Lorentz symmetry is not broken.

Therefore, we have established that half of the set of operators, specifically $\mathcal{O}_3$, $\mathcal{O}_5$, and $\mathcal{O}_6$, always vanish identically regardless of whether Majorana or Dirac fields are employed.

3.6 CPT-even $n-\bar{n}$ transition operators

We work at sufficiently low-energy scales that neutrons can be regarded as elementary particles. Due to the fact that half of the set of $B-L$ violating operators vanish identically, there are three CPT-even $n-\bar{n}$ transition operators left. They are $\mathcal{O}_1$, $\mathcal{O}_2$, and $\mathcal{O}_4$. As we have noted operator $\mathcal{O}_1$ is the familiar $n-\bar{n}$ oscillation operator, whose transition probability is suppressed in the presence of magnetic fields or matter. As for operator $\mathcal{O}_2$, it turns out that it does not contribute to $n-\bar{n}$ transition [88, 89, 90]. By a chiral rotation $\psi \to e^{i\beta\gamma^5}\psi$, in which β is the rotation angle, one can show that operator $\mathcal{O}_2$ can be rotated away and contributes to a mass term instead. Therefore, $\mathcal{O}_4$ seems the last hope of realizing an unquenched $n-\bar{n}$ transition. Note that because of the vector current j_μ in $\mathcal{O}_4$, a spin-flip between a neutron and an anitneutron becomes possible. Moreover, since a scattering process is involved, their energies are no longer required to be the same, and the quenching problem is completely solved. We will explicitly discuss this possible solution in later chapters.

CHAPTER 4

$B - L$ VIOLATION AND THEORIES OF SELF-CONJUGATE FERMIONS

In the last chapter, while studying the CPT properties of $B-L$ violating operators, we found that it is possible to write down both CPT even and odd operators that are yet also Lorentz invariant. Although the CPT-odd operators ultimately vanish identically due to the anticommuting nature of fermion fields, it is still worth wondering about why it is possible to write down these operators in the first place. To do this, we recall theories of self-conjugate particles with half-integer isospin are non-local [91, 92, 93, 94] and have anomalous CPT properties [95, 96, 97, 98].

In nature, there exists a fact that the low-lying, light hadrons fall into two types of isospin multiplets: self-conjugate multiplets, in which the antiparticles belong to the same isospin multiplet; and pair-conjugate multiplets, in which the antiparticles of the members of an isospin multiplet form a distinct isospin multiplet. For example, pions from a self-conjugate isospin multiplet, (π^+, π^0, π^-). Since the antiparticle of π^0 is itself and π^+ is the antiparticle of π^-, under charge conjugation transformation, this isospin multiplet remains itself. The K mesons (K^+, K^0), $(\bar{K}^0, K^-)$ are the case of pair-conjugate isospin multiplets, since the antiparticles of K^+ and K^0 are K^- and $\bar{K}^0$ respectively.

In attempting to understand these mesons' pattern, Carruthers [91] discovered that theories of self-conjugate bosons with half-integer $(\frac{1}{2},\ \frac{3}{2},\ \frac{5}{2}, \cdots)$ isospin would lead to a violation of locality, namely, the commutator of two self-conjugate fields with opposite isospin components do not vanish at space-like separations, which also renders the theory non-causal and hence physically unacceptable. Since weak local communitivity fails, CPT symmetry is no longer expected to hold [84], nor should the Greenberg's theorem [85] apply. This result was quickly generalized to theories of arbitrary spin [92, 93, 94, 95, 96]. Although the failure of weak locality does not really explain why the "wrong CPT" problem occurs, it does prompt us to find an interesting fact.

We note that a Majorana neutrino is a self-conjugate particle of $I = 0$, whereas the neutron and antineutron are members of pair-conjugate $I = 1/2$ multiplets. Since $p - \bar{p}$ oscillations are forbidden by electric charge conservation, a theory of $n - \bar{n}$

oscillations is not a theory of self-conjugate isofermions. We note, however, that the very quark-level operators that generate $n - \bar{n}$ oscillations [38] to be discussed in the next chapter, would also produce $p - \bar{p}$ oscillations under the isospin transformation $u \leftrightarrow d$. Since pure QCD is symmetric under $u \leftrightarrow d$ exchange in its chiral limit, $n - \bar{n}$ oscillations are indistinguishable with $p - \bar{p}$ oscillations. Then if $n - \bar{n}$ oscillation happens, neutron and proton would form a self-conjugate isofermion pair with a half-integer isospin and break weak locality. Therefore, $B - L$ violation is not compatible with pure QCD in the chiral limit.

CHAPTER 5

$n - \bar{n}$ OSCILLATIONS AND MATRIX ELEMENTS IN THE MIT BAG MODEL

5.1 Quark-level $n - \bar{n}$ oscillation operators

The effective Lagrangian for the $n-\bar{n}$ oscillation at the hadronic scale, [1]involves a set of six-fermion operators, which thus have a coefficient of dimension (mass)$^{-5}$. Here we will briefly summarize a complete set of six-fermion $n - \bar{n}$ oscillation operators with leading-mass dimension under particular conditions.

The effective Lagrangian for $n - \bar{n}$ oscillation can be written as

$$\mathcal{L}_q = \sum_{i,\chi} c_{i,\chi} (\mathcal{O}_i)_\chi + h.c. \tag{5.1}$$

where q denotes that this Lagrangian is at the quark-level, i is an integer number ranging from 1 to 3, χ is a compound chirality label, the c- number $c_{i,\chi}$ is the coupling coefficient of dimension (mass)$^{-5}$, and $\mathcal{O}_i$ is the six-fermion operator that contains two up (u) quarks and four down (d) quarks. Based on our earlier discussion of the nucleon level operators, the quark-level "building blocks" for operator $\mathcal{O}_i$ must look like

$$u^{T\alpha} C u^\beta \,, \quad d^{T\gamma} C d^\delta, \quad d^{T\rho} C d^\sigma, \tag{5.2}$$

where C is the charge conjugation matrix, and u and d denote the respective quark fields, and α, β, γ, δ, ρ and σ are color indices. Moreover, these terms always come in chiral pairs, i.e.,

$$u_L^T C u_L \,, \quad u_R^T C u_R \,, \tag{5.3}$$

since the mixed chirality terms always vanish. Finally, these operators should be invariant under color symmetry, $SU(3)_c$. There are three ways of forming an $SU(3)$ singlet from a product of six fundamental representations of $SU(3)$. However, in the

[1]An energy scale between the QCD scale (Λ_{QCD}) and the BSM scale (Λ_{BSM}).

single-generation case[2], only two color tensors occur [99]

$$(T_s)_{\alpha\beta\gamma\delta\rho\sigma} = \epsilon_{\rho\alpha\gamma}\epsilon_{\sigma\beta\delta} + \epsilon_{\sigma\alpha\gamma}\epsilon_{\rho\beta\delta} + \epsilon_{\rho\beta\gamma}\epsilon_{\sigma\alpha\delta} + \epsilon_{\sigma\beta\gamma}\epsilon_{\rho\alpha\delta}\,, \tag{5.4}$$

$$(T_a)_{\alpha\beta\gamma\delta\rho\sigma} = \epsilon_{\rho\alpha\beta}\epsilon_{\sigma\gamma\delta} + \epsilon_{\sigma\alpha\beta}\epsilon_{\rho\gamma\delta}\,. \tag{5.5}$$

These conditions eventually lead to three types of operators [38]:

$$(\mathcal{O}_1)_{\chi_1\chi_2\chi_3} = [u^{\top\alpha}_{\chi_1} C u^{\beta}_{\chi_1}][d^{\top\gamma}_{\chi_2} C d^{\delta}_{\chi_2}][d^{\top\rho}_{\chi_3} C d^{\sigma}_{\chi_3}](T_s)_{\alpha\beta\gamma\delta\rho\sigma}, \tag{5.6}$$

$$(\mathcal{O}_2)_{\chi_1\chi_2\chi_3} = [u^{\top\alpha}_{\chi_1} C d^{\beta}_{\chi_1}][u^{\top\gamma}_{\chi_2} C d^{\delta}_{\chi_2}][d^{\top\rho}_{\chi_3} C d^{\sigma}_{\chi_3}](T_s)_{\alpha\beta\gamma\delta\rho\sigma}, \tag{5.7}$$

$$(\mathcal{O}_3)_{\chi_1\chi_2\chi_3} = [u^{\top\alpha}_{\chi_1} C d^{\beta}_{\chi_1}][u^{\top\gamma}_{\chi_2} C d^{\delta}_{\chi_2}][d^{\top\rho}_{\chi_3} C d^{\sigma}_{\chi_3}](T_a)_{\alpha\beta\gamma\delta\rho\sigma}\,, \tag{5.8}$$

where χ_i can be L or R and C is the charge conjugation matrix. Note that the 24 operators are not all independent: in fact, only 18 of them are independent due to the flavor symmetry

$$(\mathcal{O}_1)_{\chi_1 LR} = (\mathcal{O}_1)_{\chi_1 RL}\,, \quad (\mathcal{O}_{2,3})_{LR\chi_3} = (\mathcal{O}_{2,3})_{RL\chi_3}\,. \tag{5.9}$$

If we expect that these operators should be also invariant under $SU(2)_L \times U(1)_Y$, then there are 6 independent operators left, namely,

$$\mathscr{P}_m = (\mathcal{O}_m)_{RRR}, \quad m = 1,\, 2,\, 3 \tag{5.10}$$

$$\begin{aligned}\mathscr{P}_4 &= [q^{Ti\alpha}_L C q^{j\beta}_L][u^{T\gamma}_R C d^{\delta}_R][d^{T\rho}_R C d^{\sigma}_R]\epsilon_{ij}(T_s)_{\alpha\beta\gamma\delta\rho\sigma} \\ &= 2(\mathcal{O}_3)_{LRR}\,,\end{aligned} \tag{5.11}$$

$$\begin{aligned}\mathscr{P}_5 &= [q^{Ti\alpha}_L C q^{j\beta}_L][q^{Tk\gamma}_L C q^{l\delta}_L][d^{T\rho}_R C d^{\sigma}_R]\epsilon_{ij}\epsilon_{kl}(T_a)_{\alpha\beta\gamma\delta\rho\sigma} \\ &= 4(\mathcal{O}_3)_{LLR}\,,\end{aligned} \tag{5.12}$$

$$\begin{aligned}\mathscr{P}_6 &= [q^{Ti\alpha}_L C q^{j\beta}_L][q^{Tk\gamma}_L C q^{l\delta}_L][d^{T\rho}_R C d^{\sigma}_R](\epsilon_{ik}\epsilon_{jl} + \epsilon_{jk}\epsilon_{il})(T_s)_{\alpha\beta\gamma\delta\rho\sigma} \\ &= 4[(\mathcal{O}_1)_{LLR} - (\mathcal{O}_2)_{LLR}]\,,\end{aligned} \tag{5.13}$$

where i, j, k, and l are SU(2) indices, and ϵ_{ij} is the totally antisymmetric SU(2)-tensor. The number of independent operators can be further reduced to 4 if an additional symmetry that emerges from antisymmetrizing pairs of epsilon tensors over four indices [100], i.e.,

$$(\mathcal{O}_2)_{mmn} - (\mathcal{O}_1)_{mmn} = 3(\mathcal{O}_3)_{mmn}\,, \tag{5.14}$$

with $m = L, R$ and $n = L, R$, is also taken into consideration. In other words, Eq. (5.14) provides us additional two relations

$$\mathscr{P}_6 = -3\mathscr{P}_5\,, \quad \mathscr{P}_2 - \mathscr{P}_1 = 3\mathscr{P}_3\,. \tag{5.15}$$

[2]Typically, (u, d) quark pair is referred as the first generation and (c, s) and (t, b) pairs are the second and third generations respectively. The "single-generation" means the involved quarks come from single pair.

and thus only 4 independent operators are left.

The matrix elements of these operators have been evaluated both in the MIT bag model by Rao and Shrock [38] and through lattice QCD (LQCD[3]) [102, 103]. Since we will compute the matrix elements of $n-\bar{n}$ conversion operators in the MIT bag model, a brief summary of the MIT bag model and of the proper definition of the bag model wave functions is necessary.

5.2 The MIT bag model

Due to the complexities of QCD, the wish for deducing hadron spectroscopy, structure, and interactions ultimately from first principles has so far been denied. Approximate models, such as the MIT bag model [86, 87], have been needed. Although the Lattice QCD (LQCD) brings us closer to our wish, the need for large computing time, makes for continuing challenges. Nowadays the MIT bag model is still a convenient tool. It incorporates several merits of QCD: (1) the QCD property of short-distance asymptotic freedom; (2) quark confinement; and (3) relativistic treatment of quarks; but it has limitations, e.g., the nucleons have to be at rest. Several variants of the MIT bag model have tried to incorporate more ingredients to overcome these limitations, e.g., models in Refs.[104, 105, 106]. In this section, we focus on the simplest version [86, 87] and briefly summarize the ingredients that are pertinent to our calculation.

5.2.1 Proper bag model wave functions

The MIT bag model we consider is static and possesses spherical symmetry. In the MIT bag theory, quarks and antiquarks are confined in a spherical cavity of radius R by a bag pressure B. Inside of this cavity, quarks and antiquarks obey the free-particle Dirac equation

$$(i\partial\!\!\!/ - m_\alpha)\psi_\alpha = 0, \tag{5.16}$$

where α labels the fermion and m_α denotes its mass. On the boundary of this cavity, there are two additional conditions given by

$$-in\!\!\!/\psi_\alpha = \psi_\alpha, \tag{5.17}$$

[3]LQCD is a non-perturbative approach to solving the QCD, a theory of quarks and gluons. It is a lattice gauge theory formulated on a grid or lattice of points in space and time. For a detailed introduction of LQCD, we refer to Ref. [101].

where n_μ is the inward normal to the surface and

$$-\sum_\alpha \frac{\partial}{\partial r}(\bar{\psi}_\alpha \psi_\alpha) = 2B \quad at\ r = R. \tag{5.18}$$

This second condition restricts the surviving quark modes to only those with total angular momentum $j = \frac{1}{2}$. Then the two such solutions with opposite parities are given by

$$\psi^s_{\alpha(k=-1)}(\mathbf{r}) = \frac{N_{\alpha(k=-1)}}{\sqrt{4\pi}} \begin{pmatrix} i j_0(p_\alpha \mathbf{r})\chi^s \\ -\epsilon_\alpha j_1(p_\alpha \mathbf{r})\sigma\cdot\hat{\mathbf{r}}\chi^s \end{pmatrix}, \tag{5.19}$$

$$\psi^s_{\alpha(k=1)}(\mathbf{r}) = \frac{N_{\alpha(k=1)}}{\sqrt{4\pi}} \begin{pmatrix} i j_1(p_\alpha \mathbf{r})\sigma\cdot\hat{\mathbf{r}}\chi^s \\ \epsilon_\alpha j_0(p_\alpha \mathbf{r})\chi^s \end{pmatrix}, \tag{5.20}$$

where

$$N_{\alpha(k=-1)} = \Big(\frac{\xi_\alpha^2 j_0^{-2}(\xi_\alpha)}{R^3[2E_\alpha R(E_\alpha R-1)+m_\alpha R]}\Big)^{\frac{1}{2}}, \tag{5.21}$$

$$N_{\alpha(k=1)} = \Big(\frac{\xi_\alpha^2 j_1^{-2}(\xi_\alpha)}{R^3[2E_\alpha R(E_\alpha R+1)+m_\alpha R]}\Big)^{\frac{1}{2}}, \tag{5.22}$$

with m_α and s denoting the quark mass and spin respectively. Also j_0 and j_1 are spherical Bessel functions, and

$$p_\alpha = \xi_\alpha/R,\ E_\alpha^2 = p_\alpha^2 + m_\alpha^2,\ \epsilon_\alpha = \sqrt{\frac{E_\alpha - m_\alpha}{E_\alpha + m_\alpha}}. \tag{5.23}$$

The first condition Eq. 5.17 determines the quantity ξ_α and eventually leads to the energy E_α through

$$j_1(\xi_\alpha) = \mp\epsilon_\alpha j_0(\xi_\alpha)\,, \tag{5.24}$$

for $k = 1$ and $k = -1$ respectively, which is equivalently written as

$$\tan\xi_\alpha = \frac{k\xi_\alpha}{k - k m_\alpha R + E_\alpha R}. \tag{5.25}$$

In next section, we quantize the MIT bag model wave function [107], i.e.,

$$\hat{\psi}_\alpha = b_\alpha u_\alpha + d_\alpha^\dagger v_\alpha\,, \tag{5.26}$$

in which u_α and v_α are always chosen as $u_\alpha \equiv \psi_{\alpha(k=-1)}$ and $v_\alpha \equiv \psi_{\alpha(k=1)}$ [38, 107]. The definition of u_α is transparent. However, the choice of v_α is subtle and not clearly stated in an early paper [107], which can lead to mistakes, as happened in Ref. [108].

Here we want to clarify the issue through Fig. 5.1 and Fig. 5.2, in which the first boundary condition with $k = \mp 1$, respectively, are considered. The horizontal values of the cross points of the two lines correspond to ξ_α, which determine the energy E_α. Note that there exist two cross points, red and green, in each figure. For $k = -1$ case, it is transparent that the ground energy should be determined by the red dot in Fig. 5.1. However, for $k = 1$ case, if we picked the green dot in Fig. 5.2 to calculate the ground energy, then the energy of quark and antiquark in field $\hat{\psi}_\alpha$ would be different, which is inconsistent with the CPT theorem. Therefore, we should also pick the red dot to evaluate the ground energy of antiparticle and hence we have

$$\bar{\xi}_{\alpha;k=1} = -\xi_{\alpha;k=-1}, \tag{5.27}$$

$$\bar{E}_{\alpha,k=1} = -E_{\alpha,k=-1}, \tag{5.28}$$

where "-" above ξ and E denotes antiparticle.

Now the true v_α for an antiquark should be

$$v_\alpha = \frac{\bar{N}_{\alpha(k=1)}}{\sqrt{4\pi}} \begin{pmatrix} -ij_1(p_\alpha \mathbf{r})\sigma \cdot \hat{\mathbf{r}}\eta^s \\ \\ \bar{\epsilon}_\alpha j_0(p_\alpha \mathbf{r})\eta^s \end{pmatrix}, \tag{5.29}$$

where

$$\begin{aligned} \bar{N}_{\alpha(k=1)} &= \Big(\frac{\xi_\alpha^2 j_1^{-2}(\xi_\alpha)}{R^3[-2E_\alpha R(-E_\alpha R+1)+m_\alpha R]}\Big)^{\frac{1}{2}} \\ &= \Big(\frac{\xi_\alpha^2 j_1^{-2}(\xi_\alpha)}{R^3[2E_\alpha R(E_\alpha R-1)+m_\alpha R]}\Big)^{\frac{1}{2}} \\ &= \Big(\frac{\xi_\alpha^2 j_0^{-2}(\xi_\alpha)}{R^3[2E_\alpha R(E_\alpha R-1)+m_\alpha R]}\Big)^{\frac{1}{2}} \bar{\epsilon}^{-1}, \end{aligned} \tag{5.30}$$

with

$$\bar{\epsilon}_\alpha = \sqrt{\frac{-E_\alpha - m_\alpha}{-E_\alpha + m_\alpha}} = \epsilon_\alpha^{-1}. \tag{5.31}$$

Putting everything together we obtain

$$v_\alpha^s = \frac{N_{\alpha(k=-1)}}{\sqrt{4\pi}} \begin{pmatrix} -i\epsilon j_1(p_\alpha \mathbf{r})\sigma \cdot \hat{\mathbf{r}}\eta^s \\ \\ j_0(p_\alpha \mathbf{r})\eta^s \end{pmatrix}. \tag{5.32}$$

Shifting the phase factor -1 leads to the proper the antiquark bag model wave function, namely,

$$v_\alpha^s = \frac{N_{\alpha(k=-1)}}{\sqrt{4\pi}} \begin{pmatrix} i\epsilon j_1(p_\alpha \mathbf{r})\sigma \cdot \hat{\mathbf{r}}\eta^s \\ \\ -j_0(p_\alpha \mathbf{r})\eta^s \end{pmatrix}. \tag{5.33}$$

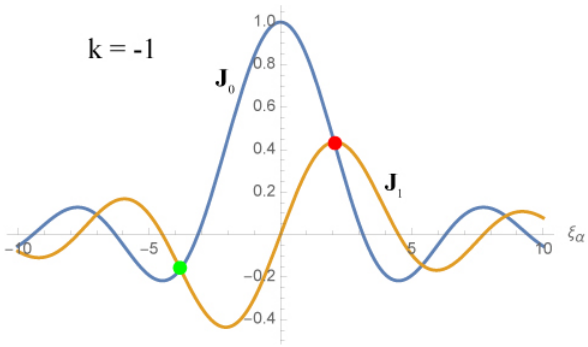

Figure 5.1: The red and green dots represent the two solutions of Eq. 5.17 with $k = -1$, which determine the corresponding two lowest energies E_α.

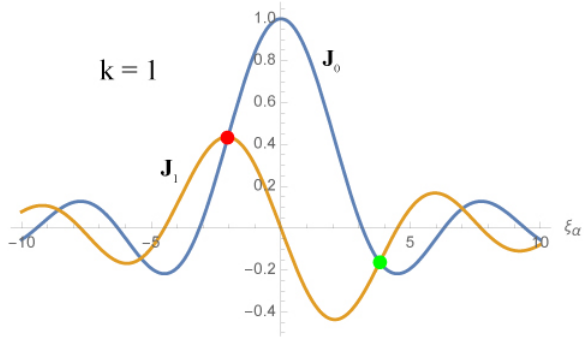

Figure 5.2: The red and green dots represent the two solutions of Eq. 5.17 with $k = 1$, which determine the corresponding two lowest energies E_α.

5.2.2 Quark fields in the MIT bag model

Now with the proper bag model wave function,

$$u_f^s(\mathbf{r}) = \frac{N_f}{\sqrt{4\pi}} \begin{pmatrix} ij_0(p_f \mathbf{r})\chi^s \\ -\epsilon_f j_1(p_f \mathbf{r})\sigma \cdot \hat{\mathbf{r}}\chi^s \end{pmatrix} \tag{5.34}$$

for quarks and

$$v_f^s(\mathbf{r}) = \frac{N_f}{\sqrt{4\pi}} \begin{pmatrix} i\epsilon_f j_1(p_f \mathbf{r})\sigma \cdot \hat{\mathbf{r}}\eta^s \\ -j_0(p_f \mathbf{r})\eta^s \end{pmatrix} \tag{5.35}$$

for antiquarks, the quantized quark field is given by [38, 107]

$$\psi_f^i(\mathbf{r}) = \sum_s [b_{s,f}^i u_f^s(\mathbf{r}) + d_{s,f}^{i\dagger} v_f^s(\mathbf{r})], \tag{5.36}$$

where $N_f = N_{\alpha(k=-1)}$, i is the color index and $b^i_{s,f}$ and $d^{i\dagger}_{s,f}$ denote quark annihilation operator and antiquark creation operators, respectively, which obey the anticommutation relations

$$\{b^i_\alpha(\mathbf{p}), b^{j\dagger}_\beta(\mathbf{p}')\} = \delta_{ij}\delta_{\alpha\beta}\delta^3(\mathbf{p}-\mathbf{p}')\,, \tag{5.37}$$

$$\{d^i_\alpha(\mathbf{p}), d^{j\dagger}_\beta(\mathbf{p}')\} = \delta_{ij}\delta_{\alpha\beta}\delta^3(\mathbf{p}-\mathbf{p}')\,, \tag{5.38}$$

with α and β denoting its other properties, such as flavor, spin, etc.

5.3 Matrix elements in the MIT bag model

To compute the matrix element of these $n-\bar{n}$ oscillation operators, i.e., $\langle\bar{n}|(\mathcal{O}_m)_{\chi_1\chi_2\chi_3}|n\rangle$, normalized spin-up neutron and antineutron wave functions are needed, which are given by

$$|n\uparrow\rangle = (1/\sqrt{18})\epsilon^{ijk}(b^{i\dagger}_{u\uparrow}b^{j\dagger}_{d\downarrow} - b^{i\dagger}_{u\downarrow}b^{j\dagger}_{d\uparrow})b^{k\dagger}_{d\uparrow}|0\rangle\,, \tag{5.39}$$

$$|\bar{n}\uparrow\rangle = (1/\sqrt{18})\epsilon^{ijk}(d^{i\dagger}_{u\uparrow}d^{j\dagger}_{d\downarrow} - d^{i\dagger}_{u\downarrow}d^{j\dagger}_{d\uparrow})d^{k\dagger}_{d\uparrow}|0\rangle\,. \tag{5.40}$$

Note that the matrix elements depend on three parameters, m_u, m_d, and R_n. We follow the argument in [38] and drop the subscripts f in Eq. (5.36) once $m_u = m_d$ is assumed. We also define the general structure of the matrix elements of these $n-\bar{n}$ oscillation operators in the bag model, namely,

$$\langle\mathcal{O}_m\rangle_{\chi_1\chi_2\chi_3} \equiv \langle\bar{n}|(\mathcal{O}_m)_{\chi_1\chi_2\chi_3}|n\rangle = [N^6p^{-3}/(4\pi)^2](I_m)_{\chi_1\chi_2\chi_3}\,, \tag{5.41}$$

where $(I_m)_{\chi_1\chi_2\chi_3}$ are dimensionless integrals. To express the final result compactly, we also define the following parameters:

$$\eta_i = 1(-1)\,,\ for\ \chi_i = R(L)\,, \tag{5.42}$$

and

$$J_a = \int_0^\xi dx\, x^2\,[\tilde{j}_1^2(x) - j_0^2(x)]^3\,, \tag{5.43}$$

$$J_b = 4\int_0^\xi dx\, x^2\tilde{j}_1^2(x)j_0^2(x)\,[\tilde{j}_1^2(x) - j_0^2(x)]\,, \tag{5.44}$$

$$J_c = \int_0^\xi dx\, x^2\,[\tilde{j}_1^2(x) + j_0^2(x)]^2[\tilde{j}_1^2(x) - j_0^2(x)]\,, \tag{5.45}$$

with $\tilde{j}_1(x) = \epsilon j_1(x)$. Now we compute the matrix elements $\langle\mathcal{O}_m\rangle_{\chi_1\chi_2\chi_3}$ with $m = 1,2,3$ and find that $(I_m)_{\chi_1\chi_2\chi_3}$ are given by

$$(I_1)_{\chi_1\chi_2\chi_3} = (-i)8\{3J_a + [\eta_2\eta_3 - 2(\eta_1\eta_2 + \eta_1\eta_3)J_b]\}\,, \tag{5.46}$$

$$(I_2)_{\chi_1\chi_2\chi_3} = (-i)2\{-3J_a + [5\eta_2\eta_3 - (\eta_1\eta_3 + \eta_2\eta_3)J_b]\}\,, \tag{5.47}$$

Table 5.1: Values of the J integrals in the two fits [109].

	Fit A	Fit B
J_a	-0.233	-0.282
J_b	0.188	0.138
J_a	-0.421	-0.420

and

$$(I_3)_{\chi_1\chi_2\chi_3} = (-i)\Big\{\frac{2}{3}\big[3J_a - [5\eta_1\eta_2 - (\eta_1\eta_3+\eta_2\eta_3)J_b]\big] - 12\eta_1\eta_2 J_c\Big\}. \qquad (5.48)$$

Note that our calculated matrix elements are the same as in Ref. [38] except for a common phase factor $-i$, which comes from the definition of the antiquark spinors. This phase factor is irrelevant to final physical quantities, since they are only related to the moduli of matrix elements.

For the purpose of comparing of $n-\bar{n}$ conversion with $n-\bar{n}$ oscillation, we also give a numerical estimation of these matrix elements. We use the same parameters as in Ref. [109, 38], which are determined in two fits: (A) $m_u = m_d = 0$, $R_n = 5.00\,\mathrm{GeV}^{-1}$; and (B) $m_u = m_d = 0.108\,\mathrm{GeV}$, $R_n = 5.59\,\mathrm{GeV}^{-1}$. Then the lowest positive solution to Eq. 5.25 with k = -1 is $\xi \simeq 2.043$ for both fits A and B and the resulting values of the three integrals are listed in Table 5.1. The factor $N^6 p^{-3}/(4\pi)^2$ in Eq. (5.41) equals $0.650\times10^{-5}\mathrm{GeV}^6$ and $0.529\times10^{-5}\mathrm{GeV}^6$ in the A and B fits, respectively. We factor out the common factor, $10^{-5}\mathrm{GeV}^6$, and list all the matrix elements $\langle\mathcal{O}_m\rangle_{\chi_1\chi_2\chi_3}$ in both fits in Table 5.2.

5.4 $n-\bar{n}$ oscillation matrix elements in lattice QCD

Matrix elements of $n-\bar{n}$ oscillation operators have also been computed using LQCD. The first LQCD calculation of these matrix elements was reported in Ref. [102]. It uses a $32^3\times256$ clover-Wilson lattices with a pion mass of 390 MeV. The results were preliminary and large uncertainty was involved. The pattern of $n-\bar{n}$ oscillation matrix elements from this bare, non-renormalized lattice calculation is quite different from the MIT bag model results [38]. Recently, these matrix elements are recomputed using LQCD with physical $N_f = 2+1$ domain wall quarks [103]. The preliminary results are non-perturbatively renormalized and converted to the $\overline{\mathrm{MS}}$ scheme.

The $n-\bar{n}$ oscillation operators are classified according to $SU(3)_{L,R}$ flavor symmetry in Table 5.3. To further classify them, it is useful to convert them to a

Table 5.2: Matrix elements of $n-\bar{n}$ oscillations in the two fits [109]

Matrix element	Fit A	Fit B
$\langle\mathcal{O}_1\rangle_{RRR}$	-6.56	-5.33
$\langle\mathcal{O}_1\rangle_{LLR}$	-4.61	-4.17
$\langle\mathcal{O}_1\rangle_{RLL}$	1.26	-0.666
$\langle\mathcal{O}_2\rangle_{RRR}$	1.64	1.33
$\langle\mathcal{O}_2\rangle_{LLR}$	2.62	1.92
$\langle\mathcal{O}_2\rangle_{RLL}$	-0.314	0.167
$\langle\mathcal{O}_3\rangle_{RRR}$	2.73	2.22
$\langle\mathcal{O}_3\rangle_{LRR}$	-3.18	-2.72
$\langle\mathcal{O}_3\rangle_{LLR}$	2.41	2.03

Table 5.3: Classification of $n-\bar{n}$ transition operators according to $SU(3)_{L,R}$ [103].

	$\mathcal{O}^{6q}$	$\mathbf{I}_R\otimes\mathbf{I}_L$
$[(RRR)_3]$	$\mathcal{O}^1_{R(RR)}+4\mathcal{O}^2_{(RR)R}$	$\mathbf{3}_R\otimes\mathbf{0}_L$
$[(RRR)_1]$	$\mathcal{O}^2_{(RR)R}-\mathcal{O}^1_{R(RR)}\equiv 3\mathcal{O}^3_{(RR)R}$	$\mathbf{1}_R\otimes\mathbf{0}_L$
$[R_1(LL)_0]$	$\mathcal{O}^2_{(LL)R}-\mathcal{O}^1_{L(LR)}\equiv 3\mathcal{O}^3_{(LL)R}$	$\mathbf{1}_R\otimes\mathbf{0}_L$
$[(RR)_1L_0]$	$3\mathcal{O}^3_{(LR)R}$	$\mathbf{1}_R\otimes\mathbf{0}_L$
$[(RR)_2L_1]_{(1)}$	$\mathcal{O}^1_{L(RR)}$	$\mathbf{2}_R\otimes\mathbf{1}_L$
$[(RR)_2L_1]_{(2)}$	$\mathcal{O}^2_{(LR)R}$	$\mathbf{2}_R\otimes\mathbf{1}_L$
$[(RR)_2L_1]_{(3)}$	$\mathcal{O}^1_{R(LR)}+2\mathcal{O}^2_{(RR)L}$	$\mathbf{2}_R\otimes\mathbf{1}_L$

$SU(2)_L \times SU(2)_R$ chiral isospin basis, in which the perturbative renormalization is diagonal [100]. There are seven other operators that can be obtained by replacing $L \leftrightarrow R$. The operators are built from left/right diquarks denoted as L, R, respectively, in the first column. Notation $(...)_I$ denotes projection on representation with total isospin I. The second column shows corresponding operators in terms of $\mathcal{O}_1, \mathcal{O}_2$, and $\mathcal{O}_3$ in Ref. [38]. The $SU(2)_{L,R}$ representation is shown in the 3rd column and the 1-loop anomalous dimension is given in the 4th column.

The lattice chosen has a lattice space $a = 0.114$ fm and volume $48^3 \times 96$. The spatial size corresponds to $m_\pi L \approx 3.9$, and the gauge configurations with $N_f = 2+1$ domain wall quarks correspond to a physical pion mass $m_\pi \approx 140$MeV.

The six-fermion operator matrix elements computed on a lattice are renormalized to a scale of 2 GeV in the $\overline{\text{MS}}$ scheme. The match between the lattice and the continuum is performed by using a one-loop perturbative calculation [100]. More recently a perturbative renormalization treatment of $n-\bar{n}$ operators can be found in Ref. [110].

The preliminary results are summarized in Table 5.4, in which Bag "A" and "B" correspond to the two fits in the MIT bag model respectively. Note that the pattern of matrix elements in LQCD is very similar to the results from the MIT bag model with bag "B". The dominant three matrix elements are almost the same, except the largest one differs in sign. However, since the physics quantities only depend on moduli of the matrix elements and if we only consider one operator at a time, then the sign difference is irrelevant. The last three matrix elements computed in LQCD are larger than the bag model calculations. It is argued that this difference can provide sharper constraints on BSM physics, and further discussion of this is still in preparation [103]. Nevertheless, the consistency of matrix elements computed in these two methods really gives us confidence in evaluating $n-\bar{n}$ conversion using the MIT bag model.

Table 5.4: Preliminary results for matrix elements of six-fermion operators and comparison to the MIT bag model results [38].

	Bag "A"	$\frac{\text{LQCD}}{\text{Bag "A"}}$	Bag "B"	$\frac{\text{LQCD}}{\text{Bag "B"}}$
$[(RRR)_3]$	0	—	0	—
$[(RRR)_1]$	8.190	5.5	6.660	6.8
$[R_1(LL)_0]$	7.230	6.1	6.090	7.2
$[(RR)_1L_0]$	-9.540	7.0	-8.160	8.1
$[(RR)_2L_1]_{(1)}$	1.260	-1.7	-0.666	3.2
$[(RR)_2L_1]_{(2)}$	-0.314	-1.7	0.167	3.2
$[(RR)_2L_1]_{(3)}$	0.630	-1.7	-0.330	3.2

CHAPTER 6

PHENOMENOLOGY OF $n\bar{n}$ CONVERSION

6.1 Spin-flip and $n - \bar{n}$ conversion

In Chap. 2, we showed that the transition probability of $n-\bar{n}$ oscillation suffers from quenching problems in the presence of magnetic fields or matter. This is generally evaluated in a 2×2 effective Hamiltonian framework, in which the initial neutron (antineutron) and its anti-particle have the same spin projection quantum number, e.g., s_z, the spin projection in the z direction, and four-momentum. Given Lorentz and CPT invariance, since the neutron and antineutron have magnetic moments of opposite sign, in the presence of external magnetic fields, their energies are different. Therefore, one member of the particle-antiparticle pair cannot spontaneously transform into the other without breaking energy-momentum conservation. To observe $n - \bar{n}$ oscillations, great efforts are needed to mitigate magnetic fields. The same argument also holds for matter effects.

On the other hand, since the neutron and antineutron have opposite magnetic moments due to the CPT symmetry, if the sign of s_z of neutron (antineutron) can be flipped during the oscillation process presumably by an external agent, such as matter or magnetic fields, then the energy of initial and final particles will remain the same even in the presence of magnetic fields, so that the transition probability is no longer suppressed. Therefore, the spin degree of freedoms of the neutron and antineutron can potentially play an important role in the study of $n - \bar{n}$ oscillations [111].

6.1.1 $n\bar{n}$ oscillation in 4×4 framework

The first attempt to achieve a non-suppressed $n - \bar{n}$ transition probability by considering spin-dependent SM effects was proposed in Ref. [111]. There it was shown that the spin-dependent SM effects involving transverse magnetic fields could flip the particle spin and eventually realize $n - \bar{n}$ transitions without quenching problems. However, this conclusion turns out to be incorrect because it is sensitive to the CPT phase constraint discussed in Chap. 2. To illustrate, I will briefly discuss the example analyzed in Ref. [111].

A neutron at rest that can oscillate to an antineutron is in a static magnetic field $\mathbf{B}_0$. Then at $t = 0$, a static transverse field $\mathbf{B}_1$ is suddenly applied. Note that $\mathbf{B}_0$

fixes the spin quantization axis, and we define $\omega_0 \equiv -\mu_n B_0$ and $\omega_1 \equiv -\mu_n B_1$, where μ_n again is the neutron magnetic moment. Instead of working in the 2×2 framework, the Hamiltonian matrix now is in the $|n(+)\rangle, |\bar{n}(+)\rangle, |n(-)\rangle, |\bar{n}(-)\rangle$ basis and is of form

$$\mathcal{H} = \begin{pmatrix} M+\omega_0 & \delta & \omega_1 & 0 \\ \delta & M-\omega_0 & 0 & -\omega_1 \\ \omega_1 & 0 & M-\omega_0 & -\delta\eta_{cpt}^2 \\ 0 & -\omega_1 & -\delta\eta_{cpt}^2 & M+\omega_0 \end{pmatrix}, \tag{6.1}$$

where M is the neutron mass and δ, as shown in Chap. 2, denotes a $n(+) \to \bar{n}(+)$ transition matrix element. The other minus signs are fixed by Hermiticity and CPT invariance. In Ref. [111], the phase η_{cpt} was set to unity, as per standard textbooks [83] and noting $|\delta| \ll |\omega_0|, |\omega_1|$, the unpolarized $n-\bar{n}$ transition probability was found to be

$$\begin{aligned} \mathcal{P}_{n\to\bar{n}}(t) &= \delta^2\Big[\frac{\omega_1^2 t^2}{\omega_0^2+\omega_1^2} + \frac{\omega_0^2}{(\omega_0^2+\omega_1^2)^2}\sin^2\left(t\sqrt{\omega_0^2+\omega_1^2}\right) \\ &\quad + \frac{\omega_0^2\omega_1^2 t}{(\omega_0^2+\omega_1^2)^{5/2}}\left(1-\sin\left(2t\sqrt{\omega_0^2+\omega_1^2}\right)\right)\Big] + \mathcal{O}(\delta^3), \end{aligned} \tag{6.2}$$

so that if $|\omega_0| \sim |\omega_1|$ the first term is of $\mathcal{O}(1)$ in magnetic fields, and thus the quenching no longer appears. However, the exact eigenvalues at $t > 0$ are

$$\begin{aligned} E_1 &= M - \sqrt{\omega_0^2 + (\delta-\omega_1)^2}, \\ E_2 &= M + \sqrt{\omega_0^2 + (\delta-\omega_1)^2}, \\ E_3 &= M - \sqrt{\omega_0^2 + (\delta+\omega_1)^2}, \\ E_4 &= M + \sqrt{\omega_0^2 + (\delta+\omega_1)^2}, \end{aligned} \tag{6.3}$$

in which one can distinguish the longitudinal and transverse fields in that the transverse field is suddenly applied. However, once the field is "on" one should no longer be able to distinguish longitudinal from transverse fields, and thus the eigenvalues should depend on the magnitude of fields only. As pointed out in Refs. [88, 112] and later confirmed in Ref. [90], this breaks rotational invariance, and hence the Lorentz invariance. Now with the correct phase $\eta_{cpt}^2 = -1$, we find that the energy eigenvalues at $t > 0$ do respect rotational symmetry, but there are only two different eigenvalues left, so that they recover the form evaluated in the 2×2 framework and

that $n(+) \to \bar{n}(-)$ and $n(-) \to \bar{n}(+)$ transitions no longer occur. As a result, $n\bar{n}$ transitions are quenched irrespective of the presence of transverse magnetic fields. Moreover, employing time-dependent magnetic fields in the manner familiar from the theory of magnetic resonance [113, 114], as discussed in Ref. [111], does not change this conclusion. However, despite the failure of this specific method, spin-dependent effects can still play a key role in $n - \bar{n}$ transitions.

6.1.2 $n - \bar{n}$ conversion operator

In Chap. 3, a $n - \bar{n}$ conversion operator was introduced. We argued that because of the vector current, the spin degree of freedom of neutron and antineutron must be considered, and spin-flip between the neutron and antineutron became possible. In this subsection, we will demonstrate explicitly that the $n - \bar{n}$ conversion operator does avoid the quenching problem in the presence of an external magnetic field.

For simplicity we make the initial neutron or antineutron stationary. Then working in the $|n(+)\rangle, |\bar{n}(+)\rangle, |n(-)\rangle, |\bar{n}(-)\rangle$ basis, and assuming that momentum transfer is trivially small (so that the following framework still works), the Hamiltonian matrix in presence of a magnetic field $\mathbf{B}_0$ is of form

$$\mathcal{H} = \begin{pmatrix} M + \omega_0 & \omega_z & 0 & \omega_x - i\omega_y \\ \omega_z & M - \omega_0 & \omega_z - i\omega_y & 0 \\ 0 & \omega_x + i\omega_y & M - \omega_0 & -\omega_z \\ \omega_x + i\omega_y & 0 & -\omega_z & M + \omega_0 \end{pmatrix}. \tag{6.4}$$

The details are given below. We set the direction of $\mathbf{B}_0$ as the quantization axis and define $\omega_0 \equiv -\mu_n B_0$. The parameter M denotes the neutron mass, and the matrix elements of $\mathcal{O}_4$ for various spin states of the neutron and antineutron are defined as follows: $\omega_x \equiv 2j^x$, $\omega_y \equiv 2j^y$, and $\omega_z \equiv 2j^z$. Note that we have incorporated a $B - L$ coefficient that is associated with the operator $\mathcal{O}_4$ into j. Therefore, $|\omega_0| \gg |\omega_x|, |\omega_y|, |\omega_z|$. Assuming $|\omega_x| \sim |\omega_y| \sim |\omega_z|$, we compute the transition probabilities of a neutron with spin $s = +$ into an antineutron in spin $s = \pm$ states respectively

$$\mathcal{P}_{n+\to\bar{n}+} = \frac{\omega_z^2}{\omega_0^2} \sin^2(t\omega_0) \cos^2(t\omega_{xy}) + \mathcal{O}(\omega_z^3) \tag{6.5}$$

$$\mathcal{P}_{n+\to\bar{n}-} = \sin^2(t\omega_{xy}) - \frac{t\omega_z^2\omega_{xy}}{\omega_0^2} \sin(t\omega_{xy}) \cos(t\omega_{xy}) - \frac{\omega_z^2}{\omega_0^2} \cos^2(t\omega_0) \sin^2(t\omega_{xy}) + \mathcal{O}(\omega_z^3), \tag{6.6}$$

where $\omega_{xy} = \sqrt{\omega_x^2 + \omega_y^2}$. It is easy to find that $\mathcal{P}_{n+\to\bar{n}+}$ is still quenched by the magnetic field, which is not surprising since the spin is not flipped. Although the last two terms in $\mathcal{P}_{n+\to\bar{n}-}$ are also quenched, the first term is independent of the external magnetic field, so that the $n(+) \to \bar{n}(-)$ process is not suppressed. It should be pointed out that although we demonstrated this in a particular case, our conclusion holds more generally. Note that since a scattering process is involved, the initial neutron and final antineutron do not have to share the same energy-momentum, and the framework we used thus far ceases to be valid, because the particles are not stationary. Therefore, we are no longer bound to the context of an oscillation framework, and the quenching problem is completely solved. Moreover, following the same analysis performed in the ILL experiment [39], one can also set a limit on η directly by utilizing a nonuniform magnetic field so that it can generate a nonzero ω_{xy} in this framework.

6.2 Effective theories of $n\bar{n}$ conversion

6.2.1 Dimensional analysis of $n - \bar{n}$ conversion operators

Before moving on to possible applications of the $n - \bar{n}$ conversion operator, we first approach the problem from the viewpoint of simple dimensional analysis. There are two kinds of fields involved: one fermion field ψ and one electromagnetic tensor $F_{\mu\nu}$ in operator $\mathcal{O}_4$. It is easy to check that the mass dimension of a fermion field with spin 1/2 is 3/2, and it is usually denoted by $[\psi] = 3/2$[1]. To be thorough, we also write down the mass dimension of the other terms in operator $\mathcal{O}_4$.

$$[\partial] = 1, \quad [F_{\mu\nu}] = 2, \quad [C] = [\gamma^\mu] = [\gamma^5] = 0. \tag{6.7}$$

Since the mass dimension of a Lagrangian density must be 4, i.e. $[\mathcal{L}] = 4$, while $[\psi^T C\gamma^\mu\gamma^5\partial^\nu F_{\nu\mu}] = 6$, there must be a coupling coefficient η with mass dimension -2 associated with this operator. Therefore, the correct form that the $n - \bar{n}$ conversion operator takes must be

$$\mathcal{O}_4 = \eta\psi^T C\gamma^\mu\gamma^5\psi\partial^\nu F_{\mu\nu} + h.c. \tag{6.8}$$

Following the same argument, one would wonder if there should also be a coupling coefficient, say η', with mass dimension one associated with the $n - \bar{n}$ oscillation operator — and the answer is positive. Now noting $[\eta/\eta'] = -3$, one cannot help

[1]Here the square brackets denote the mass dimension of the quantity in brackets.

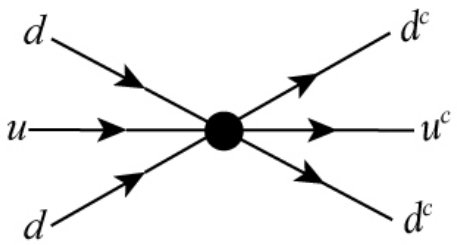

Figure 6.1: Tree diagram of a six-fermion $n - \bar{n}$ oscillation vertex.

expecting that $n - \bar{n}$ conversion will be suppressed by an additional factor of Λ_{NP}^3, where Λ_{NP} is the cutoff mass scale of new physics. This is not necessarily true because other energy scales also exist. To illustrate this explicitly, we need to find the quark-level $n - \bar{n}$ conversion operators first.

6.2.2 Quark-level $n - \bar{n}$ conversion operators

There is an inner connection between $n\bar{n}$ oscillation and conversion operators. Let us revisit the structures of these two operators, $\mathcal{O}_1$ and $\mathcal{O}_4$.

$$\mathcal{O}_1 = \eta' \psi^T C \psi + h.c., \quad \mathcal{O}_4 = \eta \psi^T C \gamma^\mu \gamma^5 \psi j_\mu + h.c., \tag{6.9}$$

with $j_\mu = \partial^\nu F_{\mu\nu}$. Note that the γ^μ structure in $\mathcal{O}_4$ can come from the interaction between $n - \bar{n}$ oscillation operator and a vector current J_μ generated by an external source. Since a neutron or antineutron contains quarks[2], we can connect the $n - \bar{n}$ conversion operator with the oscillation operator through such an external source. Moreover, this can be done via SM physics. Since quarks are explicitly involved, we must work at an energy scale above Λ_{QCD}. However, for the processes we want to consider, we can still work at energies far below the Λ_{NP}.

Although technically the current can be any vector current and it does not have to be gauged, the easiest choice should be the electromagnetic current that we explicitly showed in $\mathcal{O}_4$. We will start with the complete set of general six-fermion $n - \bar{n}$ operators listed in Chap. 5, which can also be represented graphically by Fig. 6.1. Recall there are three kinds of six-fermion $n - \bar{n}$ operators, $(\mathcal{O}_1)_{\chi_1\chi_2\chi_3}$, $(\mathcal{O}_2)_{\chi_1\chi_2\chi_3}$, and $(\mathcal{O}_3)_{\chi_1\chi_2\chi_3}$. Here we will take $(\mathcal{O}_1)_{\chi_1\chi_2\chi_3}$ as an example to demonstrate the connection between $n\bar{n}$ conversion and oscillation.

It is useful to recall the explicit form of $(\mathcal{O}_1)_{\chi_1\chi_2\chi_3}$,

$$(\mathcal{O}_1)_{\chi_1\chi_2\chi_3} = [u_{\chi_1}^{\top\alpha} C u_{\chi_1}^{\beta}][d_{\chi_2}^{\top\gamma} C d_{\chi_2}^{\delta}][d_{\chi_3}^{\top\rho} C d_{\chi_3}^{\sigma}](T_s)_{\alpha\beta\gamma\delta\rho\sigma}, \tag{6.10}$$

[2]Recall that the quarks of the SM carry both electric and color charge.

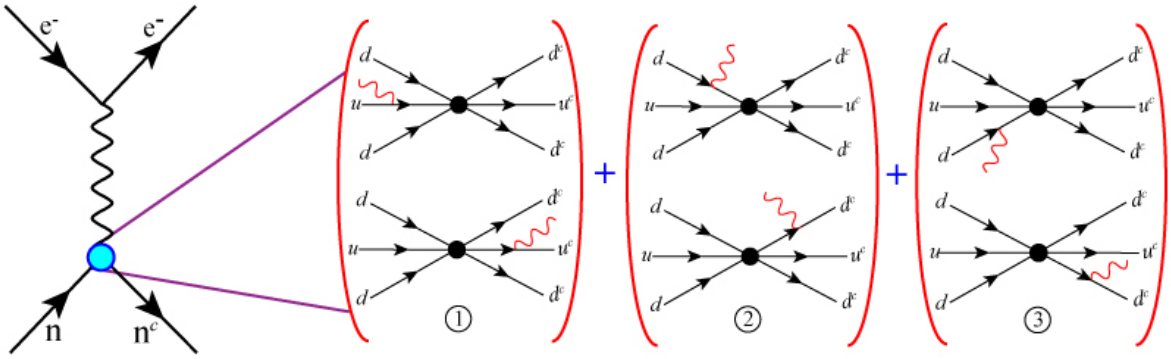

Figure 6.2: A neutron-antineutron transition is realized through electron-neutron scattering. The virtual photon emitted from the scattered electron interacts with a general six-fermion $n-\bar{n}$ oscillation vertex. ①, ②, and ③ correspond to two possible ways of attaching a photon to the three blocks.

where T_s denotes one of the color tensors. Now we can apply electromagnetic interactions to this operator. A virtual photon is generated by a scattered charged particle (e.g., electron), which is an explicit realization of an electric current. Note that there are three blocks, [...], in $(\mathcal{O}_1)_{\chi_1\chi_2\chi_3}$ and in each block there are two charged particles (quarks and antiquarks). When a virtual photon is attached to these blocks, there are six possible ways that correspond to six different Feynman diagrams as showed in Fig. 6.2. Note that we do not attach a photon line to the solid "blob" at the center — this would yield an effect that would be suppressed by higher powers of the new physics mass scale!

Let us consider the first block of this operator first. We assign the momentum p and p' for initial u quark and final u^c respectively and k as the incoming momentum of photon. Then the corresponding amplitude will be

$$\begin{aligned}\mathcal{M} &= \epsilon_\mu\Big[\frac{2e}{3}u_{\chi_1}^\top C\frac{i}{\not{p}+\not{k}-m_u}i\gamma^\mu u_{\chi_1}+\frac{2e}{3}u_{\chi_1}^\top Ci\gamma^\mu\frac{i}{-(\not{p}'-\not{k})-m_u}u_{\chi_1}\Big]\\ &\quad\times[d_{\chi_2}^{\top\gamma}Cd_{\chi_2}^{\delta}][d_{\chi_3}^{\top\rho}Cd_{\chi_3}^{\sigma}](T_s)_{\alpha\beta\gamma\delta\rho\sigma},\end{aligned}\tag{6.11}$$

where ϵ_μ denotes the polarization vector of the photon and u and d are the Dirac spinors. If we assume that the momentum transfer is small, so that the momentum of the initial u quark and final u^c are close, i.e. $p'\simeq p$ and $k\simeq 0$, then the amplitude becomes

$$\begin{aligned}\mathcal{M} &= \epsilon_\mu\Big[-\frac{4e}{3}u_{\chi_1}^\top C\gamma^\mu\frac{m_u}{p^2-m_u^2}u_{\chi_1}-\frac{2e}{3}u_{\chi_1}^\top C\frac{\not{p}\gamma^\mu-\gamma^\mu\not{p}}{p^2-m_u^2}u_{\chi_1}\Big]\\ &\quad\times[d_{\chi_2}^{\top\gamma}Cd_{\chi_2}^{\delta}][d_{\chi_3}^{\top\rho}Cd_{\chi_3}^{\sigma}](T_s)_{\alpha\beta\gamma\delta\rho\sigma}.\end{aligned}\tag{6.12}$$

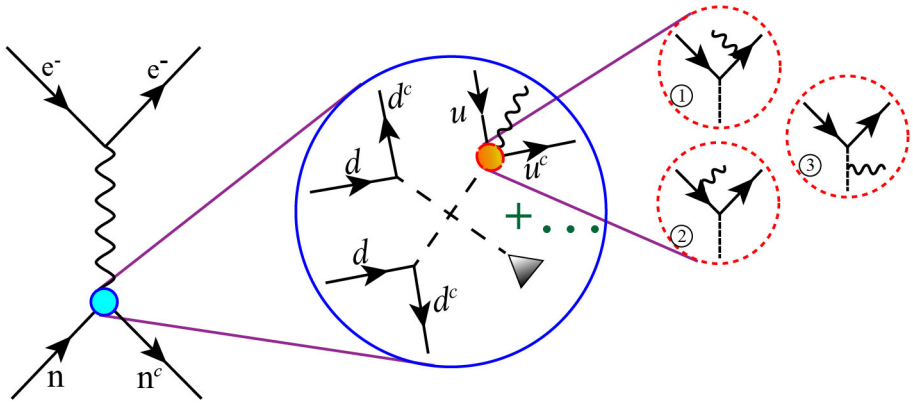

Figure 6.3: A neutron-antineutron transition is realized through electron-neutron scattering. The virtual photon emitted from the scattered electron interacts with the neutron through a six-fermion $|\Delta B| = 2$ vertex that is generated by a spontaneous $(B-L)$-symmetry breaking of the "partial unification" group $\mathrm{SU}(2)_L \otimes \mathrm{SU}(2)_R \otimes \mathrm{SU}(4')$[46]. This is shown inside of the big blue circle. Since photon can couple to any charged particle, i.e. to any of the lines in these three blocks, we only take the first block as an example. The vertex is represented by a red and gold circular area. There are three possible ways to couple the photon to this vertex. We explicitly show them within three dashed red circles.

The second term inside of the first bracket above can be dropped. Since this is not trivial, I will explicitly demonstrate it below. Note that $u^T C = \bar{v}$ in our spinor convention. From $\bar{v}\not{p} = -m\bar{v}$, it is easy to find that $\bar{v}_{\chi_1}\not{p} = -m\bar{v}_{-\chi_1}$. Therefore we have

$$\begin{aligned} u_{\chi_1}^{\top} C(\not{p}\gamma^{\mu} - \gamma^{\mu}\not{p})u_{\chi_1} &= \bar{v}_{\chi_1}(\not{p}\gamma^{\mu} - \gamma^{\mu}\not{p})u_{\chi_1} \\ &= -m_u[\bar{v}_{-\chi_1}\gamma^{\mu}u_{\chi_1} + \bar{v}_{\chi_1}\gamma^{\mu}u_{-\chi_1}]. \end{aligned} \tag{6.13}$$

Noting that $(1 \pm \gamma^5)\gamma^{\mu}(1 \mp \gamma^5) = 2\gamma^{\mu}(1 \mp \gamma^5)$, Eq. 6.13 can be further simplified to

$$u_{\chi_1}^{\top} C(\not{p}\gamma^{\mu} - \gamma^{\mu}\not{p})u_{\chi_1} = \bar{v}\gamma^{\mu}u = u^T C\gamma^{\mu}u. \tag{6.14}$$

This corresponds to an operator with the structure $\psi^T C\gamma^{\mu}\psi$, which we have showed that its CPT transformation is CPT-odd and that it vanishes identically. Eventually the amplitude can be written as

$$\mathcal{M} = \epsilon_{\mu}\Big[-\frac{4e}{3}u_{-\chi_1}^{\top} C\gamma^{\mu}\frac{m_u}{p^2 - m_u^2}u_{\chi_1}\Big][d_{\chi_2}^{\top\gamma} C d_{\chi_2}^{\delta}][d_{\chi_3}^{\top\rho} C d_{\chi_3}^{\sigma}](T_s)_{\alpha\beta\gamma\delta\rho\sigma}. \tag{6.15}$$

Now we can write down the associated effective operator as

$$\lambda \frac{-4e}{3} \frac{m_u}{p^2 - m_u^2} [u^{\top\alpha}_{-\chi_1} C\gamma^\mu u^\beta_{\chi_1}][d^{\top\gamma}_{\chi_2} C d^\delta_{\chi_2}][d^{\top\rho}_{\chi_3} C d^\sigma_{\chi_3}](T_s)_{\alpha\beta\gamma\delta\rho\sigma}. \tag{6.16}$$

Here u and d are no longer denoting Dirac spinors but the u quark and d quark fields respectively. Note that because of the electromagnetic interaction, the chirality of the initial particle and final particle in the first block has changed the sign, which fulfills the spin-flip character of the $n\bar{n}$ conversion operator $\mathcal{O}_4$. This also implies that if the particles involved cannot be massless, since it is impossible to flip the chirality of a massless particle.

Note that we have introduced a parameter λ that actually comes from the original six-fermion $\mathcal{O}_1$ operator and can be related to the coupling coefficient η' later. Simple dimensional analysis shows the mass dimension of λ to be $[\lambda] = -5$.

Before moving on to other blocks or to other $n-\bar{n}$ oscillation operators, we would like to point out that our treatment is an effective field theory (EFT) treatment, so that it should be model-independent. To demonstrate it, we will show that the model-dependent aspects drop out in the low momentum limit. We can pick a popular model in which $n-\bar{n}$ oscillation is generated by a spontaneous breaking of local $B-L$ symmetry [46]. The tree graph that induces the six-fermion $|\Delta B| = 2$ vertex, e.g., $\mathcal{O}_1$, is shown in the big blue circle in Fig. 6.3. As we did above, we focus on the first block of $(\mathcal{O}_1)_{\chi_1\chi_2\chi_3}$ first. Now there will be three different Feynman diagrams corresponding to the three different way of attaching a virtual photon to this block, because there are three charged particles (u, $\bar{u}$, and charged scalar particle) involved. The amplitude takes the form

$$\begin{aligned}
\mathcal{M} \;=\; & \Big\{ \epsilon_\mu \frac{i}{(p'-p)^2 - M^2} \Big[\frac{2e}{3} u^\top_{\chi_1} C \frac{i}{\not{p} + \not{k} - m_u} i\gamma^\mu u_{\chi_1} + \frac{2e}{3} u^\top_{\chi_1'} C i\gamma^\mu \frac{i}{-(\not{p}' - \not{k}) - m_u} u_{\chi_1} \Big] \\
& + u^\top_{\chi_1} C u_{\chi_1} \frac{i}{(p'-p)^2 - M^2} \frac{i}{(p'-p+k)^2 - M^2} \frac{4e}{3} \epsilon_\mu i(2p^\mu + 2p'^\mu + k^\mu) \Big\} \\
& \times [d^{\top\gamma}_{\chi_2} C d^\delta_{\chi_2}][d^{\top\rho}_{\chi_3} C d^\sigma_{\chi_3}](T_s)_{\alpha\beta\gamma\delta\rho\sigma},
\end{aligned} \tag{6.17}$$

where M is the mass of the charged scalar field. We can simplify the equation above by noting that both the nucleon momenta and the momentum transfer are much smaller than the scalar mass M, and that the second term is quenched by another $1/M^2$. Therefore, this amplitude can be rewritten as

$$\begin{aligned}
\mathcal{M} \;=\; & \frac{-i\epsilon_\mu}{M^2} \Big[\frac{2e}{3} u^\top_{\chi_1} C \frac{i}{\not{p} + \not{k} - m_u} i\gamma^\mu u_{\chi_1} + \frac{2e}{3} u^\top_{\chi_1'} C i\gamma^\mu \frac{i}{-(\not{p}' - \not{k}) - m_u} u_{\chi_1} \Big] \\
& \times [d^{\top\gamma}_{\chi_2} C d^\delta_{\chi_2}][d^{\top\rho}_{\chi_3} C d^\sigma_{\chi_3}](T_s)_{\alpha\beta\gamma\delta\rho\sigma}.
\end{aligned} \tag{6.18}$$

We take the same assumption as before, then the amplitude becomes

$$\begin{aligned}\mathcal{M} &= \frac{-i\epsilon_\mu}{M^2}\Big[-\frac{4e}{3}u^\top_{\chi_1}C\gamma^\mu\frac{m_u}{p^2-m_u^2}u_{\chi_1}-\frac{2e}{3}u^\top_{\chi_1'}C\frac{\not{p}\gamma^\mu-\gamma^\mu\not{p}}{p^2-m_u^2}u_{\chi_1}\Big]\\ &\quad\times[d^{\top\gamma}_{\chi_2}Cd^\delta_{\chi_2}][d^{\top\rho}_{\chi_3}Cd^\sigma_{\chi_3}](T_s)_{\alpha\beta\gamma\delta\rho\sigma}. \end{aligned}\tag{6.19}$$

Eventually the amplitude can be simplified to

$$\mathcal{M} = \frac{-i\epsilon_\mu}{M^2}\Big[-\frac{4e}{3}u^\top_{-\chi_1}C\gamma^\mu\frac{m_u}{p^2-m_u^2}u_{\chi_1}\Big][d^{\top\gamma}_{\chi_2}Cd^\delta_{\chi_2}][d^{\top\rho}_{\chi_3}Cd^\sigma_{\chi_3}](T_s)_{\alpha\beta\gamma\delta\rho\sigma}. \tag{6.20}$$

We can also write down the associated effective operator

$$\frac{-i}{M^2}\Big[-\frac{4e}{3}\frac{m_u}{p^2-m_u^2}u^{\top\alpha}_{-\chi_1}C\gamma^\mu u^\beta_{\chi_1}\Big][d^{\top\gamma}_{\chi_2}Cd^\delta_{\chi_2}][d^{\top\rho}_{\chi_3}Cd^\sigma_{\chi_3}](T_s)_{\alpha\beta\gamma\delta\rho\sigma}. \tag{6.21}$$

where u and d now denote u quark and d quark fields respectively. Now the whole effective operator shall be

$$\lambda'\frac{i}{M^6}\frac{-4e}{3}\frac{m_u}{p^2-m_u^2}[u^{\top\alpha}_{-\chi_1}C\gamma^\mu u^\beta_{\chi_1}][d^{\top\gamma}_{\chi_2}Cd^\delta_{\chi_2}][d^{\top\rho}_{\chi_3}Cd^\sigma_{\chi_3}](T_s)_{\alpha\beta\gamma\delta\rho\sigma}, \tag{6.22}$$

where λ' is introduced to make sure the mass dimension of this operator is correct — and actually it can also be related to the model [46]. Note that this operator is identical to Eq. 6.16, after a parameter definition, i.e. $\lambda \equiv i\lambda'/M^6$. Therefore, the model we considered only serves as a mechanism to generate the coupling coefficient η. Under the assumption that the conversion is mediated by electromagnetism, the structure of $n\bar{n}$ conversion operator will be the same as long as one starts with a complete set of general six-fermion $n-\bar{n}$ oscillation operators, irrespective of the model from which they arise.

We ignore the coupling coefficient λ for the moment, though we will restore it when we turn to the evaluation of the hadron matrix elements. Now we can simply write down the effective $n\bar{n}$ conversion operator as

$$(\mathcal{O}_1^\mu)^I_{\chi_1\chi_2\chi_3} = -\frac{4e}{3}\frac{m_u}{p^2-m_u^2}[u^{\top\alpha}_{-\chi_1}C\gamma^\mu u^\beta_{\chi_1}][d^{\top\gamma}_{\chi_2}Cd^\delta_{\chi_2}][d^{\top\rho}_{\chi_3}Cd^\sigma_{\chi_3}](T_s)_{\alpha\beta\gamma\delta\rho\sigma}, \tag{6.23}$$

where I denotes the first block. Following the same argument, we find the effective operators associated with the second and third blocks respectively,

$$(\mathcal{O}_1^\mu)^{II}_{\chi_1\chi_2\chi_3} = \frac{2e}{3}\frac{m_d}{p^2-m_d^2}[u^{\top\alpha}_{\chi_1}Cu^\beta_{\chi_1}][d^{\top\gamma}_{-\chi_2}C\gamma^\mu d^\delta_{\chi_2}][d^{\top\rho}_{\chi_3}Cd^\sigma_{\chi_3}](T_s)_{\alpha\beta\gamma\delta\rho\sigma}, \tag{6.24}$$

$$(\mathcal{O}_1^\mu)^{III}_{\chi_1\chi_2\chi_3} = \frac{2e}{3}\frac{m_d}{p^2-m_d^2}[u^{\top\alpha}_{\chi_1}Cu^\beta_{\chi_1}][d^{\top\gamma}_{\chi_2}Cd^\delta_{\chi_2}][d^{\top\rho}_{-\chi_3}C\gamma^\mu d^\sigma_{\chi_3}](T_s)_{\alpha\beta\gamma\delta\rho\sigma}. \tag{6.25}$$

Combining Eqs. 6.23, 6.24, and 6.25 gives the effective operator generated from $\mathcal{O}_1$

$$\begin{aligned}(\tilde{\mathcal{O}}_1)^{\mu}_{\chi_1\chi_2\chi_3} &= \Big[\frac{-4e}{3}\frac{m_u}{p^2-m_u^2}[u^{\top\alpha}_{-\chi_1}C\gamma^{\mu}u^{\beta}_{\chi_1}][d^{\top\gamma}_{\chi_2}Cd^{\delta}_{\chi_2}][d^{\top\rho}_{\chi_3}Cd^{\sigma}_{\chi_3}] \\ &+ \frac{2e}{3}\frac{m_d}{p^2-m_d^2}[u^{\top\alpha}_{\chi_1}Cu^{\beta}_{\chi_1}][d^{\top\gamma}_{-\chi_2}C\gamma^{\mu}d^{\delta}_{\chi_2}][d^{\top\rho}_{\chi_3}Cd^{\sigma}_{\chi_3}] \\ &+ \frac{2e}{3}\frac{m_d}{p^2-m_d^2}[u^{\top\alpha}_{\chi_1}Cu^{\beta}_{\chi_1}][d^{\top\gamma}_{\chi_2}Cd^{\delta}_{\chi_2}][d^{\top\rho}_{-\chi_3}C\gamma^{\mu}d^{\sigma}_{\chi_3}]\Big](T_s)_{\alpha\beta\gamma\delta\rho\sigma}. \quad (6.26)\end{aligned}$$

Putting back the current term gives the effective $n-\bar{n}$ conversion operator

$$(\tilde{\mathcal{O}}_1)_{\chi_1\chi_2\chi_3} = \frac{j_{\mu}}{q^2}(\lambda_1)_{\chi_1\chi_2\chi_3}(\tilde{\mathcal{O}}_1)^{\mu}_{\chi_1\chi_2\chi_3}, \quad (6.27)$$

where we have also put back the coupling coefficient λ with explicit labels to indicate its relevant dependence, e.g., λ_1 denotes that it is associated with operator $\mathcal{O}_1$. The other two $n-\bar{n}$ conversion operators generated from $\mathcal{O}_2$ and $\mathcal{O}_3$ respectively can also be constructed by following the same procedure.

In particular, we note that although the block structure of $(\mathcal{O}_2)_{\chi_1\chi_2\chi_3}$ is quite different from $(\mathcal{O}_1)_{\chi_1\chi_2\chi_3}$, writing down the effective operators associated with each block is straightforward. We only list the final results below.

$$\begin{aligned}(\mathcal{O}^{\mu}_2)^{I}_{\chi_1\chi_2\chi_3} &= \Big[\frac{-2e}{3}u^{\top\alpha}_{-\chi_1}C\gamma^{\mu}\frac{m_u}{p^2-m_u^2}d^{\beta}_{\chi_1} + \frac{e}{3}u^{\top\alpha}_{-\chi_1}C\gamma^{\mu}\frac{m_d}{p^2-m_d^2}d^{\beta}_{\chi_1}\Big] \\ &\times[u^{\top\gamma}_{\chi_2}Cd^{\delta}_{\chi_2}][d^{\top\rho}_{\chi_3}Cd^{\sigma}_{\chi_3}](T_s)_{\alpha\beta\gamma\delta\rho\sigma}, \quad (6.28) \\ (\mathcal{O}^{\mu}_2)^{II}_{\chi_1\chi_2\chi_3} &= [u^{\top\alpha}_{\chi_1}Cd^{\beta}_{\chi_1}]\Big[\frac{-2e}{3}u^{\top\gamma}_{-\chi_2}C\gamma^{\mu}\frac{m_u}{p^2-m_u^2}d^{\delta}_{\chi_2} + \frac{e}{3}u^{\top\gamma}_{-\chi_2}C\gamma^{\mu}\frac{m_d}{p^2-m_d^2}d^{\delta}_{\chi_2}\Big] \\ &\times[d^{\top\rho}_{\chi_3}Cd^{\sigma}_{\chi_3}](T_s)_{\alpha\beta\gamma\delta\rho\sigma}, \quad (6.29) \\ (\mathcal{O}^{\mu}_2)^{III}_{\chi_1\chi_2\chi_3} &= [u^{\top\alpha}_{\chi_1}Cd^{\beta}_{\chi_1}][u^{\top\gamma}_{\chi_2}Cd^{\delta}_{\chi_2}]\Big[\frac{2e}{3}\frac{m_d}{p^2-m_d^2}d^{\top\rho}_{-\chi_3}C\gamma^{\mu}d^{\sigma}_{\chi_3}\Big](T_s)_{\alpha\beta\gamma\delta\rho\sigma}. \quad (6.30)\end{aligned}$$

Since $(\mathcal{O}_3)_{\chi_1\chi_2\chi_3}$ has the same block structure as $(\mathcal{O}_2)_{\chi_1\chi_2\chi_3}$, we can obtain its effective operators easily by replacing $(T_s)_{\alpha\beta\gamma\delta\rho\sigma}$ by $(T_a)_{\alpha\beta\gamma\delta\rho\sigma}$.

6.3 Matrix elements of $n\bar{n}$ conversion operators in the MIT bag model

We have showed in Chap. 5 that the overall scale of the matrix elements of $n\bar{n}$ oscillation operators in the MIT bag model and LQCD is different, but it is encouraging that the pattern is similar. Therefore, it is reasonable to continue using the bag model to evaluate the six-fermion $n\bar{n}$ conversion operators. We consider the matrix element, e.g., $\langle\bar{n}\uparrow|(\mathcal{O}^{\mu}_i)^{j}_{\chi_1\chi_2\chi_3}|n\uparrow\rangle$, where $i=1,2,3$, $j=I,II,III$, and μ is the Lorentz index and χ is the chirality index. Note that in general, only the sum of the contributions

from all three blocks, j, gives an operator that will be compatible with the Ward-Takahashi identity of QED. The normalized spin-up neutron and antineutron wave functions have been shown in Eqs. (5.39, 5.40).

To make the final results as simple as possible, just as we have done in the oscillation case, we also make some useful definitions. The general structure of the matrix elements of six-fermion conversion operators are defined as

$$\begin{aligned}\langle(\tilde{\mathcal{O}}_i)\rangle^{\mu}_{\chi_1\chi_2\chi_3} &= \sum_j \langle \mathcal{O}_i^{\mu}\rangle^j_{\chi_1\chi_2\chi_3} = \sum_j \langle \bar{n}\uparrow | \int d^3\mathbf{r} (\mathcal{O}_i^{\mu})^j_{\chi_1\chi_2\chi_3} | n\uparrow\rangle \\ &= \sum_j \frac{eN^6 p^{-3}}{(4\pi)^2} \frac{m_{u/d}}{p^2 - m^2_{u/d}} (I_i^{\mu})^j_{\chi_1\chi_2\chi_3}, \end{aligned} \tag{6.31}$$

where $(I_i^{\mu})^j_{\chi_1\chi_2\chi_3}$ are dimensionless integrals and $(\mathcal{O}_i^{\mu})^j_{\chi_1\chi_2\chi_3}$ is the conversion operator obtained above. Once we put the associated coefficient λ back, then the operator, e.g., $(\mathcal{O}_1^{\mu})^I_{\chi_1\chi_2\chi_3}$, takes the form

$$\begin{aligned}& (\mathcal{O}_1^{\mu})^I_{\chi_1\chi_2\chi_3} \\ =\ & (\lambda_1)_{\chi_1\chi_2\chi_3} \frac{-4e}{3} \frac{m_u}{p^2 - m_u^2} [u^{\top\alpha}_{-\chi_1} C\gamma^{\mu} u^{\beta}_{\chi_1}][d^{\top\gamma}_{\chi_2} C d^{\delta}_{\chi_2}][d^{\top\rho}_{\chi_3} C d^{\sigma}_{\chi_3}](T_s)_{\alpha\beta\gamma\delta\rho\sigma}. \end{aligned} \tag{6.32}$$

To simplify the final expression for $(I_i^{\mu})^j_{\chi_1\chi_2\chi_3}$, we also define $\tilde{j}_1(x) \equiv \epsilon j_1(x)$ and six integrals

$$I_a = \int_0^{\xi} x^2 [j_0^2(x) - \tilde{j}_1^2(x)]^2 \Big(j_0^2(x) - \frac{1}{3}\tilde{j}_1^2(x)\Big) dx, \tag{6.33}$$

$$I_b = \int_0^{\xi} x^2 [j_0^2(x) - \tilde{j}_1^2(x)] j_0^2(x) \tilde{j}_1^2(x) dx, \tag{6.34}$$

$$I_c = \int_0^{\xi} x^2 j_0^2(x) \tilde{j}_1^4(x) dx, \tag{6.35}$$

$$I_d = \int_0^{\xi} x^2 [j_0^2(x) + \tilde{j}_1^2(x)][j_0^2(x) - \tilde{j}_1^2(x)] \Big(j_0^2(x) + \frac{1}{3}\tilde{j}_1^2(x)\Big) dx, \tag{6.36}$$

$$I_e = \int_0^{\xi} x^2 [j_0^2(x) + \tilde{j}_1^2(x)] j_0^2(x) \tilde{j}_1^2(x) dx, \tag{6.37}$$

$$I_f = \int_0^{\xi} x^2 [j_0^2(x) + \tilde{j}_1^2(x)]^2 \Big(j_0^2(x) - \frac{1}{3}\tilde{j}_1^2(x)\Big) dx. \tag{6.38}$$

For simplicity, we evaluate the matrix elements in the case of that the initial neutron and final antineutron have the same spin. A spin-flip process can also occur. However, recall that in the spin-flip case, the matrix element of the neutron level $n-\bar{n}$ conversion operator is $\omega_x - i\omega_y$. Comparing it with the matrix element ω_z in the non-spin-flip case, we expect the calculations will be twice involved. Moreover, noting the same

structure of $n-\bar{n}$ conversion operators in neutron level and quark level, we can expect that final result in the spin-flip case will be just the same as in the non-spin-flip case. Later we confirm it through explicit computations.

In the non-spin-flip case, only the z component of these operators have non-zero matrix elements, i.e. $\mu = 3$. Therefore, we have

$$(I_1^3)^I_{\chi_1\chi_2\chi_3} = -8i\Big[I_a - \frac{4}{3}\eta_2\eta_3 I_b - 8\eta_2\eta_3 I_c\Big], \tag{6.39}$$

$$(I_1^3)^{II}_{\chi_1\chi_2\chi_3} = -8i\Big[-2I_a - \frac{28}{3}\eta_1\eta_3 I_b - 8\eta_1\eta_3 I_c\Big], \tag{6.40}$$

$$(I_1^3)^{III}_{\chi_1\chi_2\chi_3} = -8i\Big[-2I_a - \frac{28}{3}\eta_1\eta_2 I_b - 8\eta_1\eta_2 I_c\Big], \tag{6.41}$$

for the first effective operator and for the second one

$$(I_2^3)^I_{\chi_1\chi_2\chi_3} = -4i\Big[-\frac{1}{2}I_a + \frac{2}{3}\eta_2\eta_3 I_b + 4(\eta_1\eta_3 + \eta_1\eta_2)I_b + 4\eta_2\eta_3 I_c\Big], \tag{6.42}$$

$$(I_2^3)^{II}_{\chi_1\chi_2\chi_3} = -4i\Big[-\frac{1}{2}I_a + \frac{2}{3}\eta_1\eta_3 I_b + 4(\eta_2\eta_3 - \eta_1\eta_2)I_b + 4\eta_1\eta_3 I_c\Big], \tag{6.43}$$

$$(I_2^3)^{III}_{\chi_1\chi_2\chi_3} = -4i\Big[\frac{5}{2}I_a + \frac{26}{3}\eta_1\eta_2 I_b + 4(\eta_2\eta_3 - \eta_1\eta_3)I_b + 4\eta_1\eta_2 I_c\Big], \tag{6.44}$$

where $\eta_i = 1(-1)$ for $\chi_i = R(L)$. Because of the antisymmetic tensor $(T_a)_{\alpha\beta\gamma\delta\rho\sigma}$ that appears in the third operator, its matrix elements are different from the other two,

$$\begin{aligned}(I_3^3)^I_{\chi_1\chi_2\chi_3} = {} & \frac{4}{3}i\Big[-\frac{1}{2}I_a + \frac{2}{3}\eta_2\eta_3 I_b + 4(\eta_1\eta_3 + \eta_1\eta_2)I_b + 4\eta_2\eta_3 I_c\Big] \\ & -4i\Big[-\eta_1\eta_2 I_d + 4\eta_2\eta_3 I_e\Big],\end{aligned} \tag{6.45}$$

$$\begin{aligned}(I_3^3)^{II}_{\chi_1\chi_2\chi_3} = {} & \frac{4}{3}i\Big[-\frac{1}{2}I_a + \frac{2}{3}\eta_1\eta_3 I_b + 4(\eta_2\eta_3 - \eta_1\eta_2)I_b + 4\eta_1\eta_3 I_c\Big] \\ & -4i\Big[-\eta_1\eta_2 I_d + 4\eta_1\eta_3 I_e\Big],\end{aligned} \tag{6.46}$$

$$\begin{aligned}(I_3^3)^{III}_{\chi_1\chi_2\chi_3} = {} & \frac{4}{3}i\Big[\frac{5}{2}I_a + \frac{26}{3}\eta_1\eta_2 I_b + 4(\eta_2\eta_3 - \eta_1\eta_3)I_b + 4\eta_1\eta_2 I_c\Big] \\ & -4i(3\eta_1\eta_2 I_f).\end{aligned} \tag{6.47}$$

Let us factor out another factor $i/3$ out of $(I_i^3)^j_{\chi_1\chi_2\chi_3}$, so that Eq. 6.31 can be rewritten as

$$\langle(\tilde{\mathcal{O}}_i)\rangle^\mu_{\chi_1\chi_2\chi_3} = \sum_j \frac{N^6 p^{-3}}{(4\pi)^2}\frac{ie}{3}\frac{m_{u/d}}{p^2 - m_{u/d}^2}(\tilde{I}_i^\mu)^j_{\chi_1\chi_2\chi_3}. \tag{6.48}$$

Recall the two fits [109] mentioned in Chap. 4: (A) $m_u = m_d = 0$, $R_n = 5.00\,\mathrm{GeV}^{-1}$; and (B) $m_u = m_d = 0.108\,\mathrm{GeV}$, $R_n = 5.59\,\mathrm{GeV}^{-1}$. Unsurprisingly, the matrix elements vanish for fit (A). The resulting values of the six integrals in

Table 6.1: Values of the I integrals in fit (B) [109, 38].

I_a	I_b	I_c	I_d	I_e	I_f
0.302	0.032	0.008	0.395	0.047	0.447

Table 6.2: Dimensionless matrix elements of $n - \bar{n}$ conversion operators.

Matrix element	Block I	Block II	Block III
$(\tilde{I}_1^3)_{RRR}$	-1.581	7.719	7.719
$(\tilde{I}_1^3)_{LLR}$	-3.243	1.930	7.719
$(\tilde{I}_1^3)_{RLL}$	-1.581	1.930	1.930
$(\tilde{I}_2^3)_{RRR}$	-0.637	0.395	-4.255
$(\tilde{I}_2^3)_{LLR}$	0.811	1.843	-4.255
$(\tilde{I}_2^3)_{RLL}$	1.427	-0.221	-2.807
$(\tilde{I}_3^3)_{RRR}$	1.032	0.688	-5.960
$(\tilde{I}_3^3)_{LRR}$	-2.814	-0.746	4.294
$(\tilde{I}_3^3)_{LLR}$	2.068	1.724	-5.960

Table 6.3: Matrix element of $\langle(\tilde{\mathcal{O}}_i)\rangle_\chi^3$ without a common factor.

$\langle(\tilde{\mathcal{O}}_1)\rangle_{RRR}^3$	$\langle(\tilde{\mathcal{O}}_1)\rangle_{LLR}^3$	$\langle(\tilde{\mathcal{O}}_1)\rangle_{RLL}^3$
37.2	32.27	14.04
$\langle(\tilde{\mathcal{O}}_2)\rangle_{RRR}^3$	$\langle(\tilde{\mathcal{O}}_2)\rangle_{LLR}^3$	$\langle(\tilde{\mathcal{O}}_2)\rangle_{RLL}^3$
-5.17	-8.07	-11.76
$\langle(\tilde{\mathcal{O}}_3)\rangle_{RRR}^3$	$\langle(\tilde{\mathcal{O}}_3)\rangle_{LRR}^3$	$\langle(\tilde{\mathcal{O}}_3)\rangle_{LLR}^3$
-14.67	18.35	-16.74

fit (B) are listed in Table 6.1, and the dimensionless matrix elements of the $n - \bar{n}$ conversion operators are given in Table 6.2. After factoring out the common factor, $[iemN^6p^{-3}]/[48\pi^2(p^2 - m^2)]$, we compute the $\langle(\tilde{\mathcal{O}}_i)\rangle_{\chi_1\chi_2\chi_3}^\mu$ with $i = 1, 2, 3$. The final results are listed in Table 6.3.

6.4 $n - \bar{n}$ conversion coupling parameter

To determine the coupling coefficient η, we have one last but not least ingredient to discuss: how the observable is related to these matrix elements. We focus on $n - \bar{n}$ oscillation first. The observable of an $n-\bar{n}$ oscillation experiment is the $n\bar{n}$ oscillation time $\tau_{n\bar{n}}$ that comes from three inputs [102]

$$\frac{1}{\tau_{n\bar{n}}} = \delta = C_{\rm BSM} C_{\rm QCD} \langle \bar{n}|\mathcal{O}|n\rangle, \tag{6.49}$$

where $C_{\rm BSM}$ is the running of the BSM theory to the weak interaction scale, $C_{\rm QCD}$ is the QCD running from weak to the nuclear scale, and $\langle \bar{n}|\mathcal{O}|n\rangle$ is the matrix element of the six-fermion $n\bar{n}$ oscillation operators. The coefficient $C_{\rm QCD}$ can be calculated because it is known at one-loop level in perturbative QCD [115, 116], and $C_{\rm BSM}$ has also been calculated in different models [117, 118, 49].

In Chap. 5, we have computed the matrix elements of $n\bar{n}$ oscillation operators and also found that oscillation operators with different labels, such as chiral indices χ_1, χ_2, χ_3, or with different tensor structure, T_a or T_s, contribute to the $n\bar{n}$ matrix elements differently. Technically, all these six-fermion $n\bar{n}$ oscillation operators contribute to the observable. However, in what follows, for simplicity, we focus on just the biggest one, i.e., $(\mathcal{O}_1)_{RRR}$. Therefore, we have

$$C_{BSM} C_{QCD} (\lambda_1)_{RRR} \frac{i N^6 p^{-3}}{(4\pi)^2} \langle \mathcal{O}_1 \rangle_{RRR} \approx \delta, \tag{6.50}$$

where λ^1_{RRR} is the coupling coefficient associated with $(\mathcal{O}_1)_{RRR}$. Similarly for $n\bar{n}$ conversion, since $\langle \mathcal{O}_1^z \rangle_{RRR}$ in Table 6.3 is also the biggest one, we obtain the relation

$$\begin{aligned} 2\eta j^z &= C'_{BSM} C'_{QCD} \langle \bar{n}|\tilde{\mathcal{O}}|n\rangle \\ &\approx \frac{j^z}{q^2} C'_{BSM} C'_{QCD} (\lambda_1)_{RRR} \frac{i N^6 p^{-3}}{(4\pi)^2} \frac{e}{3} \frac{m}{p^2 - m^2} \langle (\tilde{\mathcal{O}}_1^z) \rangle_{RRR}, \end{aligned} \tag{6.51}$$

where $\tilde{\mathcal{O}}$ denotes the six-fermion $n - \bar{n}$ conversion operator, while the left side of this equation is the matrix element of the neutron-level $n - \bar{n}$ conversion operators in the non-spin-flip case. Note that this relation would have a more complicated form, if we did not assume q^2 was small. Generally $C'_{\rm BSM}$ and $C'_{\rm QCD}$ will be different from $C_{\rm BSM}$ and $C_{\rm QCD}$, due to the electromagnetic interaction in the $n - \bar{n}$ conversion operators. However, since the ratios, $C'_{\rm BSM}/C_{\rm BSM}$ and $C'_{\rm QCD}/C_{\rm QCD}$, should be one up to very small electromagnetic corrections, we set them to unity in our calculations. Then the $n - \bar{n}$ conversion coupling coefficient can be determined as

$$\eta = \delta \frac{e}{6q^2} \frac{m}{p^2 - m^2} \frac{\langle (\tilde{\mathcal{O}}_1) \rangle^z_{RRR}}{\langle \mathcal{O}_1 \rangle_{RRR}}. \tag{6.52}$$

Note that compared with δ, η is definitely not suppressed by Λ_{NP}^3 as one might naively expect. Let us check the parameters in Eq. 6.52. The parameters m and p are fixed by fitting the masses and other parameters of the light hadron in the MIT bag model [109]. Using the fit (B), we compute $[m\langle(\tilde{\mathcal{O}}_1)\rangle^z_{RRR}]/[(p^2-m^2)\langle\mathcal{O}_1\rangle_{RRR}]$, and find that it is close to 1 GeV^{-1}. The electric charge unit e is a dimensionless constant and is about 1/3. The parameter δ is not a fundamental Lagrangian parameter, but rather the effective $n-\bar{n}$ oscillation matrix element. Therefore, η depends on q^2 in a sensitive way. By considering forward scattering, a small q^2 can be obtained, so that η can be greatly enhanced and consequently a strong limit on δ can also be set through Eq. 6.52, though it does not have to hold if η is generated in a completely independent way.

CHAPTER 7

APPLICATIONS OF $n - \bar{n}$ CONVERSION

7.1 $n - \bar{n}$ conversion cross section at low energies, mediated by electromagnetically charged particle scattering

At the neutron energy scale, the effective Lagrangian of $n - \bar{n}$ conversion through an electromagnetic current is given by

$$\mathcal{L} = i\bar{n}\partial\!\!\!/ n - m_n \bar{n} n - \eta'(n^T C n + h.c.) - \eta(n^T C\gamma^\mu\gamma^5 n\bar{\psi}\gamma_\mu\psi + h.c.), \tag{7.1}$$

where n denotes the neutron field with mass m_n, ψ represents another spin 1/2 charged particle with charge Q, and η is given in Eq. 6.52.

We now turn to the computation of the unpolarized cross section for $n+Q \to \bar{n}+Q$ to lowest order in η. The particles' momenta and spin assignments are shown in Fig. 7.1. The amplitude for this process is given by

$$\begin{aligned} i\mathcal{M} &= \eta\bar{u}_Q^{s'}(p'_Q)(\gamma^\mu)u_Q^s(p_Q)u_n^{Tr'}(p'_n)C\gamma_\mu\gamma^5 u_n^r(p_n) \\ &= \eta\bar{u}_Q^{s'}(p'_Q)(\gamma^\mu)u_Q^s(p_Q)\bar{v}_n^{r'}(p'_n)\gamma_\mu\gamma^5 u_n^r(p_n), \end{aligned} \tag{7.2}$$

where u and v are Dirac spinors and we have used the relation $u^T C = \bar{v}$. Then the

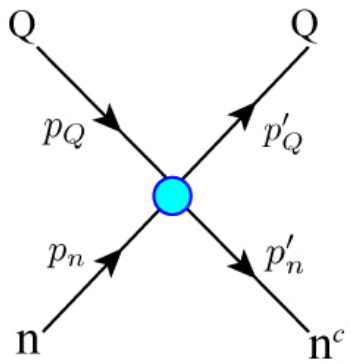

Figure 7.1: Feynman diagram for $n + Q \to \bar{n} + Q$ process at low energies. Here "Q" denotes a spin 1/2 particle with electric charge Q.

spin-averaged $\overline{|\mathcal{M}|^2}$ becomes

$$\begin{aligned}
\overline{|\mathcal{M}|^2} &= \frac{1}{4}\sum_{s,s',r,r'}|i\mathcal{M}|^2 \\
&= \frac{1}{4}\eta^2\,\mathrm{Tr}[(\not{p}'_Q+m_Q)\gamma^\mu(\not{p}_Q+m_Q)\gamma^\nu]\,\mathrm{Tr}[(\not{p}'_n-m_n)\gamma_\mu\gamma^5(\not{p}_n+m_n)\gamma_\nu\gamma^5] \\
&= \frac{8Q^2e^4|\beta|^2\delta^2}{q^4}\Big[(p'_Q\cdot p'_n)(p_Q\cdot p_n)+(p'_n\cdot p_Q)(p'_Q\cdot p_n) \\
&\qquad +2m_Q^2m_n^2-m_n^2(p'_Q\cdot p_Q)-m_Q^2(p'_n\cdot p_n)\Big], \qquad (7.3)
\end{aligned}$$

where

$$\beta=\frac{m}{p^2-m^2}\frac{(\langle\tilde{\mathcal{O}}_1\rangle)^z_{RRR}}{\langle\mathcal{O}_1\rangle_{RRR}}. \qquad (7.4)$$

The differential cross section is given by

$$d\sigma=\frac{1}{4E_QE_n|v_Q-v_n|}\frac{d^3p'_Q}{(2\pi)^3}\frac{1}{2E'_Q}\frac{d^3p'_n}{(2\pi)^3}\frac{1}{2E'_n}\overline{|\mathcal{M}|^2}(2\pi)^4\delta^4(p_Q+p_n-p'_Q-p'_n), \qquad (7.5)$$

where $|v_Q-v_n|$ is the relative velocity of the beams as viewed from the laboratory frame. To determine $d\sigma$ in terms of basic kinematic variables, such as energies and angles, we must pick a frame. However, the total cross section is a Lorentz scalar and thus frame independent. In this thesis, we choose the fixed-target frame, which is the laboratory frame. In this frame, two processes are possible. The first one is charged particle scattering with a neutron target, and the other one is neutron beam scattering with a charged particle target.

Let us consider the second possibility, in which a neutron (n) scattering with a charged particle Q becomes an antineutron, $n+Q\to\bar{n}+Q$, first. The initial and final 4-momenta can be written as follows:

$$\begin{aligned}
p_n&=(E_n,\mathbf{p}_n); \quad p'_n=(E'_n,\mathbf{p}'_n); \\
p_Q&=(m_Q,0); \quad p'_Q=(E'_Q,\mathbf{p}'_Q). \qquad (7.6)
\end{aligned}$$

Now the Lorentz invariant quantities in Eq. 7.3 can be written as

$$\begin{aligned}
q^2=(p'_n-p_n)^2 &= 2m_n^2-2E_nE'_n+2|\mathbf{p_n}||\mathbf{p}'_n|\cos\theta, \qquad (7.7)\\
(p_n\cdot p'_n) &= E_nE'_n-|\mathbf{p_n}||\mathbf{p}'_n|\cos\theta, \qquad (7.8)\\
(p_Q\cdot p'_Q) &= m_Q^2-m_n^2+E_nE'_n-|\mathbf{p_n}||\mathbf{p}'_n|\cos\theta, \qquad (7.9)\\
(p_Q\cdot p'_n)(p_n\cdot p'_Q) &= m_Q^2E'^2_n, \qquad (7.10)\\
(p'_Q\cdot p'_n)(p_Q\cdot p_n) &= m_Q^2E_n^2, \qquad (7.11)
\end{aligned}$$

where θ is the scattering angle in the laboratory frame.

In deriving Eq. 6.52 in last chapter, we assumed that the energies of initial neutron and final antineutron are comparable. This can occur in the target-rest frame, with physical scattering, if we work in the limit of $m_n \ll m_Q$ — just like a ping-pong ball bouncing against a steel ball. The bounced ping-pong ball can have the same energy but moves in a different direction and leaves the steel ball roughly at rest. Therefore, we have $E_n \approx E'_n$ and $|\mathbf{p}'_n| \approx |\mathbf{p}_n|$, and the Lorentz-invariant quantities of interest can be simplified to

$$\begin{aligned} q^2 &= -4|\mathbf{p_n}|^2 \sin^2\left(\frac{\theta}{2}\right), && (7.12)\\ (p_n \cdot p'_n) &= E_n^2 - |\mathbf{p_n}|^2 \cos\theta, && (7.13)\\ (p_Q \cdot p'_Q) &= 2|\mathbf{p_n}|^2 \sin^2\left(\frac{\theta}{2}\right) + m_Q^2; && (7.14)\\ (p_Q \cdot p'_n)(p_n \cdot p'_Q) &= (p'_Q \cdot p'_n)(p_Q \cdot p_n) = m_Q^2 E_n^2. && (7.15) \end{aligned}$$

The total cross section then is given by

$$\sigma = \frac{Q^2 2\pi\alpha^2 |\beta|^2 \delta^2}{8|\mathbf{p_n}|^4} \int_{\theta_0} d\theta \sin\theta \frac{2m_n^2 + |\mathbf{p_n}|^2(1+\cos\theta) - \frac{2m_n^2}{m_Q^2}|\mathbf{p_n}|^2 \sin^2(\theta/2)}{\sin^4(\theta/2)}. \quad (7.16)$$

Note that this cross section is divergent at $\theta = 0$. This singularity also occurs in case of scattering by purely Coulombic interactions. The standard procedure is to introduce some phenomenological parameter θ_0 for cutting off the cross section with angles $\theta < \theta_0$. This parameter can be determined by considering the experimental set up.

Note that in the case $m_Q \ll m_n$ the above arguments also apply to the first possible process, in which a charged particle Q scatters with a neutron (n) target and the neutron becomes an antineutron, $Q + n \to Q + \bar{n}$. Its cross section can be obtained simply by exchanging $\mathbf{p}_n \leftrightarrow \mathbf{p}_Q$ and $m_n \leftrightarrow m_Q$.

7.2 Some experimental proposals

The event rate for a fixed-target experiment is given by [119]

$$\frac{dR}{dt} = \mathcal{L}\sigma = \phi \rho_T L \sigma, \quad (7.17)$$

where $\mathcal{L}$ denotes luminosity with units $\mathrm{cm}^{-2}\mathrm{s}^{-1}$, R is the number of events, ϕ is the flux of incoming particles, i.e., the number of particles per second [1], ρ_T is the number

[1] We define the flux density as the number of particles per second and per area, whereas the flux is the number of particles per second. We note that different usages appear in the literature.

density of target, L is the length of target, and finally σ is the total cross section. Therefore, to maximize R, high flux of incoming particles and high density of target are essential.

Note that cross section is proportional to the squared charge Q^2, naively one would pick heavy nuclei as probes to flip the spin projection of quarks in neutrons, since it contains many protons. However, if the neutrons are of sufficiently low energy, they would see the heavy atoms as electrically neutral, so that we set this aside as a possibility for now.

For the first possible process, possible "Q" beam we are considering is either a proton or an electron beam. Electron beams with high flux have been constructed for the DarkLight experiment at Jlab [120]. The goal of this experiment is to search for the dark matter in 10-100 MeV range, so the energy of electron will be around 100 MeV. It may be possible to arrange a beam of the same flux with lower energy. Therefore, when we perform a numerical estimation of the $Q + n \to Q + \bar{n}$ process in a later section, this beam will be our primary choice. However, high-flux proton beams at lower energies certainly work too. Since free neutron targets do not exist, the possible effective neutron target we would like to consider is liquid deuterium, because at certain temperatures, its density can be promisingly large.

In case of second possible process , one can use a free neutron beam. For example, a free neutron beam of low energy (2×10^{-4}eV) and very high flux was used in a $n-\bar{n}$ oscillation search at the ILL [39]. The possible "Q" targets we want to consider are an electron plasma and liquid deuterium. Electrons can be confined into a plasma by a magnetic field. Although there exists a limiting density called the Brillouin density [121], $n_B = \epsilon_0 B^2/2m_e$, in a high magnetic field B, an electron plasma with high density is still possible. In the second case, we pick liquid deuterium, not only because of its possible high particle density, but also because of its low neutron absorption rate. To maximize the chance of observing $n - \bar{n}$ conversion, the loss of neutrons in the process must be minimized.

A little bit of summary seems necessary now. In this section, we have proposed different ways of realizing $n-\bar{n}$ conversion. The first one is an electron beam scattering from a liquid deuterium target; the second one is a neutron beam scattering from electron plasma confined by a large magnetic field; and the final one is neutron beam scattering from a liquid deuterium target. We will explicitly estimate each case and set limits on the $n - \bar{n}$ oscillation parameter δ.

7.3 $n-\bar{n}$ conversion limits on δ

(1) $\mathbf{n+e\to\bar{n}+e}$ **case:**

The total cross section is

$$\sigma=\frac{2\pi\alpha^2|\beta|^2\delta^2}{8|\mathbf{p_n}|^4}\int_{\theta_0}d\theta\sin\theta\frac{2m_n^2+|\mathbf{p_n}|^2(1+\cos\theta)-\frac{2m_n^2}{m_e^2}|\mathbf{p_n}|^2\sin^2(\theta/2)}{\sin^4(\theta/2)}, \quad (7.18)$$

with

$$\beta \equiv \frac{1}{6}\frac{m}{p^2-m^2}\frac{(\langle\tilde{\mathcal{O}}_1\rangle)^z_{RRR}}{\langle\mathcal{O}_1\rangle_{RRR}}. \quad (7.19)$$

Using the results obtained in the last chapter, we compute $\beta\simeq 0.92$ GeV^{-1}. We also use the mass of an electron $m_e=5.10\times10^{-4}$ GeV, and, for simplicity, set the masses of a neutron and a proton equal, $m_n=m_p=0.939$ GeV. The angular integration in Eq. 7.18 is divergent at $\theta=0$. Therefore, we will apply a cutoff angle θ_0, which is based on a setup for a T violation search in neutron transmission experiment [122]. The concept for this experiment is different. However, there they want to detect forward scattering with angles no larger than an angle of $\theta_0\approx0.003$ in radians. Therefore it seems that we can also use this angle as an estimate of the smallest possible experimental scattering angle. The angular integral in Eq. (7.18) for forward scattering process is about 1.7×10^6 and that does not vary very much for $|\mathbf{p_n}|\in(10\text{ eV}, 10\text{ MeV})$, since the small denominator dominates the total integration. For the same reason, the cross section for $n+d\to\bar{n}+d$ is also close to that of $n+e\to\bar{n}+e$ process. We want to use parameters as achieved by or anticipated in a particular experiment in our numerical estimates. Due to their high luminosity, the neutron beam we consider is from the ILL [39], and the relevant parameters are listed below:

$$\phi \simeq 1.7\times10^{11}\text{ ns}^{-1}=1.7\times10^{20}\text{ s}^{-1}, \quad (7.20)$$

$$E_n \simeq 2\times10^{-3}\text{ eV}\Rightarrow v_n\simeq600\text{ m/s}, \quad |\mathbf{p_n}|\simeq2\text{ keV}. \quad (7.21)$$

For a neutron beam of such energy, the cross section is found to be

$$\sigma_{n+e}\simeq1.7\times10^{21}\Big(\frac{\delta}{1\text{ GeV}}\Big)^2\Big(\frac{2\text{ keV}}{|\mathbf{p}_n|}\Big)^4\text{ b}. \quad (7.22)$$

The Brillouin density [121] of electron plasma confined by a magnetic field B is given by $n_B=\epsilon_0B^2/2m_e$, where ϵ_0 is the vacuum permittivity. Then for a 10 T magnetic

field, $n_B = 0.5 \times 10^{15}$ cm^{-3}. If such a neutron beam scatters with a one meter long electron plasma target for one year, and no signal is found, we can set a limit on δ:

$$\delta < 1.6 \times 10^{-21} \Big(\frac{|\mathbf{p_n}|}{2 \text{ keV}}\Big)^2 \sqrt{\frac{1 \text{ yr}}{\text{t}}} \sqrt{\frac{1.7 \times 10^{11} \text{ ns}^{-1}}{\phi}} \sqrt{\frac{1 \text{ m}}{L}} \frac{10 \text{ T}}{B} \text{ GeV}, \tag{7.23}$$

or equally $\tau_{n\bar{n}} > 4 \times 10^{-4}$s. Compared with the current limit $\delta < 2.46 \times 10^{-33}$ GeV from SuperK [40], this setup does not seem promising. Note that if we can manage to keep the same neutron flux as at the ILL but with much lower momentum $|\mathbf{p_n}| \simeq 10$ eV from Ref. [122][2], σ will be 1.6×10^9 times bigger, and a better limit can be obtained, $\delta < 0.4 \times 10^{-25}$ GeV.

(2) $\mathbf{n + d \to \bar{n} + d}$ **case:**

The target we prefer is liquid deuterium, because the neutron capture rate is low and the neutron density can be high at very low temperatures. For example, at 19 K its density can be $\rho = 0.17$ g/cm^3 [123], which corresponds to $\rho = 5 \times 10^{22}$ cm^{-3}. As for the neutron capture rate, we note that the thermal neutron disappearing cross section in liquid deuterium is $\sigma_c \approx 0.5$ mb [124]. Its effect on neutron flux can be characterized by

$$\Delta N = \phi \rho \Delta T \Delta L \sigma_c, \tag{7.24}$$

where ΔN is the number of captured neutrons during time ΔT and in a ΔL long deuterium target with density ρ. Since $N = \phi \Delta T$, we have

$$\Delta N = N \rho \sigma_c \Delta L \,, \tag{7.25}$$

so that if N_0 is the initial number of neutrons, we compute the number of neutrons N remaining after traversing length L is

$$N = N_0 e^{-\sigma_c L \rho}, \tag{7.26}$$

and the corresponding flux is

$$\phi = \phi_0 e^{-\sigma_c L \rho}. \tag{7.27}$$

It turns out that for a one meter long target of such density, the thermal neutron capture effects have very limited impact on the flux ϕ, $\phi/\phi_0 \simeq 0.998$. We apply

[2]Note that given such a low kinetic energy, half of the neutrons will be repelled by the large magnetic field applied to the electron plasma.

the same parameters as for the neutron beams from ILL [39] and compute the cross section

$$\sigma_{n+d} \simeq 3.4\times 10^{21}\Big(\frac{\delta}{1\text{ GeV}}\Big)^2\Big(\frac{2\text{ keV}}{|\mathbf{p}_n|}\Big)^4\text{ b}, \tag{7.28}$$

which is twice that of σ_{n+e} because both the electron and proton are considered in the process. Then running the experiment for 1 year without observing a single event can set a limit on δ:

$$\begin{aligned}\delta \;<\; & 1.05\times 10^{-25}\Big(\frac{|\mathbf{p_n}|}{2\text{ keV}}\Big)^2\sqrt{\frac{1\text{ yr}}{\text{t}}}\sqrt{\frac{1.7\times 10^{11}\text{ ns}^{-1}}{\phi}}\\ & \times\sqrt{\frac{1\text{ m}}{L}}\sqrt{\frac{5\times 10^{22}\text{ cm}^{-3}}{\rho}}\text{GeV}.\end{aligned} \tag{7.29}$$

In the future if a slow neutron (10 eV) beam with flux comparable to that at the ILL can be generated, then it can set a more severe limit on δ, $\delta < 3.67\times 10^{-30}$ GeV.

(3) $\mathbf{e+n\to e+\bar{n}}$ **case:**

From the high flux point of view, we consider the electron beam used in the DarkLight experiment [120]. The luminosity of the electron beam scattering on H_2 gas of density $\rho = 10^{19}/\text{cm}^2$ is $\mathcal{L} = 2\times 10^{36}\text{ cm}^{-2}\text{s}^{-1}$. Then the flux of electron beams can be easily obtained

$$\phi = \frac{\mathcal{L}}{\rho} = 2\times 10^{17}s^{-1}. \tag{7.30}$$

Since DarkLight experiment aims to search for dark photon in the $10-100$ MeV range, the energy of the electrons is about 100 MeV. The angular cutoff θ_0 for electron comes from a quantum mechanical effect. To obtain a reasonable probability of scattering, the incident trajectory must be localized to within $\Delta x \sim r_a$. Here r_a is the Thomas-Fermi radius of atom

$$r_a = \frac{1}{\alpha m_e Z^{1/3}}, \tag{7.31}$$

where Z is the atomic number of target nucleus. Then, according to the uncertainty principle, the incident momentum is uncertain by an amount $\Delta p \sim 1/r_a$. Because of the Coulomb interaction, the incident particle receives a momentum Δp perpendicular to its original direction. It will therefore be deflected through a small angle [125]

$$\theta = \frac{\Delta p}{p}. \tag{7.32}$$

In this case, the scattering angle is $\theta_0 \sim 1/pr_a = \alpha Z^{1/3} m_e/p$, which for deuterium is $\theta_0 = 3\times 10^{-5}$. We find the total cross section is

$$\sigma_{e+d} \simeq 2.9\times 10^4 \Big(\frac{\delta}{1\text{ GeV}}\Big)^2 \Big(\frac{100\text{ MeV}}{|\mathbf{p}_n|}\Big)^4 \text{ b} \tag{7.33}$$

Compared with previous two cases, it is much smaller because of the high energy of electrons. Let us also choose a liquid deuterium target at 19 K as source of neutrons, then running the experiment for 1 year without observing one single event sets limits on δ:

$$\begin{aligned}\delta &< 0.345\times 10^{-7}\Big(\frac{|\mathbf{p_n}|}{100\text{ MeV}}\Big)^2 \sqrt{\frac{1\text{ yr}}{\text{t}}}\sqrt{\frac{2\times 10^{17}\text{ s}^{-1}}{\phi}} \\ &\times\sqrt{\frac{1\text{ m}}{L}}\sqrt{\frac{5\times 10^{22}\text{ cm}^{-3}}{\rho}}\text{GeV},\end{aligned} \tag{7.34}$$

which is the worst one among the three cases. This is not surprising, because although the flux of electron beams is big enough, the high energy of electron really dwarfs the total cross section.

7.4 $n-\bar{n}$ conversion limits on η

In previous sections, we have explicitly showed that $n-\bar{n}$ conversion can set limits on $n-\bar{n}$ oscillation time, due to the electromagnetic connection between these two processes. In this section, we want to set a limit on η directly by using $n-\bar{n}$ conversion.

Let us consider a general conversion process, in which a particle A scattering with another particle B results in an antiparticle of B. We denote it as $A+B\to A+\bar{B}$. The Feynman diagram for the process is the same as in Fig. 7.1 and its amplitude is given by Eq. 7.2 but with different labels. The spin-averaged $\overline{|\mathcal{M}|^2}$ takes the form of

$$\begin{aligned}\overline{|\mathcal{M}|^2} &= 8|\eta|^2[(p'_A\cdot p'_B)(p_A\cdot p_B)+(p'_A\cdot p_B)(p_A\cdot p'_B)-m_A^2(p_B\cdot p'_B) \\ &\quad -m_B^2(p_A\cdot p'_A)+2m_A^2m_B^2].\end{aligned} \tag{7.35}$$

Since the total cross section is Lorentz invariant, we can evaluate it in any frames. In this case, we chose the center-of-mass (CM) frame in which the computation is much easier. The differential cross section is given by

$$\begin{aligned}\Big(\frac{d\sigma}{d\Omega}\Big)_{cm} &= \frac{1}{4E_AE_B|v_A-v_B|}\frac{|\boldsymbol{p_A}|}{(2\pi)^2 4E_{cm}}\overline{|\mathcal{M}|^2}, \\ &= \frac{1}{64\pi^2E_{cm}^2}\overline{|\mathcal{M}|^2},\end{aligned} \tag{7.36}$$

by noting that

$$|v_A - v_B| = \left|\frac{\boldsymbol{p_A}}{E_A} - \frac{\boldsymbol{p_B}}{E_B}\right| = \boldsymbol{p_A}\left|\frac{1}{E_A} + \frac{1}{E_B}\right| = \frac{\boldsymbol{p_A} E_{cm}}{E_A E_B}, \tag{7.37}$$

where E_{cm} is the center-of-mass energy, $\boldsymbol{p_A}$ is the spacial momentum, and v is the velocity of the particles. In the CM frame, we have

$$\begin{aligned} p_A &= (E_A, \boldsymbol{p_A}), \quad p'_A = (E'_A, \boldsymbol{p'_A}), & (7.38)\\ p_B &= (E_B, -\boldsymbol{p_A}), \quad p'_B = (E'_B, -\boldsymbol{p'_A}), & (7.39) \end{aligned}$$

and

$$\begin{aligned} (p'_A \cdot p'_B) &= (p_A \cdot p_B) = \frac{1}{2}(E_{cm}^2 - m_A^2 - m_B^2), & (7.40)\\ (p'_A \cdot p_B) &= (p_A \cdot p'_B) = E'_A E_B + |\boldsymbol{p_A}||\boldsymbol{p'_A}|\cos\theta, & (7.41)\\ (p'_A \cdot p_A) &= E'_A E_A - |\boldsymbol{p_A}||\boldsymbol{p'_A}|\cos\theta, & (7.42)\\ (p'_B \cdot p_B) &= (p'_A \cdot p_A) + m_B^2 - m_A^2, & (7.43) \end{aligned}$$

where parameters with the label $'$ belong to the outgoing particles and θ is the scattering angle between $\boldsymbol{p'_A}$ and $\boldsymbol{p_A}$. We compute the total cross section

$$\begin{aligned} \sigma &= \frac{|\eta|^2}{4\pi E_{cm}^2}\Big[\frac{1}{2}(E_{cm}^2 - m_A^2 - m_B^2)^2 + 2m_A^4 + 2m_A^2 m_B^2 \\ &\quad -2E_A E'_A(m_A^2 + m_B^2) + 2E_A'^2 E_B^2 + \frac{2}{3}|\boldsymbol{p_A}|^2|\boldsymbol{p'_A}|^2\Big], \end{aligned} \tag{7.44}$$

where

$$\begin{aligned} |\boldsymbol{p'_A}|^2 &= \frac{(E_{cm}^2 + m_B^2 - m_A^2)^2}{4E_{cm}^2} - m_B^2, & (7.45)\\ E'_A &= \sqrt{|\boldsymbol{p'_A}|^2 + m_A^2}. & (7.46) \end{aligned}$$

Since we want to utilize the same experimental setups that were used in previous sections to set limits on η, we shall rewrite the total cross section in the lab frame, in which we assume the target particle B is at rest, i.e. $p_A = (E_A, \boldsymbol{p}_A)$ and $p_B = (m_B, 0)$. Now the total cross section is given by

$$\begin{aligned} \sigma &= \frac{|\eta|^2\gamma^2}{4\pi E_{cm}^2}\Big[\frac{1}{2}(\frac{E_{cm}^2}{\gamma^2} - m_A^2 - m_B^2)^2 + 2m_A^4 + 2m_A^2 m_B^2 \\ &\quad -2(\gamma E_A - \gamma\boldsymbol{\beta}\cdot\boldsymbol{p}_A)\tilde{E}'_A(m_A^2 + m_B^2) + 2\tilde{E}_A'^2(\gamma m_B)^2 \\ &\quad +\frac{2}{3}(\gamma|\beta|m_B)^2|\boldsymbol{P'_A}|^2\Big], \end{aligned} \tag{7.47}$$

where

$$|\boldsymbol{P'_A}|^2 = \frac{(E_{cm}^2 + \gamma^2 m_B^2 - \gamma^2 m_A^2)^2}{4\gamma^2 E_{cm}^2} - m_B^2, \quad (7.48)$$

$$\tilde{E}_A'^2 = \frac{(E_{cm}^2 + \gamma^2 m_B^2 - \gamma^2 m_A^2)^2}{4\gamma^2 E_{cm}^2} - m_B^2 + m_A^2, \quad (7.49)$$

with

$$\boldsymbol{\beta} = \frac{\boldsymbol{p_A}}{E_{cm}}, \quad \gamma = \frac{1}{\sqrt{1-\beta^2}}. \quad (7.50)$$

Note that all the parameters in Eq. 7.47 are in the lab frame.

Now we can check the limits on η set by the previous three proposals. In the $n + e \to \bar{n} + e$ case, i.e., neutrons scattering with an electron plasma, we obtain

$$|\beta| = \frac{|\boldsymbol{p_n}|}{E_n + m_e} = \simeq 2.13 \times 10^{-6}, \quad (7.51)$$

$$\gamma = \frac{1}{\sqrt{1-\beta^2}} \simeq 1, \quad (7.52)$$

$$\sigma \simeq 8.30 \times 10^{-8} |\eta|^2 \text{ GeV}^2. \quad (7.53)$$

Running the experiment for one year without observing one single event sets a limit on η

$$|\eta| < 1.74 \times 10^{-5} \frac{2 \text{ keV}}{|\boldsymbol{p_n}|} \sqrt{\frac{1 \text{ yr}}{\text{t}}} \sqrt{\frac{1.7 \times 10^{11} \text{ ns}^{-1}}{\phi}} \sqrt{\frac{1 \text{ m}}{L}} \frac{10 \text{ T}}{B} \text{ GeV}^{-2}. \quad (7.54)$$

In the $n + d \to \bar{n} + d$ case, we consider that neutrons scatter with protons in a deuterium target, so that the density of protons is determined by deuterium. We compute the total cross section

$$|\beta| = \frac{|\boldsymbol{p_n}|}{E_n + m_p} \simeq 1.07 \times 10^{-6},$$

$$\gamma = \frac{1}{\sqrt{1-\beta^2}} \simeq 1\,, \quad (7.55)$$

$$\sigma \simeq 7.00 \times 10^{-2} |\eta|^2 \text{ GeV}^2\,, \quad (7.56)$$

and obtain the limit on η

$$|\eta| < 1.2 \times 10^{-12} \frac{2 \text{ keV}}{|\boldsymbol{p_n}|} \sqrt{\frac{1 \text{ yr}}{\text{t}}} \sqrt{\frac{1.7 \times 10^{11} \text{ ns}^{-1}}{\phi}}$$
$$\sqrt{\frac{1 \text{ m}}{L}} \sqrt{\frac{5 \times 10^{22} \text{ cm}^{-3}}{\rho_T}} \text{ GeV}^{-2}. \quad (7.57)$$

In the $e+n \to e+\bar{n}$ case, electrons utilized in the Darklight experiment [120] scatter with a neutron target, liquid deuterium. We compute the relevant parameters and the total cross:

$$|\beta| = \frac{|\boldsymbol{p_e}|}{E_e + m_n} \simeq 0.096\,, \tag{7.58}$$

$$\gamma = \frac{1}{\sqrt{1-\beta^2}} = 1.00466, \tag{7.59}$$

$$\sigma \simeq 2.0 \times 10^{-3} |\eta|^2 \mathrm{GeV}^2. \tag{7.60}$$

We can set a limit on η

$$|\eta| < 2.07 \times 10^{-10} \frac{100\ \mathrm{MeV}}{|\boldsymbol{p_e}|} \sqrt{\frac{1\ \mathrm{yr}}{\mathrm{t}}} \sqrt{\frac{2 \times 10^{17}\ \mathrm{s}^{-1}}{\phi}} \sqrt{\frac{1\ \mathrm{m}}{L}} \sqrt{\frac{5 \times 10^{22}\ \mathrm{cm}^{-3}}{\rho_T}}\ \mathrm{GeV}^{-2}. \tag{7.61}$$

Note that it appears that the second and third processes yield better limits on η.

7.5 Conclusion and discussion

In this chapter, we have considered $n-\bar{n}$ conversion as it would be mediated by an electromagnetic current. We worked out the total cross section in different cases: for (1) charged particles scattering from a deuterium target and for (2) neutrons scattering from charged particles or from particles with electrically charged constituents. Due to various considerations, we narrow down three possible conversion processes: electron beams scattering with a liquid deuterium target, neutrons scattering from an electron plasma, and neutrons scattering from a liquid deuterium target. Given currently available experimental setups, we perform preliminary estimations of various limits on δ. It appears low energy neutrons scattering from a liquid deuterium target is the most promising method. For the same experimental setups, we estimate the limits on η directly also.

CHAPTER 8

CP VIOLATION AND NEUTRON-ANTINEUTRON OSCILLATION

Recently, it was claimed that the observation of $n-\bar{n}$ oscillation produced by the $n-\bar{n}$ oscillation operator $\psi^T C\psi + h.c.$ would also imply the breaking of CP symmetry [88], and this result has been called into question [89, 53, 90]. However, this does not mean CP violation cannot appear in $n-\bar{n}$ oscillations. A new mechanism of breaking the detailed balance, and thus of breaking CP symmetry, through the inclusion of exotic particles that couple to both n and $\bar{n}$ has been proposed in Ref. [90]. Their phenomenological analysis of CP violation in the $n-\bar{n}$ system is the same as in the neutral meson oscillation system. Therefore, in this chapter, we will briefly discuss the phenomenology of CP violation for neutral flavored mesons, and in particular we will focus on the B meson system. Since we have also done some works that is related to CP violation in the $B\bar{B}$ system, this will be briefly discussed, too.

8.1 Introduction of CP violation

In Chap. 3, we have discussed the discrete symmetries, C, P, and T, in Nature. Also we have showed how fermion fields (Dirac or Majorana fields) transform under CP, which is the product of two components: C and P. However, we have said little about the physical consequences of this operation. We know that charge conjugation transforms a particle into the corresponding anti-particle, e.g., if we apply C to an electron, we will obtain a positron. Also parity is the transformation that inverts the spatial coordinates, i.e. $\mathbf{x} \to -\mathbf{x}$. If we apply P to an moving electron with a velocity $\mathbf{v}$ from left to right, the electron will flip direction and end up moving with a velocity -$\mathbf{v}$, from right to left. In other words, parity produces the "mirror" image of reality.

Therefore, when we apply a CP transformation to an electron moving with a velocity $\mathbf{v}$ we will obtain a positron moving with a velocity -$\mathbf{v}$. When we apply a CP transformation to a composite system, such as e^+ and e^-, we find that it backs to itself. This means that matter will transform to its anti-matter under CP. This can be illustrated by a "CP-mirror" that returns the mirror image of matter (Fig. 8.1). Naturally, we expect not only that our "anti-self" would wave back at us in the CP-mirror but also that Nature would respect CP symmetry. However, our intuitive

Figure 8.1: A CP mirror world[126]

expectation was vetoed in 1964 by the discovery of Christensen, Cronin, Fitch, and Turlay [127], that the long-lived (CP-odd) kaon state did sometimes decay into the CP-even two pion state. This result immediately shows that CP symmetry is violated. Therefore, we need to examine how CP non-conservation manifests itself, and then ask what theories will give such effects.

One of the ways in which CP non-conservation can appear is as a rate difference between two processes that are the CP conjugates of each other. One may wonder how such a rate difference can appear. Consider, for example, a particle decay for which two different terms in the Lagrangian can contribute. The amplitude for such a process can be written as

$$\mathcal{A}(A \to B) = a_1 r_1 e^{i\phi_1} + a_2 r_2 e^{i\phi_2}, \tag{8.1}$$

where a_1 and a_2 are two different, possibly complex, coupling constants in the theory. The transition amplitudes associated with each coupling are given by $re^{i\phi}$ that also can have both a real part (magnitude) and a phase (absorptive part). The physical source of this phase comes from the contribution of multiple real intermediate states to the process via rescattering effects. The phases ϕ are usually called strong phases because the rescattering effects among the various coupled channels are dominated

by strong interactions. These phases are the same for a process and its CP conjugate, since the strong interaction respects CP symmetry. The phase of the coupling constants are often called weak phases because the relevant complex couplings are in the weak interaction sector of the SM. Writing down the amplitude for the CP conjugate process, we find

$$\bar{\mathcal{A}}(\bar{A} \to \bar{B}) = a_1^* r_1 e^{i\phi_1} + a_2^* r_2 e^{i\phi_2}. \tag{8.2}$$

Note that the weak phases change sign between a process and its CP conjugate process, while the strong phases do not. Computing the difference in rates for these two processes, which breaks CP symmetry, we find

$$|\mathcal{A}|^2 - |\bar{\mathcal{A}}|^2 = 2r_1 r_2 \Im(a_1 a_2^*) \sin(\phi_1 - \phi_2). \tag{8.3}$$

This shows CP violation will vanish if the two coupling constants are real. In addition it vanishes if the difference of the strong phases is zero. The CP-violating effect associated with the comparison of two CP-related decay rates is often called direct CP violation, and it is characterized by the condition $|\bar{\mathcal{A}}/\mathcal{A}| \neq 1$. There are also more types of CP violation that we will discuss later.

The phase of any single complex coupling in a Lagrangian is not a physically meaningful quantity, because in general it can be redefined and even made to vanish by redefining related fields. However, such a rephasing of fields can never change the relative phase between two couplings that contribute to the same process. This is because both terms involve the same set of fields, and hence both changes in the same way under any rephasings of those fields. These rephasing-invariant quantities are the physically meaningful phases in Lagrangian.

Note that the CP-violating rate difference in Eq. 8.3 also depends on a difference of strong phases. Typically, they are very difficult to calculate, since strong phases are associated with strong interaction physics effects that in general cannot be evaluated in perturbation theory. One of the things that makes the study of the neutral but flavored mesons interesting is that we can find other types of CP-violating effects, in which the role played by strong phases can be replaced by other complex quantities that are relevant to the process of meson mixing with its CP conjugate meson. In such case, we can relate a CP-violating effect directly to the phase-difference in the Lagrangian couplings without any calculation of strong-interaction quantities. We will discuss these types of CP violation in later sections.

8.2 CP violation for neutral flavored mesons mixing

The phenomenology of CP violation for neutral flavored mesons is particularly interesting, since many of the observables can be cleanly interpreted. The phenomenology is different for different mesons, such as K^0, D^0, B^0, and B_s^0, decays, since each of these systems is governed by different decay rates, oscillations, and lifetime splittings. However, the general considerations are identical for all flavored neutral mesons.

8.2.1 Charged- and neutral-hadron decays

We define decay amplitudes of M, which could be charged or neutral, and its CP conjugate $\overline{M}$ to a final state f and its CP conjugate $\bar{f}$ as

$$\begin{aligned} \mathcal{A}_f &= \langle f|\mathcal{H}|M\rangle, \quad \overline{\mathcal{A}}_f = \langle f|\mathcal{H}|\overline{M}\rangle, \\ \mathcal{A}_{\bar{f}} &= \langle \bar{f}|\mathcal{H}|M\rangle, \quad \overline{\mathcal{A}}_{\bar{f}} = \langle \bar{f}|\mathcal{H}|\overline{M}\rangle, \end{aligned} \tag{8.4}$$

where $\mathcal{H}$ is the effective Hamiltonian governing the weak interactions at the b quark mass scale. Applying the CP transformation on these states introduces phases ξ_M and ξ_f that depend on their flavor content. In general

$$CP|M\rangle = e^{i\xi_M}|\bar{M}\rangle, \quad CP|f\rangle = e^{i\xi_f}|\bar{f}\rangle, \tag{8.5}$$

then

$$CP|\bar{M}\rangle = e^{-i\xi_M}|M\rangle, \quad CP|\bar{f}\rangle = e^{-i\xi_f}|f\rangle, \tag{8.6}$$

so that $(CP)^2 = 1$. The phases ξ_M and ξ_f are arbitrary and can be chosen by convention, e.g., $\xi = 0$ or $\xi = \pi$: the physical results are convention independent. Note that if CP is conserved by the dynamics, $[CP, \mathcal{H}]$=0, then $\mathcal{A}_f$ and $\bar{\mathcal{A}}_{\bar{f}}$ have the following relations

$$\bar{\mathcal{A}}_{\bar{f}} = e^{i(\xi_f - \xi_M)}\mathcal{A}_f. \tag{8.7}$$

8.2.2 Neutral meson mixing

A state that is a superposition of M^0 and $\overline{M}^0$ at $t = 0$,

$$|\psi(0)\rangle = a(0)|M^0\rangle + b(0)|\overline{M}^0\rangle, \tag{8.8}$$

will evolve in time and acquire components that describe all possible final states $\{f_1, f_2, ...\}$, i.e.,

$$|\psi(t)\rangle = a(t)|M^0\rangle + b(t)|\overline{M}^0\rangle + c_1(t)|f_1\rangle + c_2(t)|f_2\rangle + ... \tag{8.9}$$

Here we only interested in the values of $a(t)$ and $b(t)$. Then the time evolution is determined by a 2×2 effective Hamiltonian $\mathbf{H}$ that is not Hermitian, since the mesons not only oscillate but also decay. This matrix is written in the basis of the two flavor eigenstates and can also be written in terms of Hermitian matrices $\mathbf{M}$ and $\mathbf{\Gamma}$ as

$$\mathbf{H} = \mathbf{M} - \frac{i}{2}\mathbf{\Gamma}. \tag{8.10}$$

$\mathbf{M}$ and $\mathbf{\Gamma}$ are associated with $(M^0, \overline{M}^0) \leftrightarrow (M^0, \overline{M}^0)$ via off-shell (dispersive) and on-shell (absorptive) intermediate states, respectively. The diagonal elements of $\mathbf{M}$ and $\mathbf{\Gamma}$ correspond to the flavor-conserving transitions $M^0 \leftrightarrow M^0$ and $\overline{M}^0 \leftrightarrow \overline{M}^0$, while the off-diagonal parts are associated with flavor-changing transitions $M^0 \leftrightarrow \overline{M}^0$.

The Hamiltonian $\mathbf{H}$ has two mass eigenstates M_H and M_L[1] where the H and L stand for heavy and light, which really means heavier and less heavy, since the mass difference may be tiny. We can write these two states in the basis of flavor eigenstates,

$$\begin{aligned} |M_L\rangle &= p|M^0\rangle + q|\overline{M}^0\rangle, \\ |M_H\rangle &= p|M^0\rangle - q|\overline{M}^0\rangle, \end{aligned} \tag{8.11}$$

with $|q|^2 + |p|^2 = 1$[2]. The real and imaginary parts of the eigenvalues $\omega_{L,H}$ corresponding to $|M_{L,H}\rangle$ represent their mass and decay widths, respectively.

Solving the eigenvalue problem of $\mathbf{H}$

$$\begin{pmatrix} \mathbf{M} - \frac{i}{2}\mathbf{\Gamma} & \mathbf{M}_{12} - \frac{i}{2}\mathbf{\Gamma}_{12} \\ \mathbf{M}^*_{12} - \frac{i}{2}\mathbf{\Gamma}^*_{12} & \mathbf{M} - \frac{i}{2}\mathbf{\Gamma} \end{pmatrix} \psi = \lambda\psi, \tag{8.12}$$

one can obtain

$$\lambda_\pm = \mathbf{M} - \frac{i}{2}\mathbf{\Gamma} \pm \sqrt{(\mathbf{M}_{12} - \frac{i}{2}\mathbf{\Gamma}_{12})(\mathbf{M}^*_{12} - \frac{i}{2}\mathbf{\Gamma}^*_{12})}, \tag{8.13}$$

where $\lambda_\pm$ are the eigenvalues, $\mathbf{M}_{12}$ quantifies the contribution from weak box-diagrams, and $\mathbf{\Gamma}_{12}$ is a measure of the contribution from the virtual, intermediate on-shell particle decay. Splitting $\lambda_\pm$ into the real and imaginary parts, we have

$$\lambda_\pm = M_{H,L} - \frac{i}{2}\Gamma_{H,L}. \tag{8.14}$$

[1]The labels H and L are meant to denote that we view the system in the weak eigenstates (as opposed to the flavor) basis. In the B system the weak eigenstate differ significantly in mass and hence the labels H an L, whereas for kaons, suitable labels are L and S because the lifetime difference is more striking.

[2]Note in this framework we have assumed CPT symmetry intact. However, CPT violation in mixing can be considered by introducing a papameter z. A relevant introduction can be found in Ref.[128].

Then it is fairly easy to obtain the relation below

$$\left(\frac{q}{p}\right)^2 = \frac{\mathbf{M}_{12}^* - (i/2)\mathbf{\Gamma}_{12}^*}{\mathbf{M}_{12} - (i/2)\mathbf{\Gamma}_{12}}, \tag{8.15}$$

$$\frac{q}{p} = -\frac{2(\mathbf{M}_{12}^* - (i/2)\mathbf{\Gamma}_{12}^*)}{\Delta M - (i/2)\Delta\Gamma}, \tag{8.16}$$

where

$$\Delta M = M_H - M_L, \quad \Delta\Gamma = \Gamma_H - \Gamma_L. \tag{8.17}$$

Note if CP is a symmetry of $\mathbf{H}$, then $\mathbf{\Gamma}_{12}/\mathbf{M}_{12}$ is real, which leads to $|q/p| = 1$.

8.2.3 Classification of CP violation

Three types of CP violation can be potentially observed in meson decay, and two of them have already been discussed. We follow the discussion in Ref. [129].

I. **CP violation in decay (Direct CP violation):**
Its condition is given by

$$|\bar{\mathcal{A}}_{\bar{f}}/\mathcal{A}_f| \neq 1. \tag{8.18}$$

In charged meson decays, this is the only possible source of CP violation, since mixing effects cannot appear. The CP asymmetries are defined by

$$A \equiv \frac{\Gamma(M^- \to f^-) - \Gamma(M^+ \to f^+)}{\Gamma(M^- \to f^-) + \Gamma(M^+ \to f^+)} = \frac{|\bar{\mathcal{A}}_{f^-}/\mathcal{A}_{f^+}|^2 - 1}{|\bar{\mathcal{A}}_{f^-}/\mathcal{A}_{f^+}|^2 + 1}. \tag{8.19}$$

II. **CP violation in mixing:**
This appears if $|q/p| \neq 1$. In charged-current semileptonic neutral meson decays $M, \overline{M} \to l^{\pm}X$, this is the only source of CP violation, and it can be measured via the asymmetry of "wrong-sign" decays induced by oscillations:

$$\begin{aligned} A(t) &\equiv \frac{\Gamma[\overline{M}^0(t) \to l^+X] - \Gamma[M^0(t) \to l^-X]}{\Gamma[\overline{M}^0(t) \to l^+X] + \Gamma[M^0(t) \to l^-X]} \\ &= \frac{1 - |q/p|^4}{1 + |q/p|^4}. \end{aligned} \tag{8.20}$$

Interestingly this asymmetry of time-dependent decay rates is actually time-independent.

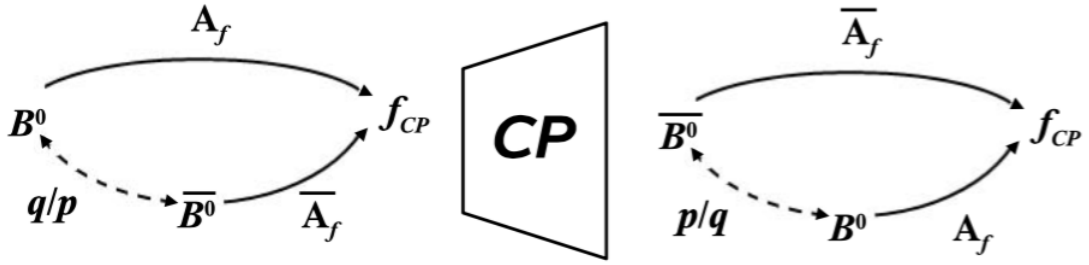

Figure 8.2: Effect of the CP transformation on B^0 decay to a CP eigenstate f_{CP}. The asymmetry is due to the interference between mixing, described by parameters p and q, and the decay amplitudes A_f and $\bar{A}_f$.

III. **CP violation in the interference of mixing and direct decay:**
In this third type of CP violation there exist final states which may be reached from either M^0 or $\overline{M}^0$, and the CP violation results from the interference between the decays of mixed and of unmixed neutral mesons (see Fig. 8.2). The asymmetry in this case is given by

$$A(t) \equiv \frac{\Gamma[\overline{M}^0(t) \to f_{CP}] - \Gamma[M^0(t) \to f_{CP}]}{\Gamma[\overline{M}^0(t) \to f_{CP}] + \Gamma[M^0(t) \to f_{CP}]}, \tag{8.21}$$

and the CP violation condition is given by

$$\Im(\lambda_f) \neq 0, \tag{8.22}$$

such that

$$\lambda_f \equiv \frac{q}{p}\frac{\bar{\mathcal{A}}_f}{\mathcal{A}_f}. \tag{8.23}$$

A more detailed discussion of CP violation and its classification can be found in the book by Bigi and Sanda [75].

8.3 CP violation in the B system

8.3.1 Time evolution of the B states and time-dependent observables

Now we focus on CP violation in the neutral B-meson system. As in the general case, the $B\bar{B}$ system can be described by a 2×2 effective Hamiltonian $H = M - (i/2)\Gamma$, where M and Γ are Hermitian matrices. CP or CPT symmetry ensures that $M_{11} = M_{22}$ and $\Gamma_{11} = \Gamma_{22}$. Writing H is in the flavor basis $(|B^0\rangle, |\overline{B}^0\rangle)$, we have two eigenvalues ω_L and ω_H,

$$\omega_{H,L} \equiv m_{H,L} - \frac{i}{2}\Gamma_{H,L}, \tag{8.24}$$

corresponding to the two eigenstates $|B_H\rangle$ and $|B_L\rangle$, respectively. Under CPT symmetry, the light and heavy mass eigenstates can be written as

$$\begin{aligned} |B_L\rangle &= p|B^0\rangle + q|\overline{B}^0\rangle, \\ |B_H\rangle &= p|B^0\rangle - q|\overline{B}^0\rangle. \end{aligned} \tag{8.25}$$

To evaluate the measurable quantities, we first need to understand the time evolution of states which begin, e.g., as pure B^0 meson states at t=0. That is,

$$|B^0(t=0)\rangle = (|B_H\rangle + |B_L\rangle)/2p. \tag{8.26}$$

Since $|B_L\rangle$ and $|B_H\rangle$ are mass eigenstates, the time-evolution of $|B(t=0)\rangle$ is trivial,

$$|B^0(t)\rangle = g_+|B^0\rangle + (q/p)g_-|\overline{B}^0\rangle, \tag{8.27}$$

where we have introduced

$$g_\pm = \frac{1}{2}\Big(e^{-i\omega_H t} \pm e^{-i\omega_L t}\Big). \tag{8.28}$$

The time-dependent state that is a pure $\overline{B}^0$ state at $t=0$ can be obtained in a similar way,

$$|\overline{B}^0(t)\rangle = (p/q)g_-|B^0\rangle + g_+|\overline{B}^0\rangle. \tag{8.29}$$

It is now straightforward to derive any time-dependent quantities necessary for CP violating observables. For example, the time-dependent rate to reach a particular CP eigenstate f with CP eigenvalue ξ_f can be written as

$$\begin{aligned} \Gamma[B^0(t)\to f] &\propto |\mathcal{A}(B(t)\to f)|^2 \\ &= \mathcal{N}_f|\mathcal{A}(B^0\to f)|^2\Big[|g_+|^2 + |\lambda_f g_-|^2 + 2\Re[g_+^* g_- \lambda_f]\Big], \end{aligned} \tag{8.30}$$

with

$$\lambda_f = \frac{q}{p}\frac{\mathcal{A}(\overline{B}^0\to f)}{\mathcal{A}(B^0\to f)} = \xi_f \frac{q}{p}\frac{\mathcal{A}(\overline{B}^0\to \bar{f})}{\mathcal{A}(B^0\to f)}. \tag{8.31}$$

Note that $\mathcal{N}_f$ is a common, time-independent, normalization factor. With Eq. 8.30 and 8.31 in hand, other CP violating quantities (time-dependent or independent) can also be easily constructed. With this it is straightforward to check the last equation in Eq. 8.20 simply by substituting Eq. 8.30 into Eq. 8.20.

When neutral pseudoscalar mesons are produced coherently in pairs from the decay of a vector resonance, $V\to M^0\overline{M}^0$, the time-dependent decay rate has a form

similar to Eq. 8.30. For example, since the $\Upsilon(4S)$ state has definite flavor and CP, at the $\Upsilon(4S)$ resonance, neutral-B mesons are produced in coherent p-wave pairs,

$$\begin{aligned} |i\rangle &= \frac{1}{\sqrt{2}}[B^0(t_1)\overline{B}^0(t_2) - \overline{B}^0(t_1)B^0(t_2)] \\ &= \frac{1}{\sqrt{2}}[B_+(t_1)B_-(t_2) - B_-(t_1)B_+(t_2)], \end{aligned} \tag{8.32}$$

where t_1 or t_2 represents the life-time of the state, and $|B_\pm\rangle$ are normalized linear combinations of B^0 and $\overline{B}^0$ such that $CP|B_\pm\rangle = \pm|B_\pm\rangle$.

If we subsequently observe one B-meson to decay to state f_1 at time $t_0 = 0$ and the other decay to state f_2 at a later time t, then if both B^0 and $\overline{B}^0$ can decay to f_1 and f_2, we cannot in general know from which B meson f_1 or f_2 came. To simplify the final time-dependent decay rate, we introduce the helpful definitions

$$\begin{aligned} A_1 &\equiv \mathcal{A}(B^0 \to f_1), \quad A_2 \equiv \mathcal{A}(B^0 \to f_2), \\ \bar{A}_1 &\equiv \mathcal{A}(\overline{B}^0 \to f_1), \quad \bar{A}_2 \equiv \mathcal{A}(\overline{B}^0 \to f_2). \end{aligned} \tag{8.33}$$

Now the overall amplitude is given by

$$\mathcal{A} = a_+ g_+ + a_- g_-, \tag{8.34}$$

where

$$\begin{aligned} a_+ &= \bar{A}_1 A_2 - A_1 \bar{A}_2 \\ a_- &= \Big[\frac{p}{q} A_1 A_2 - \frac{q}{p}\bar{A}_1 \bar{A}_2\Big]. \end{aligned} \tag{8.35}$$

Note that Eq. 8.28 produces two relations below

$$|g_\pm|^2 = \frac{1}{2}e^{\Gamma t}[\cosh(\Delta\Gamma t/2) \pm \cos(\Delta m_B t)], \tag{8.36}$$

and

$$g_+^* g_- = -\frac{1}{2}e^{-\Gamma t}[\sinh(\Delta\Gamma t/2) + i\sin(\Delta m_B t)], \tag{8.37}$$

where $\Gamma = (\Gamma_{11} + \Gamma_{22})/2$, $\Delta\Gamma = \Gamma_M - \Gamma_L$, and $\Delta m_B = M_H - M_L$. We find the decay rate

$$\begin{aligned} \Gamma(t) \;\propto\; e^{-\Gamma t}\Big\{ &\frac{1}{2}c_+ \cosh(\Delta\Gamma t/2) + \frac{1}{2}c_- \cos(\Delta m_B t) \\ &-\Re(s)\sinh(\Delta\Gamma t/2) + \Im(s)\sin(\Delta m_B t)\Big\}, \end{aligned} \tag{8.38}$$

where

$$c_\pm = |a_+|^2 \pm |a_-|^2, \quad s = a_+^* a_-. \tag{8.39}$$

Note that Eq. 8.38 will reduce to Eq. 8.30 with $A_1 = 0, \bar{A}_1 = 1$. A final state f_1 with $A_1 = 0$ or $\bar{A}_1 = 0$ is called a tagging state, because it identifies the decaying meson as $\bar{B}^0$ or B^0, respectively. Once one meson is tagged, it sets the clock for its time evolution.

8.3.2 The golden modes

There are many possible CP eigenstate channels for $b \to c\bar{c}s$, such as $J/\psi K_S$, $J/\psi K_L$, $\psi' K_S$, $\eta_c K_S$, etc.). We would like to focus on the channel $B \to J/\psi K$. There are two weak decay Feynman diagrams that can contribute to B decays to leading order in the effective weak interaction coupling strength G_F. They are called "tree" and "penguin" diagrams as shown in Figs. 8.3 and 8.4. The d or s in these two figures are called spectator quarks, because although they are present in the initial B meson, they are not directly involved in the decay. Its amplitude is given by

$$A_{J/\psi K} = (V_{cb}^* V_{cs}) T_{J/\psi K} + (V_{ub}^* V_{us}) P_{J/\psi K}, \tag{8.40}$$

where $T_{J/\psi K} = t_{J/\psi K} + p^c_{J/\psi K} - p^t_{J/\psi K}$ and $P^u_{J/\psi K} = p^u_{J/\psi K} - p^t_{J/\psi K}$ with t_f and p^q_f denoting the contributions from tree diagram as in Fig. 8.3 and penguin diagram in Fig. 8.4, respectively. The complex parameters, "V", are the matrix elements of the Cabibbo-Kobayashi-Maskawa (CKM) [130, 131] matrix, which are written as follows:

$$V_{CKM} = \begin{pmatrix} V_{ud} & V_{us} & V_{ub} \\ V_{cd} & V_{cs} & V_{cb} \\ V_{td} & V_{ts} & V_{tb} \end{pmatrix}. \tag{8.41}$$

It is a unitary matrix, and leads to the following relation

$$V_{ud} V_{ub}^* \; + \; V_{cd} V_{cb}^* \; + \; V_{td} V_{tb}^* = 0, \tag{8.42}$$

which can be described by a unitary triangle as in Fig. 8.5. The three CKM unitary angles, ϕ_1, ϕ_2, and ϕ_3, are defined as

$$\phi_1 = \pi - \arg\Big(\frac{V_{tb}^* V_{td}}{V_{cb}^* V_{cd}}\Big), \tag{8.43}$$

$$\phi_2 = \arg\Big(-\frac{V_{tb}^* V_{td}}{V_{ub}^* V_{ud}}\Big), \tag{8.44}$$

$$\phi_3 = \arg\Big(-\frac{V_{ub}^* V_{ud}}{V_{cb}^* V_{cd}}\Big). \tag{8.45}$$

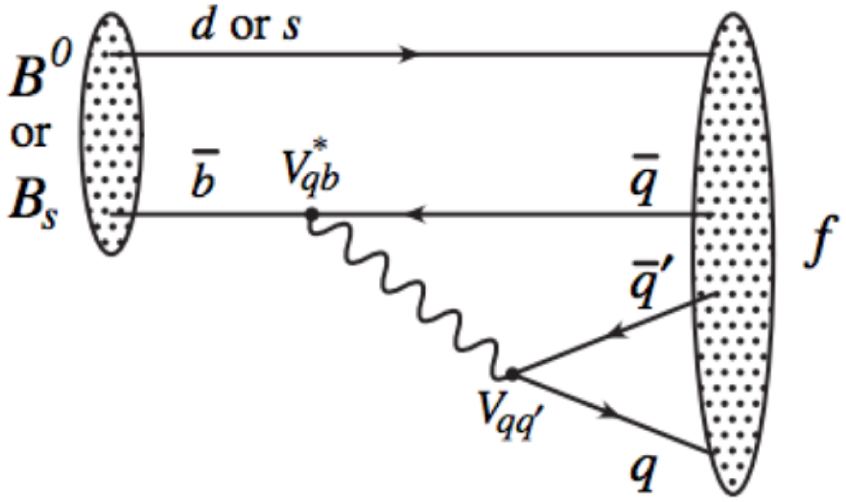

Figure 8.3: Feynman diagram for tree amplitude contributing to $B^0 \to f$ or $B_s \to f$ [129].

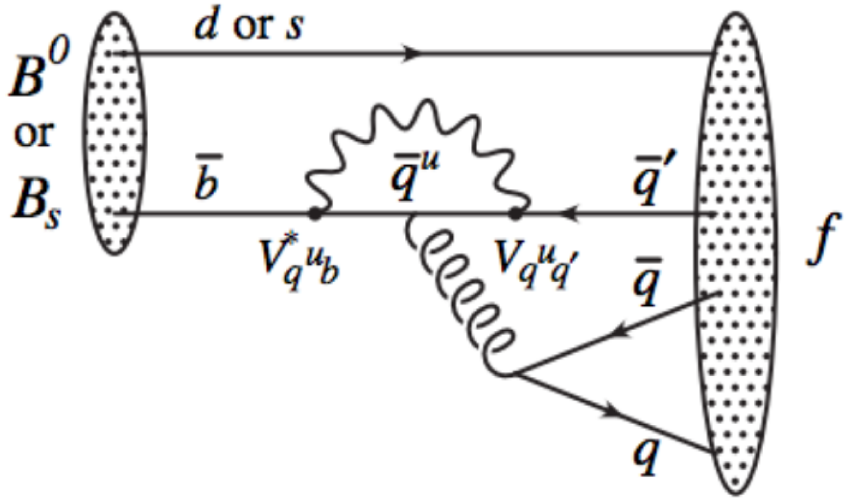

Figure 8.4: Feynman diagram for the penguin amplitude contributing to $B^0 \to f$ or $B_s \to f$ [129], where $q^u = u, c, t$ is the quark in the loop.

Note another notation is often used in many papers, in which the three CKM angles are labeled as α, β, and γ. The corresponding relations between the two sets of CKM unitary angles are $\alpha = \phi_2$, $\beta = \phi_1$, and $\gamma = \phi_3$. We see that $T_{J/\psi K}$ and $P_{J/\psi K}$ are associated with different combinations of the CKM matrix elements. Generally the names "tree" (T) and "penguin" (P) are associated with contributions that multiply distinct combinations of CKM matrix elements. We note $T_{J/\psi K}$ is the dominant

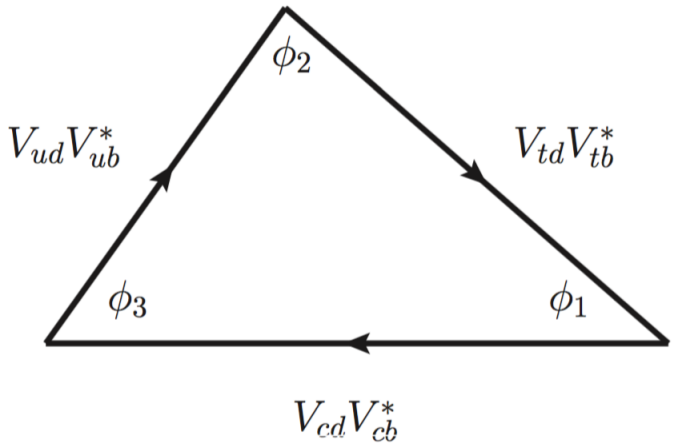

Figure 8.5: CKM triangle of Eq. 8.42 in the complex plane.

contribution, and $P^u_{J/\psi K}$ is a smaller effect. The particular channels $B \to J/\psi K_{S,L}$ are very interesting to physicists for analyzing CP violation in B decay. They are also referred to as the golden modes. However, to study CP violation in these channels, there is one subtlety that must be considered. That is, a B^0 meson actually decays into a final state $J/\psi K^0$, while a $\bar{B}^0$ decays into a different final state $J/\psi \bar{K}^0$. The common final state only results from $K^0 - \bar{K}^0$ oscillation. Consequently, a phase factor $(V^*_{cd}V_{cs})/(V_{cd}V^*_{cs})$ associated with the neutral K mixing also plays a role. Now the λ for $B \to J/\psi K_S$ is given by

$$\lambda_{J/\psi K_S} = \left(\frac{q}{p}\right)_{B^0} \left(\eta_{J/\psi K_S} \frac{\bar{A}_{J/\psi K_s}}{A_{J/\psi K_s}}\right) \times \frac{V^*_{cd}V_{cs}}{V_{cd}V^*_{cs}}. \tag{8.46}$$

For $B \to J/\psi K_{S,L}$, its penguin contribution P^u to A_f in the SM can be neglected, hence the name "golden modes," and we have

$$\lambda_{J/\psi K_S} = -e^{i2\beta}. \tag{8.47}$$

8.3.3 Time reversal violation in B physics

CP violation has been observed using the $K - \overline{K}$ and $B - \overline{B}$ systems. Various modes and methods to analyze CP violation in B physics have been reviewed, e.g., in Refs. [132, 133]. Since there is no evidence of CPT symmetry violation[3], the existence of CP violation implies that time reversal symmetry is also violated. However, it is still of great interest to observe T violation directly in a single experiment. Previously a direct observation of time-reversal violation in $K - \overline{K}$ had been reported

[3]The CPT violation limit from the mass difference between K^0 and $\overline{K}^0$ is found to be $|m_{\overline{K}^0} - m_{K^0}|/m_{K^0} \leq 0.6 \times 10^{-18}$ at 90% CL [57].

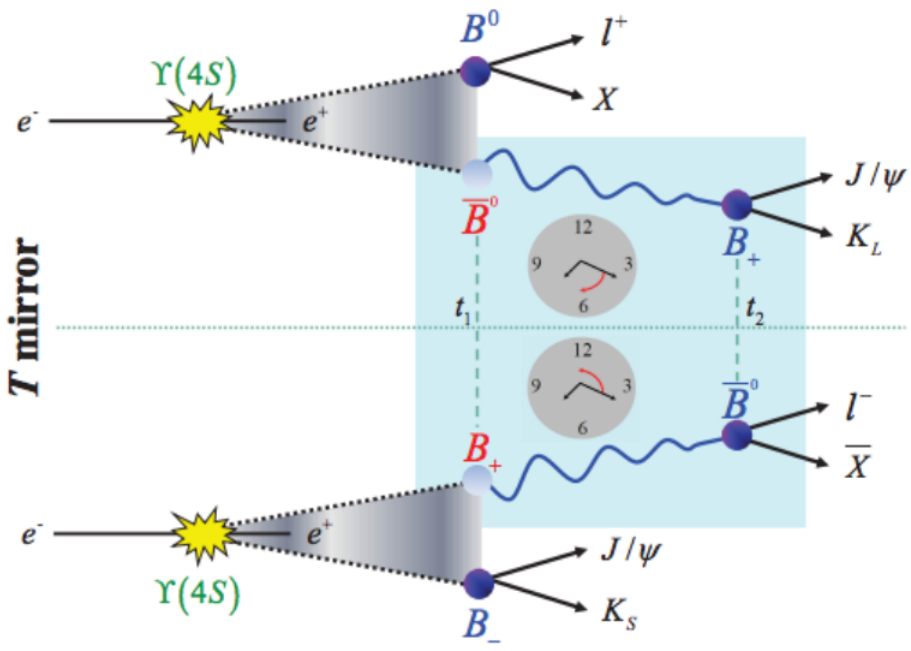

Figure 8.6: Basic concept of the time-reversal experiment in B physics [138].

by CPLEAR [134]. However, the interpretation of the experiment as a test of T has been criticized [135, 136], because the time-reversal quantity they formed is not really time dependent. In 2012, the BaBar Collaboration observed direct T violation [3] by exploiting the coherent $B\bar{B}$ system produced in $\Upsilon(4S)$ decays. This is because the flavor- or CP-state of a B meson can be determined, or "tagged," at a time t by measuring the decay of the other B meson at that instant, since the $\Upsilon(4S)$ state has definite flavor and CP. With this construction the asymmetry flips sign when the sign of t, in effect, is reversed.

This idea was first proposed in a seminal paper by Bañuls and Bernabéu, in which they shown that by selecting suitable combinations of flavor and CP tags of the $B-$mesons in the entangled pair, CP, T, and CPT asymmetries [137] can all be constructed. It is probably worth briefly sketching their idea to test T reversal symmetry in a B factory experiment [3, 137]. There is a beautiful figure illustrating the foundations of the time-reversal experiment, which is produced in Fig. 8.6 [138]. Electron-positron collisions at a B factory can produce $\Upsilon(4S)$ resonances. In the top panel, the first B decays into a ℓ^+X final state at t_1. This final state filters the quantum-mechanical state of the other B as $\bar{B}^0$ at the same time. In other words, the other B meson is "tagged" without measuring it specifically. The "tagged" meson is observed later at t_2 to decay into a final state $J/\psi K_L$ indicating that the B meson is

in a B_+ state. Therefore, this time-ordered event class $(\ell^+X, J/\psi K_L)$ demonstrates a transition $\overline{B}^0 \to B_+$ in the elapsed time $t = t_2 - t_1$. To test time-reversal, a T-mirrored transition $B_+ \to \overline{B}^0$ needs to be constructed. As shown in the bottom panel, one B_+ state is tagged by observing the other B meson decaying into the $J/\psi K_S$ final state at t_1. Then the observation of $\ell^-\overline{X}$ at t_2 projects the $\overline{B}^0$ state and the event class $(J/\psi K_S, \ell^-\overline{X})$ indicates the wanted T-mirrored transition. By carefully selecting the event classes, other possible comparisons to test T can be constructed. We show some possibilities in Table 8.1. Similar ideas can also be applied to CP and CPT symmetry tests and are illustrated in Tables 8.2 and 8.3, respectively.

Reference		T- conjugate	
Transition	final state	Transition	final state
$\overline{B}^0 \to B_-$	$(\ell^+X, J/\psi K_S)$	$B_- \to \overline{B}^0$	$(J/\psi K_L, \ell^-X)$
$\overline{B}^0 \to B_+$	$(\ell^+X, J/\psi K_L)$	$B_+ \to \overline{B}^0$	$(J/\psi K_S, \ell^-X)$
$B_+ \to B^0$	$(J/\psi K_S, \ell^+X)$	$B^0 \to B_+$	$(\ell^-X, J/\psi K_L)$
$B_- \to B^0$	$(J/\psi K_L, \ell^+X)$	$B^0 \to B_-$	$(\ell^-X, J/\psi K_S)$

Table 8.1: Possible comparisons for T tests in the experimental B factory scheme [139].

Reference		CP-conjugate	
Transition	final state	Transition	final state
$\overline{B}^0 \to B_-$	$(\ell^+X, J/\psi K_S)$	$B^0 \to B_-$	$(\ell^-X, J/\psi K^0_S,)$
$\overline{B}^0 \to B_+$	$(\ell^+X, J/\psi K_L)$	$B^0 \to B_+$	$(\ell^-X, J/\psi K_L)$
$B_+ \to B^0$	$(J/\psi K_S, \ell^+X)$	$B_+ \to \overline{B}^0$	$(J/\psi K_S, \ell^-X)$
$B_- \to B^0$	$(J/\psi K_L, \ell^+X)$	$B_- \to \overline{B}^0$	$(J/\psi K_L, \ell^-X)$

Table 8.2: Possible comparisons for CP tests in the experimental B factory scheme [139].

The BaBar collaboration [3] uses the final states $J/\psi K_L$ and $J/\psi K_S$ as CP tags and the sign of the charged lepton in $\ell^\pm X$ as a flavor tag, and they measure time-dependent, T violating asymmetries, such as $A_T = (\Gamma(B^0 \to B_+) - \Gamma(B_+ \to B_0))/(\Gamma(B^0 \to B_+) + \Gamma(B_+ \to B_0))$. Their final reported T violation measurement

Reference		CPT-conjugate	
Transition	final state	Transition	final state
$\overline{B}^0 \to B_-$	$(\ell^+X, J/\psi K_S)$	$B_- \to B^0$	$(J/\psi K_L, \ell^+X)$
$B^0 \to B_-$	$(\ell^-X, J/\psi K_S)$	$B_- \to \overline{B}^0$	$(J/\psi K_L, \ell^-X)$
$B_+ \to B^0$	$(J/\psi K_S, \ell^+X)$	$\overline{B}^0 \to B_+$	$(\ell^+X, J/\psi K_L)$
$B_+ \to \overline{B}^0$	$(J/\psi K_S, \ell^-X)$	$B^0 \to B_+$	$(\ell^-X, J/\psi K_L)$

Table 8.3: Possible comparisons for CPT tests in the experimental B factory scheme [139].

has an effective significance of 14σ [3]. There are possible subtleties in the interpretation of the BaBar measurement, e.g., the presence of direct CP violation, CPT violation, wrong strangeness decays, and wrong sign semileptonic decays that were all ignored. These effects have been considered in Ref. [140], and found to be negligibly small. We have also explicitly considered how the presence of direct CP violation in kaon decay can affect the interpretation of A_T [54]. Nevertheless, since these effects are all known to be relatively very small, the BaBar's collaboration's measurement can be considered a meaningful direct demonstration of the violation of T reversal symmetry.

8.3.4 Generalized T violation method to trap penguin

Now we would like to generalize the analysis of A_T to consider different choices of CP tags for which the dominant amplitudes have the same weak phase; these would represent alternates to those listed in Table 8.1. Before doing that, we first revisit the decay rate of the coherent $B\bar{B}$ meson system as considered in Eq. 8.38.

We neglect the refinements resulting from the possible presence of CPT violation, wrong-sign semileptonic decays, and wrong strangeness decays. We also neglect CP violation in $B\bar{B}$ mixing and set the width difference of the B-meson weak eigenstates to zero, i.e., $\Gamma_H - \Gamma_L = 0$. The time-dependent decay rate for $B\bar{B}$ mesons produced in $\Upsilon(4S)$ decay, in which one B decays to final state f_1 at time t_1 and the other decays to final state f_2 at a later time t_2 is thus given by

$$\begin{aligned} \Gamma_{(f_1)_\perp, f_2} &= \mathcal{N}_1\mathcal{N}_2 e^{-\Gamma(t_1+t_2)}[1 + C_{(1)_\perp,2}\cos(\Delta m_B\, t) \\ &+ S_{(1)_\perp,2}\sin(\Delta m_B\, t)]\,, \end{aligned} \tag{8.48}$$

with $\Gamma \equiv (\Gamma_H + \Gamma_L)/2$, $\Delta m_B \equiv m_H - m_L$, $t = t_2 - t_1 \geq 0$, $S_{(1)_\perp,2} \equiv C_1 S_2 - C_2 S_1$, and $C_{(1)_\perp,2} \equiv -[C_2 C_1 + S_2 S_1]$. Moreover, $C_f \equiv (1 - |\lambda_f|^2)/(1 + |\lambda_f|^2)$ and $S_f \equiv 2\Im(\lambda_f)/(1 + |\lambda_f|^2)$, where $\lambda_f \equiv (q/p)(\bar{A}_f/A_f)$, noting $A_f \equiv A(B^0 \to f)$, $\bar{A}_f \equiv A(\bar{B}^0 \to f)$, and $\mathcal{N}_f \equiv A_f^2 + \bar{A}_f^2$, and q and p are the usual $B\bar{B}$ mixing parameters. Since we neglect wrong-sign semileptonic decay, $C_{\ell^+X} = -C_{\ell^-X} = 1$. Defining normalized rates as per $\Gamma'_{(f_1)_\perp,f_2} \equiv \Gamma_{(f_1)_\perp,f_2}/(\mathcal{N}_{f_1}\mathcal{N}_{f_2})$ we have, in the case of the asymmetry illustrated in Fig. 8.6,

$$A_T = \frac{\Gamma'_{(\ell^+X)_\perp,J/\psi K_L} - \Gamma'_{(J/\psi K_S)_\perp,\ell^-X}}{\Gamma'_{(\ell^+X)_\perp,J/\psi K_L} + \Gamma'_{(J/\psi K_S)_\perp,\ell^-X}}\,. \tag{8.49}$$

Note that normalizing each rate is important to a meaningful experimental asymmetry because the $J/\psi K_S$ (or, more generally, $c\bar{c}K_S$) and $J/\psi K_L$ final states have different reconstruction efficiencies [139]. BaBar constructs four different asymmetries, based on four distinct subpopulations of events, namely, those for $\Gamma_{(\ell^+X)_\perp,c\bar{c}K_S}$ ($\bar{B}^0 \to B_-$), $\Gamma_{(c\bar{c}K_S)_\perp,\ell^+X}$ ($B_+ \to B^0$), $\Gamma_{(\ell^+X)_\perp,J/\psi K_L}$ ($\bar{B}^0 \to B_+$), $\Gamma_{(J/\psi K_L)_\perp,\ell^+X}$ ($B_- \to B^0$), and their T conjugates, respectively, and finds the measurements of the individual asymmetries to be compatible [3]. We note that the normalization factors $\mathcal{N}_f$ for general CP tags will differ; nevertheless, meaningful experimental asymmetries can be constructed through the use of normalized decay rates as already implemented in BaBar's A_T analysis [3].

Now we generalize the choice of CP final states, so that $J/\psi K_S \to f_o$ and $J/\psi K_L \to f_e$, where "o" ("e") denotes a CP-odd (even) final state. The possible CP asymmetries list in Table 8.2 can be generalized to general CP final states and be defined as

$$\begin{aligned} A_{CP}^{e+} &\equiv \frac{\Gamma'_{(\ell^-X)_\perp,f_e} - \Gamma'_{(\ell^+X)_\perp,f_e}}{\Gamma'_{(\ell^-X)_\perp,f_e} + \Gamma'_{(\ell^+X)_\perp,f_e}} \\ &= C_e \cos(\Delta m_B\, t) - S_e \sin(\Delta m_B\, t)\,, \end{aligned} \tag{8.50}$$

$$\begin{aligned} A_{CP}^{e-} &\equiv \frac{\Gamma'_{(f_e)_\perp,\ell^-X} - \Gamma'_{(f_e)_\perp,\ell^+X}}{\Gamma'_{(f_e)_\perp,\ell^-X} + \Gamma'_{(f_e)_\perp,\ell^+X}} \\ &= C_e \cos(\Delta m_B\, t) + S_e \sin(\Delta m_B\, t)\,, \end{aligned} \tag{8.51}$$

where $A_{CP}^{e+} \to A_{CP}^{o+}$ and $A_{CP}^{e-} \to A_{CP}^{o-}$ follow by replacing $f_e \to f_o$. Note that A_{CP}^{f+}

and A_{CP}^{f-} employ distinct data samples. Moreover,

$$\begin{aligned} A_T^{o+} &\equiv \frac{\Gamma'_{(f_o)_\perp,\ell^- X} - \Gamma'_{(\ell^+ X)_\perp,f_e}}{\Gamma'_{(f_o)_\perp,\ell^- X} + \Gamma'_{(\ell^+ X)_\perp,f_e}} \\ &= \frac{(C_e + C_o)\cos(\Delta m_B\, t) + (S_o - S_e)\sin(\Delta m_B\, t)}{2 + (C_o - C_e)\cos(\Delta m_B\, t) + (S_o + S_e)\sin(\Delta m_B\, t)}\,, \qquad (8.52) \\ A_T^{o-} &\equiv \frac{\Gamma'_{(\ell^- X)_\perp,f_o} - \Gamma'_{(f_e)_\perp,\ell^+ X}}{\Gamma'_{(\ell^- X)_\perp,f_o} + \Gamma'_{(f_e)_\perp,\ell^+ X}} \\ &= \frac{(C_e + C_o)\cos(\Delta m_B\, t) - (S_o - S_e)\sin(\Delta m_B\, t)}{2 + (C_o - C_e)\cos(\Delta m_B\, t) - (S_o + S_e)\sin(\Delta m_B\, t)}\,, \qquad (8.53) \\ A_T^{e+} &\equiv \frac{\Gamma'_{(f_e)_\perp,\ell^- X} - \Gamma'_{(\ell^+ X)_\perp,f_o}}{\Gamma'_{(f_e)_\perp,\ell^- X} + \Gamma'_{(\ell^+ X)_\perp,f_o}} \\ &= \frac{(C_e + C_o)\cos(\Delta m_B\, t) - (S_o - S_e)\sin(\Delta m_B\, t)}{2 - (C_o - C_e)\cos(\Delta m_B\, t) + (S_o + S_e)\sin(\Delta m_B\, t)}\,, \qquad (8.54) \\ A_T^{e-} &\equiv \frac{\Gamma'_{(\ell^- X)_\perp,f_e} - \Gamma'_{(f_o)_\perp,\ell^+ X}}{\Gamma'_{(\ell^- X)_\perp,f_e} + \Gamma'_{(f_o)_\perp,\ell^+ X}} \\ &= \frac{(C_e + C_o)\cos(\Delta m_B\, t) + (S_o - S_e)\sin(\Delta m_B\, t)}{2 - (C_o - C_e)\cos(\Delta m_B\, t) - (S_o + S_e)\sin(\Delta m_B\, t)}\,, \qquad (8.55) \end{aligned}$$

which correspond to possible T asymmetries in Table 8.1 with general CP final states. Each time-dependent asymmetry has four parameters made distinguishable by the various time-dependent functions, and they can be measured experimentally. Indeed the individual asymmetries can be simultaneously fit for $S_o + S_e$, $S_o - S_e$, $C_o + C_e$, and $C_o - C_e$.

The possible CP final states that share a dominant weak phase with each other and with $J/\psi K_{S,L}$ are $f_{o'} = \phi K_S$, ηK_L, $\eta' K_L$, $\rho^0 K_S$, ωK_S, $\pi^0 K_L$ and $f_{e'} = \phi K_L$, ηK_S, $\eta' K_S$, $\rho^0 K_L$, ωK_L, $\pi^0 K_S$, respectively. These are the two-body "sin(2β)" modes commonly studied[4] to test its universality [143, 144]. Not only can we use these modes to form the A_T asymmetries we have discussed thus far [145], such as the comparison of $\bar{B}^0 \to B_{o'}$ with $B_{o'} \to \bar{B}^0$, we can form two more for each one: e.g., we can compare $\bar{B}^0 \to B_{o'}$ to $B_o \to \bar{B}^0$, as well as $\bar{B}^0 \to B_o$ to $B_{o'} \to \bar{B}^0$. Turning to Eq. (8.55), we see that the parameters associated with the $\sin(\Delta m_B t)$ terms in these comparisons are, e.g., $S_{o'} - S_e$ and $S_{o'} + S_e$. In $S_{o'} + S_e$ the dominant weak phase contributions (in the SM) cancel, and the small terms, namely, the penguin contributions, as well as possible contributions from new physics, are determined directly.

[4]Three-body decays, such as $K_S K_S K_S$ or $K^+ K^- K_S$, have also been studied, though determining the CP content of the $K^+ K^- K_S$ Dalitz plot requires an angular moment analysis [141, 142].

Here to demonstrate this, we first work out the parameter λ. As defined in Ref. [146], we can also rewrite Eqs. 8.40 as

$$A_{\overline{B}\to f} = (V_{cb}^* V_{cs}) a_f^c + (V_{ub}^* V_{us}) a_f^u \propto 1 + e^{-i\gamma} d_f, \tag{8.56}$$

where

$$d_f = \left| \frac{V_{ub} V_{us}^*}{V_{cb} V_{cs}^*} \right| \frac{a_f^u}{a_f^c}, \tag{8.57}$$

in which "a_f^c" and "a_f^u" contain the magnitudes of the amplitude associated with each phase, including diagrammatic tree and penguin contributions and γ is another CKM unitarity angle, $\gamma \equiv \arg[-(V_{ub}V_{us}^*)/(V_{cb}V_{cs}^*)]$. Moreover, the parameter λ becomes

$$\lambda_f = -\eta_{CP}^f e^{-2i\beta} \frac{1 + d_f e^{-i\gamma}}{1 + d_f e^{i\gamma}}, \tag{8.58}$$

where $CP|f\rangle = \eta_{CP}^f |f\rangle$. A simple calculation gives us: [146]

$$\begin{aligned} S_f &= -\eta_{CP}^f \frac{\sin(2\beta) + 2\Re(d_f)\sin(2\beta+\gamma) + |d_f|^2 \sin(2\beta+2\gamma)}{1 + |d_f|^2 + 2\Re(d_f)\cos(\gamma)}, \\ C_f &= \frac{-2\Im(d_f)\sin(\gamma)}{1 + |d_f|^2 + 2\Re(d_f)\cos(\gamma)}. \end{aligned} \tag{8.59}$$

We remind the reader that we denote all wrong phase contributions as "penguin contributions". Note that setting the smaller, penguin contributions to zero, i.e. $a_f^u = 0$, we obtain a simplified expressions $C_f = 0$, $S_f = -\eta_{CP}^f \sin(2\beta)$ for all f. It is convenient to define ΔS_f such that $S_f = -\eta_{CP}^f(\sin(2\beta) + \Delta S_f)$.

Several theoretical studies have been made of the deviations of S_f, measured through A_{CP}^{f+}, from $\sin(2\beta)$ in the SM [146, 147, 148]. Experimentally one can form

$$\Delta S_f = -\eta_{CP}^f S_f - \sin(2\beta) \tag{8.60}$$

using the determination of $\sin(2\beta)$ in $B \to c\bar{c}\, K_S$ and $J/\Psi K_L$ final states [149, 3], though the error in ΔS_f is dominantly that in S_f. We now compare this procedure to our A_T method with generalized CP tags. In this new case, assuming $\sin(2\beta)$ universality, the $\sin(2\beta)$ term in S_f cancels, yielding

$$(S_e + S_o) = \Delta S_o - \Delta S_e \tag{8.61}$$

and providing a direct measurement of the difference of deviations from $\sin(2\beta)$ for the chosen CP tags. If we use a "golden mode" for which $\Delta S_{e(o)} \approx 0$, such as $J/\Psi K_{S,L}$, to define $\sin(2\beta)$, then $S_e + S_o \approx \pm\sin(2\beta_{o(e)}) \mp \sin(2\beta) \pm \Delta S_{o(e)}$, where the upper sign

is associated with o. Thus we test the deviation of S_f from $\sin(2\beta)$ through a single asymmetry measurement, whereas a "double" difference appears in Eq. (8.60). Of course $\sin(2\beta)$ in $B \to c\bar{c}\,K_S$, $J/\Psi K_L$ decays is very well known (0.677 ± 0.020 [133]), so that it is more pertinent to note that the asymmetry A_T can directly employ these highly precise decay samples as well [149, 3].

An asymmetry A_T generally requires the comparison of the rates $((\ell^\pm X)_\perp, f_{o(e)})$ and $((f_{e'(o')})_\perp, \ell^\pm X)$, or of their time conjugates, while A_{CP} only requires the comparison of the $((\ell^\pm X)_\perp, f_{o'(e')})$ rates. Thus in the case of $\eta' K_S$, e.g., the determination of $S_{e'}$ via A_{CP} employs two subsamples of limited statistics, whereas the determination of $S_{e'} + S_o$ via A_T is formed from the comparison of a limited statistics sample with the plentiful statistics of $c\bar{c}K_S$. Consequently, we expect improved access to $\Delta S_{e'}$, for any of the CP-even modes that probe $\sin(2\beta)$, and analogous improvements to the determination of $\Delta S_{o'}$ for any of the CP-odd modes. Current experimental results for S_f have limited precision in many of the $\sin(2\beta)$ modes previously listed as CP-tag candidates (e.g., $-\eta^f_{CP} S_{\pi^0 K_S} = 0.57 \pm 0.17$; $-\eta^f_{CP} S_{\omega K_S} = 0.45 \pm 0.24$ [133]). Our method will be of greatest impact for these more poorly known modes. Comparing these results against predicted values of $\Delta S_{o'(e')}$ in the SM should then yield sharper tests of new physics; diverse sources of the latter have been proposed [150, 151, 152, 153, 148].

The method we have proposed can be generalized to other sorts of decay modes, such as those that probe $\sin(2\alpha)$. The basic idea is that the CP-tagging modes are chosen so that their dominant decay amplitudes are identical. In the cases we have considered above, the CP-even and odd tags are chosen with a common dominant weak phase of $\sin(2\beta)$. In so doing, A_T is no longer a true test of T, but we introduce new observables that permit a direct measurement of small departures from weak-phase universality. If the dominant weak phase is universal, then these observables measure the penguin pollution in these decays.

8.4 CP violation in $n\bar{n}$ oscillations

In this section, I will argue how the indeterminacy of the CP transformation property of operator $\mathcal{O}_1$ disproves this claim, how the indeterminacy is related to field rephasing discussed in Ref. [89], and thus that the observation of $n - \bar{n}$ oscillation itself cannot also prove the existence of CP violation in this system. However, sufficient conditions for CP violation to be manifest in $n - \bar{n}$ oscillations have been discussed in Ref. [90], and its brief summary will also be presented in this section.

8.4.1 Indeterminate CP transformation phase

In Chap. 3, we found that only half of the B-L violating operators remain once the correct phase constraint is applied. Now we turn to the analysis of the CP properties of the surviving B-L violating operators:

$$\mathcal{O}_1 = \psi^T C\psi + h.c. \qquad \overset{\mathbf{CP}}{\Longrightarrow} -(\eta_c\eta_p)^2\,, \tag{8.62}$$

$$\mathcal{O}_2 = \psi^T C\gamma_5\psi + h.c. \qquad \overset{\mathbf{CP}}{\Longrightarrow} -(\eta_c\eta_p)^2\,, \tag{8.63}$$

$$\mathcal{O}_4 = \psi^T C\gamma^\mu\gamma_5\psi\,\partial^\nu F_{\mu\nu} + h.c. \qquad \overset{\mathbf{CP}}{\Longrightarrow} -(\eta_c\eta_p)^2\,, \tag{8.64}$$

where we have left the phase dependence explicit. Previously, we have determined that $\eta_p^2 = -1$. However, the CP transformation properties of the operators are not definite, since they are given by η_c^2, and η_c is not determined.

Explicit examples of the indeterminate nature of the CP transformation, illustrated through the phase rotation $\psi \to \psi' = e^{i\theta}\psi$, can be found in Ref. [89]. The noted phase rotation has the effect of changing $\eta_c \to e^{2i\theta}\eta_c$, $\eta_t \to e^{-2i\theta}\eta_t$, with η_p unchanged, under $\psi \to \psi'$ in the C, T, and P transformations, respectively. Note that, in Ref. [89], the phase conventions $\eta_c = \eta_p = 1$ and $\eta_t = i$ are chosen. Although these choices are consistent with the phase constraint we found for the CPT transformation, they are not consistent with the phase constraints for P and TC, though this does not impact their conclusion. If η_c^2 were set to -1, then Eq. 8.62 gives the result reported in Ref. [88].

In the absence of external fields, the possibility of a free $n-\bar{n}$ oscillations is controlled by $|\delta|^2$ [55]. Referring to Eqs. 8.62, 8.63, though only Eq. 8.62 can operate, one finds that the probability transforms as $|\eta_c|^2 = 1$. In other words, although δ does not have definite CP, its associated observable is always CP even. Therefore, the observation of free $n-\bar{n}$ oscillations itself cannot imply the existence of CP violation.

8.4.2 CP violation in $n-\bar{n}$ oscillations through on-shell decays

Recall the system of two neutral mesons that can mix can be described by a 2×2 effective Hamiltonian H. The same idea can also apply to any neutral spin-1/2 system that can oscillate. In vacuum, the H for $n-\bar{n}$ system is given by [90]

$$H = \begin{pmatrix} m_n - \frac{i}{2}\Gamma_n & M_{12} - \frac{i}{2}\Gamma_{12} \\ M_{12}^* - \frac{i}{2}\Gamma_{12}^* & m_n - \frac{i}{2}\Gamma_n \end{pmatrix}, \tag{8.65}$$

with

$$m_n = m_n^*, \qquad \Gamma_n = \Gamma_n^*. \tag{8.66}$$

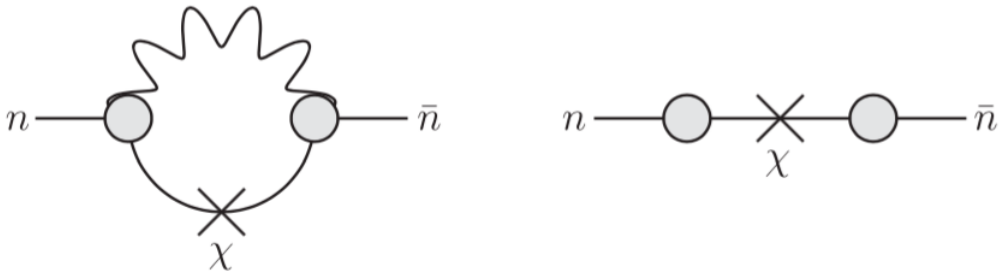

Figure 8.7: The left-hand and right-hand Feynman diagrams as per the model of Ref. [90] gives contributions to Γ_{12} and M_{12}, respectively. The crosses represent χ mass insertions, and the blobs are the high-dimension operators responsible for $n-\chi$ and $\bar{n}-\chi$ transitions. Note that only the imaginary part of the left-hand diagram contributes to Γ_{12}.

It is argued that CP violation in interference between mixing and decays (the third kind of CP violation) is possible in $n-\bar{n}$ system, which leads to a difference between the transition probability of $n \to \bar{n}$ and $\bar{n} \to n$ [90],

$$\frac{P_{|n\rangle\to|\bar{n}\rangle}}{P_{|\bar{n}\rangle\to|n\rangle}} - 1 = \frac{2\Im(M_{12}\Gamma_{12}^*)}{|M_{12}|^2 - |\Gamma_{12}|^2/4 - \Im(M_{12}\Gamma_{12}^*)}. \tag{8.67}$$

In order to observe a non-zero effect, both M_{12} and Γ_{12} cannot be zero. Now it should be obvious that the failure of detailed balance though the operator $\mathcal{O}_1$ itself is impossible, since Γ_{12} vanishes in this case. To break detailed balance, Eq. 8.67 also shows that M_{12} and Γ_{12} cannot be real simultaneously. The authors of Ref. [90] show that Γ_{12} can be realized through an intermediate on-shell χ and photon γ, while M_{12} is from an off-shell intermediate χ exchange. The Feynman diagrams responsible for the two processes are shown in Fig. 8.7. It turns out that CP violation in $n-\bar{n}$ oscillations cannot be a significant effect, and larger CP violation should be expected in a neutral baryon oscillation system which is less directly constrained by nuclear stability. Possible candidates are $\Lambda - \bar{\Lambda}$ or $\Xi^0 - \bar{\Xi}^0$ oscillations [90].

CHAPTER 9

SUMMARY

In the SM, $B - L$ symmetry is perfectly conserved, therefore any observation of $B - L$ violation demonstrates the existence of new physics. $B - L$ violation in the baryon sector can appear in two possible ways, through $|\Delta B| = 1$ or $|\Delta B| = 2$ processes. Using dimensional analysis with current experimental results shows that the observation of $|\Delta B| = 2$ processes would suggest a relatively low scale of new physics. The typical process is $n - \bar{n}$ oscillations, which, if observed, can also help determine the Majorana character of neutrinos. However, the ability to discover $n-\bar{n}$ oscillations is very sensitive to the "environment". In the presence of magnetic field or matter effects, the energies of a neutron and antineutron become different, and the $n - \bar{n}$ transition probability becomes suppressed. Unless the magnetic fields and matter effects are reduced to the extent that a "quasi-free" condition is realized, the transition probability is always quenched.

In order to explore other possibilities for the discovery of $B - L$ violation in the quark sector, we studied the Lorentz invariant $B - L$ violating operators with lowest mass dimensions. After applying the CPT transformation to these operators, we found that they did not possess a definite CPT transformation property. Moreover, half of them vanish due to the anti-commuting nature of fermion fields. What is worse is that due to arbitrary choices of phase convention, a "wrong CPT" problem appears. We found, rather, that the arbitrary phases that appear in discrete symmetry transformations are not arbitrary. We determined the restrictions on the phases associated with the discrete symmetry transformations C, P, and T of fermion fields that appears in theories of $B-L$ violation by generalizing the earlier work of Ref. [19]. We found that the phase associated with the transformation of a fermon field under CPT, η_{cpt}, must always be imaginary and that the phase associated with P, η_p, or equally CT, η_{ct}, must be imaginary for fermions for which a P transformation exists. However, phases associated with other discrete symmetries or combinations of discrete symmetries, e.g., CP, remain indeterminate for $B - L$ violating operators. Nevertheless, with correct η_{cpt} applied, the "wrong" CPT problem is automatically solved as we describe in Chap. 3.

We connected the ability to write down CPT odd operators, though they even-

tually vanish identically, to theories of self-conjugate isofermions, for which locality fails [91, 92, 93, 94], and the CPT properties are anomalous. From the study of self-conjugate isofermions, we found that it is impossible to study $n-\bar{n}$ oscillations in QCD in the chiral limit.

Although the phase constraint on η_{cpt} determined that magnetic fields do indeed quench $n-\bar{n}$ oscillations mediated by the operator $\psi^T C\psi + h.c.$, we argued that spin dependence could still play a key role in $n-\bar{n}$ transitions. In particular, we proposed a $n-\bar{n}$ conversion operator associated with an electromagnetic current. We studied the $n-\bar{n}$ transition probability in a 4×4 effective Hamiltonian framework in the soft photon emission limit. We showed that the spin-flip effect does result in a non-quenching transition probability that is no longer sensitive to the presence of magnetic fields or matter.

We proposed a new mechanism, which we call $n-\bar{n}$ conversion, in which the change of a neutron into an antineutron is mediated by an external source, as can occur in a scattering process. At the nuclear level, that is at low energy scales smaller than Λ_{QCD}, naive dimension analysis implies that $n-\bar{n}$ conversion processes will be suppressed by 3 powers of the new-physics scale, Λ_{BSM}, compared with $n-\bar{n}$ oscillation processes. However, we found that this numerical comparison need not hold, by studying an explicit example. That is, we related $n-\bar{n}$ conversion to $n-\bar{n}$ oscillation by including electromagnetic interactions in the energy scale between Λ_{QCD} and Λ_{BSM}. Starting with a complete set of $n-\bar{n}$ operators at such an intermediate energy scale, we dressed each electrically charged quark with a soft photon to determine the effective six-fermion $n-\bar{n}$ oscillation operators. The coupling parameter of the conversion operators below energy scale Λ_{QCD} can be connected to the matrix elements of six-fermion conversion operators, which we evaluated in the MIT bag model. Then, due to the inner connections between six-fermion oscillation and conversion operators, a relation between the low energy coupling parameters associated with oscillation and conversion operators was established. We found that not only are $n-\bar{n}$ conversion processes not suppressed, but rather that they can be greatly enhanced. The possibility of $n-\bar{n}$ conversions provides opportunities to explore $n-\bar{n}$ transitions through scattering experiments. Moreover, due to their connection to $n-\bar{n}$ oscillations, we can compare the sensitivity of such experiments, under limited assumptions, to $n-\bar{n}$ oscillation experiments. As a result of our analysis, we focused on forward scattering processes, and we considered three possible reactions: (1) electrons scattering with a neutron target transfer the neutrons into antineutrons; (2) neutrons scattering with a electron plasma becomes antineutrons;

and (3) neutrons scattering with deuterium target turn into antineutrons. Using the experimentally established technical parameters, we found that slow neutrons scattering with a liquid deuterium target appears to be the most promising proposal. We also performed preliminary estimation of the limits on η for the same proposals and found that proposals (1) and (3) appear to be good choices.

Finally, CP violation in particle-antiparticle systems has been discussed. We generalized the analysis of the time dependent T-violating asymmetry in Ref. [3] to consider different choices of CP tags for which the dominant amplitudes have the same weak phase. We found that it is possible to measure departures from the universality of $\sin(2\beta)$ directly. If $\sin(2\beta)$ is universal, as in the Standard Model, our method permits the direct determination of penguin effects in these channels.

We have also considered the possibility of CP violation in $n - \bar{n}$ oscillations. We showed that due to the indefinite phase associated with CP transformation of $n - \bar{n}$ oscillation operators, the appearance of $n - \bar{n}$ oscillations does not break CP symmetry, in contrast to claims in the literature [88]. However, CP violation in $n - \bar{n}$ oscillations can occur by breaking the detailed balance. One mechanism, e.g., breaking the detailed balance through the appearance of an intermediate state that couples to both n and $\bar{n}$ [90], is briefly discussed.

APPENDIX A

PHASE RESTRICTIONS FOR TWO-COMPONENT FIELDS

In this section we develop the phase restrictions associated with the discrete-symmetry transformations of two-component Majorana fields. We develop these in two different ways: the first by connecting Dirac fields, and our earlier phase constraints, with two-component Majorana fields and the second by analyzing the transformation properties of two-component Majorana fields directly.

In Weyl representation, a Dirac spinor can be written as

$$\psi = \begin{pmatrix} \xi^\alpha \\ \\ \eta_{\dot\beta} \end{pmatrix} . \tag{A.1}$$

where α and β can be 1 or 2. Here we employ the undotted and dotted notation used by Refs. [154, 155]. The undotted contravariant spinor ξ^α and the covariant spinor ξ_α are in the $(\frac{1}{2}, 0)$ representation of the Lorentz group SO(3,1), whereas the dotted covariant spinor $\eta_{\dot\beta}$ and the contravariant spinor $\eta^{\dot\beta}$ are in the $(0, \frac{1}{2})$ representation. One can raise or lower the undotted indices using the metric of SL(2,C)

$$g_{\alpha\beta} = \begin{pmatrix} 0 & 1 \\ \\ -1 & 0 \end{pmatrix} = i\sigma^2_{\alpha\beta}, \tag{A.2}$$

$$g^{\alpha\beta} = \begin{pmatrix} 0 & -1 \\ \\ 1 & 0 \end{pmatrix} = -i\sigma^2_{\alpha\beta}\,, \tag{A.3}$$

i.e.,

$$\xi^\alpha = g^{\alpha\beta}\xi_\beta = -i\sigma^2_{\alpha\beta}\xi_\beta\,, \tag{A.4}$$

and use the same metric for dotted indices.

Since the C and P transformations of Eqs. (3.1,3.2) connect the $(\frac{1}{2}, 0)$ and $(0, \frac{1}{2})$ representations of the Lorentz group and thus the two two-component fields in Eq. (A.1), a particular two-component field cannot transform into itself under P or C. However, it can transform into itself under CP or CPT (or T) [154, 155], so that phase constraints may exist for these particular transformations. We will now determine them in two different ways.

In Chap. 3, we found the phase constraints associated with the discrete-symmetry transformations of a Dirac field. Revisiting the CP and CPT transformations in Weyl representation, we find

$$\mathbf{CP}\begin{pmatrix}\xi^{\alpha}(\mathbf{x},t)\\ \\ \eta_{\dot\beta}(\mathbf{x},t)\end{pmatrix}(\mathbf{CP})^{-1} = \eta_{cp} i\gamma^0\gamma^2\begin{pmatrix}\xi^{\alpha\dagger}(-\mathbf{x},t)\\ \\ \eta^{\dagger}_{\dot\beta}(-\mathbf{x},t)\end{pmatrix}, \tag{A.5}$$

$$\mathbf{CPT}\begin{pmatrix}\xi^{\alpha}(x)\\ \\ \eta_{\dot\beta}(x)\end{pmatrix}(\mathbf{CPT})^{-1} = -\eta_{cpt}\gamma^5\begin{pmatrix}\xi^{\alpha\dagger}(-x)\\ \\ \eta^{\dagger}_{\dot\beta}(-x)\end{pmatrix}. \tag{A.6}$$

Since in Weyl representation

$$i\gamma^0\gamma^2 = \begin{pmatrix}-i\sigma^2 & 0\\ \\ 0 & i\sigma^2\end{pmatrix};\quad \gamma^5 = \begin{pmatrix}-1 & 0\\ \\ 0 & 1\end{pmatrix} \tag{A.7}$$

we use Eq. (A.4), e.g., to find

$$\mathbf{CP}\xi^{\alpha}(\mathbf{x},t)(\mathbf{CP})^{-1} = -\eta_{cp}\xi^{\dagger}_{\alpha}(-\mathbf{x},t), \tag{A.8}$$

$$\mathbf{CP}\eta_{\dot\alpha}(\mathbf{x},t)(\mathbf{CP})^{-1} = -\eta_{cp}\eta^{\dot\alpha\dagger}(-\mathbf{x},t), \tag{A.9}$$

$$\mathbf{CPT}\xi^{\alpha}(x)(\mathbf{CPT})^{-1} = \eta_{cpt}\xi^{\alpha\dagger}(-x), \tag{A.10}$$

$$\mathbf{CPT}\eta_{\dot\alpha}(x)(\mathbf{CPT})^{-1} = -\eta_{cpt}\eta^{\dagger}_{\dot\alpha}(-x), \tag{A.11}$$

where we note, as per Chap. 3, that $\eta_{cpt} \equiv \eta_c\eta_p\eta_t = \pm i$. Here we find no direct constraint on the phase $\eta_{cp} \equiv \eta_c\eta_p$, or η_t for that matter, because the analysis of Chap. 3 determined that the combinations $\eta^*_{cp}\lambda$ and $\eta_t\lambda$ were imaginary and real, respectively. Since the phase λ has no meaning in the current context, no conclusions on η_{cp} or η_t can follow.

An alternate path to these results comes from the analysis of the plane-wave expansion of the two-component Majorana field $\xi_a(x)$ [156, 157]:

$$\xi_{\alpha}(x) = \sum_s \int \frac{d^3\mathbf{p}}{(2\pi)^{3/2}(2E_{\mathbf{p}})^{1/2}}[x_{\alpha}(\mathbf{p},s)a(\mathbf{p},s)e^{-ipx} + \lambda y_{\alpha}(\mathbf{p},s)a^{\dagger}(\mathbf{p},s)e^{ipx}], \tag{A.12}$$

where x_α and y_α are two-component spinors, whose definition can be found in Ref. [157]. Note that we have included a phase factor λ in $\xi_a(x)$, in analogy to the analysis of Chap. 3. It is trivial to check that the phase λ included here functions in the same way as in Eq. (3.40) and that it is forced to 1 when $\xi_\alpha(x)$ is used to constuct a Dirac

field [1]. Using the CP transformation of $\xi_\alpha(\mathbf{x},t)$ [154, 155]

$$\mathbf{CP}\xi_\alpha(\mathbf{x},t)(\mathbf{CP})^{-1} = \eta_{cp}(\xi^\alpha)^\dagger(-\mathbf{x},t) \tag{A.13}$$

and the relations [157]

$$\begin{aligned}(x^\alpha)^\dagger(\mathbf{p},s) &= x^{\dagger\dot\alpha}(\mathbf{p},s) = -y_\alpha(-\mathbf{p},s)\,, &\text{(A.14)}\\ (y^\alpha)^\dagger(\mathbf{p},s) &= y^{\dagger\dot\alpha}(\mathbf{p},s) = x_\alpha(-\mathbf{p},s) &\text{(A.15)}\end{aligned}$$

yield

$$\begin{aligned}\mathbf{CP}a(\mathbf{p},s)(\mathbf{CP})^{-1} &= \eta_{cp}\lambda^* a(-\mathbf{p},s)\,, &\text{(A.16)}\\ \mathbf{CP}a^\dagger(\mathbf{p},s)(\mathbf{CP})^{-1} &= -\eta_{cp}\lambda^* a^\dagger(-\mathbf{p},s)\,. &\text{(A.17)}\end{aligned}$$

Since **CP** is a unitary operator, taking the Hermitian conjugate of either relation proves that $\eta_{cp}\lambda^*$ must be imaginary.

Under CPT, we have

$$\mathbf{CPT}\xi^\alpha(x)(\mathbf{CPT})^{-1} = \eta_{cpt}(\xi^\alpha)^\dagger(-x)\,. \tag{A.18}$$

Using the relations [157]

$$\begin{aligned}x^{\dagger\dot\alpha}(\mathbf{p},-s) &= 2sy^{\dagger\dot\alpha}(\mathbf{p},s)\,, &\text{(A.19)}\\ y^{\dagger\dot\alpha}(\mathbf{p},-s) &= -\frac{1}{2s}x^{\dagger\dot\alpha}(\mathbf{p},s)\,, &\text{(A.20)}\end{aligned}$$

we find

$$\begin{aligned}\mathbf{CPT}a(\mathbf{p},s)(\mathbf{CPT})^{-1} &= -\frac{1}{2s}\lambda^*\eta_{cpt}a(\mathbf{p},-s)\,, &\text{(A.21)}\\ \mathbf{CPT}a^\dagger(\mathbf{p},s)(\mathbf{CPT})^{-1} &= 2s\lambda\eta_{cpt}a^\dagger(\mathbf{p},-s)\,. &\text{(A.22)}\end{aligned}$$

Noting that **CPT** is an antiunitary operator, as in Chap. 3, we can take the Hermitian conjugate of either equation to show that η_{cpt} must be imaginary. Alternatively, after Ref. [19], we define $\mathbf{CPT}|0\rangle = |0\rangle$ and note

$$\begin{aligned}1 &= \langle 0|a(\mathbf{p},s)a^\dagger(\mathbf{p},s)|0\rangle\\ &= \langle 0|\mathbf{CPT}a(\mathbf{p},s)\mathbf{CPT}^{-1}\mathbf{CPT}a^\dagger(\mathbf{p},s)\mathbf{CPT}^{-1}|0\rangle\,. &\text{(A.23)}\end{aligned}$$

Then using Eqs. (A.21,A.22) shows that $\eta_{cpt} = \pm i$.

In summary, we have used two methods to find the phase constraints on **CP** and **CPT** for two-component fields, and have obtained the same results, which are that η_{cp} itself is unconstrained, though $\eta_{cp}\lambda^*$ must be imaginary, and η_{cpt} is always $\pm i$.

[1] Although the notation for a Dirac field employed by Refs. [154, 155] and [157] differs, our results are unchanged.

BIBLIOGRAPHY

[1] J. H. Christenson, J. W. Cronin, V. L. Fitch, and R. Turlay, "Evidence for the 2π Decay of the K_2^0 Meson," *Phys. Rev. Lett.* 13, 138, 1964.

[2] L. Wolfenstein, "Violation of CP Invariance and the Possibility of Very Weak Interactions," *Phys. Rev. Lett.* 13, 562, 1964.

[3] J. P. Lees *et al.* [BaBar Collaboration], "Observation of Time Reversal Violation in the B^0 Meson System," *Phys. Rev. Lett.* 109, 211801, 2012

[4] A. Sakharov, "Violation of CP Invariance, C Asymmetry, and Baryon Asymmetry of the Universe," *JETP* 5, 24, 1967

[5] G. 't Hooft, "Symmetry Breaking Through Bell-Jackiw Anomalies," *Phys. Rev. Lett.* 37, 8, 1976.

[6] S. Dimopoulos and L. Susskind, "On the Baryon Number of the Universe," *Phys. Rev. D* 18, 4500, 1978.

[7] N. S. Manton, "Topology in the Weinberg-Salam Theory," *Phys. Rev. D* 28, 2019, 1983.

[8] F. R. Klinkhamer and N. S. Manton, "A Saddle Point Solution in the Weinberg-Salam Theory," *Phys. Rev. D* 30, 2212, 1984.

[9] V. A. Kuzmin, V. A. Rubakov, and M. E. Shaposhnikov, "On the Anomalous Electroweak Baryon Number Nonconservation in the Early Universe," *Phys. Lett. B* 155, 36, 1985.

[10] G. Gelmini and E. Roulet, "Neutrino masses," *Rept. Prog. Phys.* 58, 1207, 1995. [hep-ph/9412278].

[11] V. N. Gribov and B. Pontecorvo, "Neutrino astronomy and lepton charge," *Phys. Lett. B* 28, 493, 1969.

[12] S. M. Bilenky and B. Pontecorvo, "Neutrino Oscillations With Large Oscillation Length in Spite of Large (Majorana) Neutrino Masses?," *Sov. J. Nucl. Phys.* 38, 248, 1983. [Lett. Nuovo Cim. 37, 467 (1983)] [Yad. Fiz. 38, 415 (1983)].

[13] S. R. Elliott and P. Vogel, "Double beta decay," *Ann. Rev. Nucl. Part. Sci.* 52, 115, 2002. [hep-ph/0202264].

[14] J. D. Vergados, H. Ejiri, and F. Simkovic, "Theory of Neutrinoless Double Beta Decay," *Rept. Prog. Phys.* 75, 106301, 2012

[15] W. Rodejohann, "Neutrinoless Double beta Decay and Neutrino Physics," *J. Phys. G* 39, 124008, 2012

[16] J. Schechter and J. W. F. Valle, "Neutrinoless Double beta Decay in SU(2) x U(1) Theories," *Phys. Rev. D* 25, 2951, 1982.

[17] M. Doi, T. Kotani, H. Nishiura, K. Okuda, and E. Takasugi, "CP Violation in Majorana Neutrinos," *Phys. Lett. B* 102, 323, 1981.

[18] L. Wolfenstein, "CP Properties of Majorana Neutrinos and Double beta Decay," *Phys. Lett. B* 107B, 77, 1981.

[19] B. Kayser, "CPT, CP, and C Phases and their Effects in Majorana Particle Processes," *Phys. Rev. D* 30, 1023, 1984.

[20] A. Zee, "A Theory of Lepton Number Violation, Neutrino Majorana Mass, and Oscillation," *Phys. Lett. B* 93, 389, 1980. Erratum: [Phys. Lett. B 95, 461 (1980)].

[21] P. Minkowski, "$\mu \to e\gamma$ at a Rate of One Out of 10^9 Muon Decays?," *Phys. Lett. B* 67, 421, 1977.

[22] M. Gell-Mann, P. Ramond, and R. Slansky, in "Supergravity," ed. by P. van Nieuwenhuizen and D. Z. Freedman, *North Holland Publishing Company*, 1979.

[23] R. N. Mohapatra and G. Senjanovic, "Neutrino Mass and Spontaneous Parity Violation," *Phys. Rev. Lett.* 44, 912, 1980.

[24] K. S. Babu, R. N. Mohapatra, and S. Nasri, "Post-Sphaleron Baryogenesis," *Phys. Rev. Lett.* 97, 131301, 2006

[25] M. Claudson, L. J. Hall, and I. Hinchliffe, "Cosmological Baryon Generation At Low Temperatures," *Nucl. Phys. B* 241, 309, 1984.

[26] J. M. Cline and S. Raby, "Gravitino induced baryogenesis: A Problem made a virtue," *Phys. Rev. D* 43, 1781, 1991.

[27] K. Benakli and S. Davidson, "Baryogenesis in Models with a low Quantum Gravity Scale," *Phys. Rev. D* 60, 025004, 1999.

[28] D. J. H. Chung and T. Dent, "Standard Model Maryogenesis through four fermion operators in Brane worlds," *Phys. Rev. D* 66, 023501, 2002.

[29] B. Dutta, Y. Mimura and R. N. Mohapatra, "Observable N - anti-N oscillation in high scale Seesaw Models," *Phys. Rev. Lett.* 96, 061801, 2006.

[30] K. S. Babu, R. N. Mohapatra and S. Nasri, "Unified TeV Scale Picture of Baryogenesis and Dark Matter," *Phys. Rev. Lett.* 98, 161301, 2007.

[31] K. S. Babu, P. S. Bhupal Dev, E. C. F. S. Fortes, and R. N. Mohapatra, "Post-Sphaleron Baryogenesis and an Upper Limit on the Neutron-Antineutron Oscillation Time," *Phys. Rev. D* 87, 115019, 2013.

[32] J. M. Arnold, B. Fornal, and M. B. Wise, "Simplified Models with Baryon Number Violation but no Proton Decay," *Phys. Rev. D* 87, 075004, 2013.

[33] K. S. Babu and R. N. Mohapatra, "Determining Majorana Nature of Neutrino from Nucleon Decays and $n - \bar{n}$ oscillations," *Phys. Rev. D* 91, 013008, 2015.

[34] V. A. Kuzmin, "CP violation and baryon asymmetry of the universe," *Pisma Zh. Eksp. Teor. Fiz.* 12, 335, 1970. [*JETP Lett.* 12, 228, 1970.]

[35] F. Wilczek and A. Zee, "Operator Analysis of Nucleon Decay," *Phys. Rev. Lett.* 43, 1571, 1979.

[36] L. F. Abbott and M. B. Wise, "The Effective Hamiltonian for Nucleon Decay," *Phys. Rev. D* 22, 2208, 1980.

[37] E. Kearns, *Talk presented at the ISOUP Symposium*, 2013.

[38] S. Rao and R. Shrock, "$n \leftrightarrow \bar{n}$ Transition Operators and Their Matrix Elements in the MIT Bag Model," *Phys. Lett. B* 116, 238, 1982.

[39] M. Baldo-Ceolinp, *et al*, "A New Experimental Limit on Neutron-antineutron Oscillations" *Z. Phys. C* 63, 409, 1994.

[40] K. Abe *et al.* [Super-Kamiokande Collaboration], "The Search for $n-\bar{n}$ oscillation in Super-Kamiokande I," *Phys. Rev. D* 91, 072006, 2015.

[41] S. Weinberg, "Varieties of Baryon and Lepton Nonconservation," *Phys. Rev. D* 22, 1694, 1980.

[42] H. A. Weldon and A. Zee, "Operator Analysis of New Physics," *Nucl. Phys. B* 173, 269, 1980.

[43] K. S. Babu and R. N. Mohapatra, "B-L Violating Proton Decay Modes and New Baryogenesis Scenario in SO(10)," *Phys. Rev. Lett.* 109, 091803, 2012.

[44] K. S. Babu and R. N. Mohapatra, "B-L Violating Nucleon Decay and GUT Scale Baryogenesis in SO(10)," *Phys. Rev. D* 86, 035018, 2012.

[45] S. Seidel *et al.*, "Search for Multitrack Nucleon Decay," *Phys. Rev. Lett.* 61, 2522, 1988.

[46] R. N. Mohapatra and R. E. Marshak, "Local B-L Symmetry of Electroweak Interactions, Majorana Neutrinos and Neutron Oscillations," *Phys. Rev. Lett.* 44, 1316. 1980. Erratum:*Phys. Rev. Lett.* 44, 1643, 1980].

[47] T. K. Kuo and S. T. Love, "Neutron Oscillations and the Existence of Massive Neutral Leptons," *Phys. Rev. Lett.* 45, 93, 1980.

[48] J. F. Nieves, "Baryon and Lepton Number Nonconserving Processes and Intermediate Mass Scales," *Nucl. Phys. B* 189, 182, 1981.

[49] K. S. Babu and R. N. Mohapatra, "Coupling Unification, GUT-Scale Baryogenesis and Neutron-Antineutron Oscillation in SO(10)," *Phys. Lett. B* 715, 328, 2012. [arXiv:1206.5701 [hep-ph]].

[50] D. G. Phillips, II *et al.*, "Neutron-Antineutron Oscillations: Theoretical Status and Experimental Prospects," *Phys. Rept.* 612, 1, 2016

[51] R. N. Mohapatra, "Neutron-Anti-Neutron Oscillation: Theory and Phenomenology," *arXiv:* 0902.0834 [hep-ph], 2009.

[52] B. O. Kerbikov, "Quantum Damping of Neutron-antineutron Oscillations," *arXiv:*1704.07117, 2017 [hep-ph].

[53] S. Gardner and X. Yan, "CPT, CP, and C transformations of fermions, and their consequences, in theories with B-L violation," *Phys. Rev. D* 93, 096008, 2016. [arXiv:1602.00693 [hep-ph]].

[54] R. Dadisman, S. Gardner, and X. Yan, "Trapping Penguins with Entangled B Mesons," *Phys. Lett. B* 754, 1, 2016. [arXiv:1409.6801 [hep-ph]].

[55] R. N. Mohapatra and R. E. Marshak, "Phenomenology Of Neutron Oscillations," *Phys. Lett. B* 94, 183, 1980.

[56] R. Cowsik and S. Nussinov, "SOME CONSTRAINTS ON DELTA B = 2 n anti-n OSCILLATIONS," *Phys. Lett. B* 101, 237, 1981.

[57] C. Patrignani *et al.* [Particle Data Group], "Review of Particle Physics," *Chin. Phys. C* 40, 100001, 2016.

[58] D. Milstead, "A New High Sensitivity Search for Neutron-antineutron Oscillations at the ESS," *PoS EPS -HEP2015*, 603, 2015. [arXiv:1510.01569]

[59] C. B. Dover, A. Gal and J. M. Richard, "Neutron Anti-neutron Oscillations In Nuclei," *Phys. Rev. D* 27, 1090, 1983.

[60] C. B. Dover, A. Gal and J. M. Richard, "Limits On The Neutron Anti-neutron Oscillation Time From The Stability Of Nuclei," *Phys. Rev. C* 31, 1423, 1985.

[61] C. B. Dover, A. Gal and J. M. Richard, "Neutron-antineutron Oscillations in Nuclei." *Nucl. Instrum. Methods Phys. Res., Sect. A* 284, 13, 1989.

[62] E. Friedman and A. Gal, "Realistic Calculations of Nuclear Disappearance lifetimes induced by n anti-n oscillations," *Phys. Rev. D* 78, 016002, 2008. [arXiv:0803.3696 [hep-ph]].

[63] B. Aharmim *et* al. [SNO Collaboration], "The search for neutron-antineutron oscillations at the Sudbury Neutrino Observatory," *arXiv*:1705.00696 [hep-ex].

[64] J. Chung *et al.*, "Search for neutron anti-neutron oscillations using multiprong events in Soudan 2," *Phys. Rev. D* 66, 032004, 2002. [hep-ex/0205093].

[65] B. O. Kerbikov, M. S. Lukashov, Y. A. Kamyshkov, and L. J. Varriano, "Damping and Decoherence in Neutron Oscillations," *arXiv:*1512.03398 [hep-ph].

[66] A. Kossakowski, "On quantum statistical mechanics of non-Hamiltonian systems," *Rep. Math. Phys.* 3, 247, 1972.

[67] G. Lindblad, "On the Generators of Quantum Dynamical Semigroups," *Commun. Math. Phys.* 48, 119, 1976.

[68] F. Bloch, "Nuclear Induction," *Phys. Rev.* 70, 460, 1946.

[69] C. Csaki, E. Kuflik, and T. Volansky, "Dynamical R-Parity Violation," *Phys. Rev. Lett.* 112, 131801, 2014. [arXiv:1309.5957 [hep-ph]].

[70] J. L. Goity and M. Sher, "Bounds on $\Delta B = 1$ couplings in the supersymmetric standard model," *Phys. Lett. B* 346, 69, 1995. Erratum: [*Phys. Lett. B* 385, 500, 1996]

[71] C. Berger *et al.* [Frejus Collaboration], "Lifetime limits on (B-L) violating nucleon decay and dinucleon decay modes from the Frejus experiment," *Phys. Lett. B* 269, 227, 1991.

[72] M. Litos *et al.*, "Search for Dinucleon Decay into Kaons in Super-Kamiokande," *Phys. Rev. Lett.* 112, 131803, 2014.

[73] J. Gustafson *et al.* [Super-Kamiokande Collaboration], "Search for dinucleon decay into pions at Super-Kamiokande," *Phys. Rev. D* 91, 072009, 2015. [arXiv:1504.01041 [hep-ex]].

[74] R. Feynman, "The Character of Physical Law," *The MIT Press*, Cambridge, Massachusetts, London, England, 1967.

[75] I. I. Y. Bigi and A. I. Sanda, "CP violation," *Camb. Monogr. Part. Phys. Nucl. Phys. Cosmol.* 9, 1, 2000.

[76] A. Halprin, S. T. Petcov and S. P. Rosen, "Effects of Light and Heavy Majorana Neutrinos in Neutrinoless Double Beta Decay," *Phys. Lett. B* 125, 335, 1983.

[77] B. Kayser and A. S. Goldhaber, "CPT and CP Properties of Majorana Particles, and the Consequences," *Phys. Rev. D* 28, 2341, 1983.

[78] G. Feinberg and S. Weinberg, "On the phase factors in inversions," *Nuovo Cimento* 14, 571, 1959.

[79] P. A. Carruthers, "Spin and Isospin in Particle Physics," *Gordon and Breach, New York*, p.133, 1971.

[80] W. C. Haxton and G. J. Stephenson, "Double beta Decay," *Prog. Part. Nucl. Phys.* 12, 409, 1984.

[81] G. C. Branco, L. Lavoura, and J. P. Silva, *CP Violation* (Oxford University Press, New York, 1999)

[82] R. N. Mohapatra and P. B. Pal, "Massive neutrinos in physics and astrophysics. Second edition," *World Sci. Lect. Notes Phys.* 72, 1, 2004.

[83] M. E. Peskin and D. V. Schroeder, "An Introduction To Quantum Field Theory," *Westview Press*, 1995.

[84] R. F. Streater and A. S. Wightman, "PCT, spin and statistics, and all that," *Princeton University Press, Princeton*, 2000.

[85] O. W. Greenberg, "CPT violation implies violation of Lorentz invariance," *Phys. Rev. Lett.* 89, 231602, 2002. [hep-ph/0201258].

[86] A. Chodos, R. L. Jaffe, K. Johnson, C. B. Thorn, and V. F. Weisskopf, "A New Extended Model of Hadrons," *Phys. Rev. D* 9, 3471, 1974.

[87] A. Chodos, R. L. Jaffe, K. Johnson, and C. B. Thorn, "Baryon Structure in the Bag Theory," *Phys. Rev. D* 10, 2599, 1974.

[88] Z. Berezhiani and A. Vainshtein, "Neutron-Antineutron Oscillation as a Signal of CP Violation," *arXiv:1506.05096* [hep-ph].

[89] K. Fujikawa and A. Tureanu, "Neutron-antineutron oscillation and parity and CP symmetries," *arXiv:1510.00868 [hep-ph]*, 2015.

[90] D. McKeen and A. E. Nelson, "CP Violating Baryon Oscillations," *Phys. Rev. D* 94, 076002, 2016. [arXiv:1512.05359 [hep-ph]].

[91] P. Carruthers, "Locality and the isospin of self-conjugate bosons," *Phys. Rev. Lett.* 18, 353, 1967.

[92] Huan Lee, "Nonexistence of self-conjugate particles with half-integral isospin," *Phys. Rev. Lett.* 18, 1098, 1967.

[93] G. N. Fleming and E. Kazes, "Microcausality and the Representations of Self-Conjugate Bosons," *Phys. Rev. Lett.* 18, 764, 1967.

[94] Y. S. Jin, "General proof of Carruthers theorem," *Phys. Lett. B* 24, 411, 1967.

[95] P. Carruthers, "Local field theory and isospin invariance. 1. free field theory of spinless bosons," *J. Math. Phys.* 9, 928, 1968.

[96] P. Carruthers, "Local field theory and isospin invariance. 2. free field theory of arbitrary spin particles," *J. Math. Phys.* 9, 1835, 1968.

[97] P. Carruthers, "Local field theory and isospin invariance. 3. interactions of self-conjugate isofermion fields," *Phys. Rev.* 172, 1406, 1968.

[98] P. Carruthers, "Isospin symmetry, TCP , and local field theory," *Phys. Lett. B* 26, 158, 1968.

[99] S. Rao and R. E. Shrock, "Six Fermion $(B-L)$ Violating Operators of Arbitrary Generational Structure," *Nucl. Phys. B* 232, 143, 1984.

[100] W.E. Caswell, J. Milutinovic, and G. Senjanovic, "Matter - antimatter transition operators: a manual for modeling," *Phys. Lett. B* 122, 373, 1983.

[101] R. Gupta, "Introduction to lattice QCD: Course," *hep-lat/*9807028.

[102] M. I. Buchoff, C. Schroeder, and J. Wasem, "Neutron-antineutron oscillations on the lattice," *PoS LATTICE 2012*, 128, 2012. [arXiv:1207.3832 [hep-lat]].

[103] S. Syritsyn, M. I. Buchoff, C. Schroeder, and J. Wasem, "Neutron-antineutron oscillation matrix elements with domain wall fermions at the physical point," *PoS LATTICE 2015*, 132, 2016.

[104] A. Chodos and C. B. Thorn, "Chiral invariance in a bag theory," *Phys. Rev. D* 12, 2733, 1975

[105] A. W. Thomas, "Chiral Symmetry and the Bag Model: A New Starting Point for Nuclear Physics," *Adv. Nucl. Phys.* 13, 1, 1984.

[106] C. J. Benesh and G. A. Miller, "Deep Inelastic Structure Functions in the MIT Bag Model," *Phys. Rev. D* 36, 1344, 1987.

[107] R. E. Shrock and S. B. Treiman, "$K^0 \leftrightarrow \bar{K}^0$ Transition Amplitude in the MIT Bag Model," *Phys. Rev. D* 19, 2148, 1979.

[108] J. Pasupathy, "The Neutron - Anti-neutron Transition Amplitude in the MIT Bag Model", *Phys. Lett. B* 114, 172, 1982.

[109] T. A. DeGrand, R. L. Jaffe, K. Johnson, and J. E. Kiskis, "Masses and Other Parameters of the Light Hadrons," *Phys. Rev. D* 12, 2060, 1975.

[110] M. I. Buchoff and M. Wagman, "Perturbative Renormalization of Neutron-Antineutron Operators," *Phys. Rev. D* 93, 016005, 2016. [arXiv:1506.00647 [hep-ph]].

[111] S. Gardner and E. Jafari, "Phenomenology of n-$\bar{n}$ Oscillations Revisited," *Phys. Rev. D* 91, 096010, 2015. [arXiv:1408.2264 [hep-ph]].

[112] M. Voloshin (private communication)

[113] I. I. Rabi, "Some constraints on $\delta B = 2$ $n - \bar{n}$ oscillations," *Phys. Rev.* 51, 652, 1937.

[114] C. Cohen-Tannoudji *e*t al., "Quantum Mechanics," *Cambridge University Press, Cambridge, England*, 2000.

[115] P. T. Winslow and J. N. Ng, "Neutron-Antineutron Oscillations in a Warped Extra Dimension," *Phys. Rev. D* 81, 106010, 2010. [arXiv:1003.1424 [hep-th]].

[116] M. Ozer, "Neutron Anti-neutron Oscillations And Renormalization Effects For Delta B = 2 Six Quark Operators," *Phys. Rev. D* 26, 3159, 1982.

[117] S. Nussinov and R. Shrock, "N - anti-N oscillations in models with large extra dimensions," *Phys. Rev. Lett.* 88, 171601, 2002. [hep-ph/0112337].

[118] K. S. Babu, P. S. Bhupal Dev and R. N. Mohapatra, "Neutrino mass hierarchy, neutron - anti-neutron oscillation from baryogenesis," *Phys. Rev. D* 79, 015017, 2009. [arXiv:0811.3411 [hep-ph]].

[119] W. Herr and B. Muratori, "Concept of luminosity," *https://cds.cern.ch/record/941318/files/p361.pdf*

[120] J. Balewski *et al.*, "The DarkLight Experiment: A Precision Search for New Physics at Low Energies," *arXiv:*1412.4717 [physics.ins-det].

[121] L. Brillouin, "A Theorem of Larmor and Its Importance for Electrons in Magnetic Fields," *Phys. Rev.* 67, 260, 1945.

[122] J. D. Bowman and V. Gudkov, "Search for time reversal invariance violation in neutron transmission," *Phys. Rev. C* 90, 065503, 2014. [arXiv:1407.7004 [hep-ph]].

[123] Clusius, K., and Bartholome E., "Calorische und Thermische Eigenschaften des Kondensierten Schweren Wasserstoffs", *Z. physik. Chem. B* 30, 237-57, 1935.

[124] E. T. Jurney, P. J. Bendt, and J. C. Browne, "Thermal neutron capture cross section of deuterium," *Phys. Rev. C* 25, 2810, 1982.

[125] R. C. Fernow, "Introduction to Experimental Particle Physics," *Cambridge University Press*, 1989.

[126] G. Sciolla, "The Mystery of CP Violation," MIT Physics Annual, 27/ 04/ 14 (2006)

[127] J. H. Christenson, J. W. Cronin, V. L. Fitch, and R. Turlay, "Evidence for the 2π Decay of the K_2^0 Meson," *Phys. Rev. Lett.* 13, 138, 1964.

[128] K. Nakamura *et al.* [Particle Data Group], "Review of Particle Physics," *JPG* 37, 075021, 2010

[129] Y. Nir, "CP violation in meson decays," *arXiv:hep-ph/0510413*, 2005.

[130] N. Cabibbo, "Unitary Symmetry and Leptonic Decays," *Phys. Rev. Lett.* 10, 531, 1963.

[131] M. Kobayashi and T. Maskawa, "CP Violation in the Renormalizable Theory of Weak Interaction," *Prog. Theor. Phys.* 49, 652, 1973.

[132] Y. Nir and H. R. Quinn, "CP violation in B physics," *Ann. Rev. Nucl. Part. Sci.* 42, 211, 1992.

[133] A. J. Bevan *et al.* [BaBar and Belle Collaborations], "The Physics of the B Factories," *Eur. Phys. J. C* 74, 3026, 2014.

[134] A. Angelopoulos *et al.* [CPLEAR Collaboration], "First direct observation of time reversal noninvariance in the neutral kaon system," *Phys. Lett. B* 444, 43, 1998.

[135] L. Wolfenstein, "The search for direct evidence for time reversal violation," *Int. J. Mod. Phys. E* 8, 501, 1999.

[136] L. Wolfenstein, "CP violation," *arXiv:hep-ph/0011400*, 2000.

[137] M. C. Banuls and J. Bernabeu, "CP, T and CPT versus temporal asymmetries for entangled states of the B(d) system," *Phys. Lett. B* 464, 117, 1999. [hep-ph/9908353].

[138] J. Bernabeu and F. Martinez-Vidal, "Colloquium: Time-reversal violation with quantum-entangled B mesons," *Rev. Mod. Phys.* 87, 165, 2015. [arXiv:1410.1742 [hep-ph]].

[139] J. Bernabeu, F. Martinez-Vidal, and P. Villanueva-Perez, "Time Reversal Violation from the entangled B0-antiB0 system," *JHEP* 1208, 064, 2012. [arXiv:1203.0171 [hep-ph]].

[140] E. Applebaum, A. Efrati, Y. Grossman, Y. Nir, and Y. Soreq, "Subtleties in the $BABAR$ measurement of time-reversal violation," *Phys. Rev. D* 89, 076011, 2014. [arXiv:1312.4164 [hep-ph]].

[141] T. Gershon and M. Hazumi, "Time dependent CP violation in $B^0 \to P^0 P^0 X^0$ decays," *Phys. Lett. B* 596, 163, 2004. [hep-ph/0402097].

[142] J. P. Lees *et al.* [BaBar Collaboration], "Study of CP violation in Dalitz-plot analyses of $B^0 \to K^+K^-K^0(S)$, $B^+ \to K^+K^-K^+$, and $B^+ \to K^0(S)K^0(S)K^+$," *Phys. Rev. D* 85, 112010, 2012. [arXiv:1201.5897 [hep-ex]].

[143] J. Beringer *et al.* [Particle Data Group Collaboration], "Review of Particle Physics (RPP)," *Phys. Rev. D* 86, 010001, 2012.

[144] T. Aushev *et al.*, "Physics at Super B Factory," *arXiv:1002.5012 [hep-ex]*, 2010.

[145] A. Bevan, G. Inguglia, and M. Zoccali, "Neutral meson tests of time-reversal symmetry invariance," *arXiv:1302.4191 [hep-ph]*, 2013.

[146] M. Beneke, "Corrections to $\sin(2\beta)$ from CP asymmetries in $B^0 \to (\pi^0, \rho^0, \eta, \eta', \omega, \phi)K(S)$ decays," *Phys. Lett. B* 620, 143, 2005.

[147] H. -Y. Cheng, C. -K. Chua, and A. Soni, "Effects of final-state interactions on mixing-induced CP violation in penguin-dominated B decays," *Phys. Rev. D* 72, 014006, 2005. [hep-ph/0502235].

[148] G. Buchalla, G. Hiller, Y. Nir, and G. Raz, "The Pattern of CP asymmetries in B —¿ s transitions," *JHEP* 0509, 074, 2005. [hep-ph/0503151v3].

[149] I. Adachi *et al.*, "Precise measurement of the CP violation parameter $\sin(2\phi_1)$ in $B^0 \to (c\bar{c})K^0$ decays," *Phys. Rev. Lett.* 108, 171802, 2012. [arXiv:1201.4643 [hep-ex]].

[150] Y. Grossman and M. P. Worah, "CP asymmetries in B decays with new physics in decay amplitudes," *Phys. Lett. B* 395, 241, 1997. [hep-ph/9612269].

[151] G. Hiller, "First hint of nonstandard CP violation from $B \to \Phi K(S)$ decay," *Phys. Rev. D* 66, 071502, 2002. [hep-ph/0207356].

[152] G. Burdman, "Flavor violation in warped extra dimensions and CP asymmetries in B decays," *Phys. Lett. B* 590, 86, 2004. [hep-ph/0310144].

[153] A. J. Buras, R. Fleischer, S. Recksiegel, and F. Schwab, "Anatomy of prominent B and K decays and signatures of CP violating new physics in the electroweak penguin sector," *Nucl. Phys. B* 697, 133, 2004.

[154] V. B. Berestetskii, E. M. Lifshitz, and L. P. Pitaevskii, "Quantum Electrodynamics," *Butterworth-Heinemann, Oxford, UK*, 1982.

[155] Q. Duret and B. Machet, "Discrete symmetries and the propagator approach to coupled fermions in Quantum Field Theory. Generalities. The case of a single fermion-antifermion pair," *Annals Phys.* 325, 2041, 2010

[156] K. M. Case, "Reformulation of the Majorana Theory of the Neutrino," *Phys. Rev.* 107, 307, 1957.

[157] H. K. Dreiner, H. E. Haber, and S. P. Martin, "Two-component spinor techniques and Feynman rules for quantum field theory and supersymmetry," *Phys. Rept.* 494, 1, 2010.

VITA

Education

Ph.D. in Physics, University of Kentucky (expected) *2012-2017.*

M.S. in Physics, Institute of Modern Physics, CAS, China *2007-2010.*

B.S. in Physics, Sichuan University, China *2003-2007.*

Research

- New method of directly testing the universality of $\sin(2\beta)$ and/or measuring penguin contributions in the entangled $B\bar{B}$ system.
- Phase constraints on discrete symmetry transformations (C, P, T) of Dirac fermions with $B - L$ violation.
- Development of new mechanism to set a limit on $B - L$ violating scale. That is $n - \bar{n}$ conversion, i.e., the transition of a neutron into an antineutron through the interaction with an external source, and its connection to $n - \bar{n}$ oscillation, in which a neutron transforms into an antineutron spontaneously.
- Neutron-antineutron transition operators and their matrix elements in the MIT bag model.

Professional development

- **National Nuclear Physics Summer School (NNPSS)**, MIT, July 18 – 29, 2016.
- **Theoretical Advanced Study Institute (TASI)**, University of Colorado, Boulder, June 6 – July 1, 2016.
- **Fundamental Neutron Physics Summer School**, University of Tennessee, June 14 – 20 2015.

Publications

[1] S. Gardner and X. Yan, "CPT, CP, and C transformations of fermions, and their consequences, in theories with $B-L$ violation," *Phys. Rev. D* 93, 096008 (2016), arXiv:1602.00693 [hep-ph].

[2] R. Dadisman, S. Gardner, and X. Yan, "Trapping Penguins with Entangled B mesons," *Phys. Lett. B* 754, 1 (2016), arXiv:1409.6801 [hep-ph].

[3] X. Yan, J. Wang, and Y. Yang, "Structure of ^{6}He in the frame of a cluster model," *Chin. Phys. C* 35, 550 (2011).

Talks and posters

- *Neutron-antineutron conversion: an alternate path to exploring B-L violation with baryons*, Talk, Indiana University Cyclotron Seminar, April 27, 2017.
- *Neutron-antineutron transitions*, Talk, 3rd PIKIO Meeting, held at Indiana University, March 4, 2017.
- $n-\bar{n}$ *transitions*, Talk, University of Kentucky Nuclear Physics Seminars, December 1, 2016.
- *Discrete-symmetry Phase Constraints in* $B-L$ *violation theories*, Poster, NNPSS 2016, MIT, July 22, 2016.
- *Phase constraints on discrete symmetries in* $n-\bar{n}$ *oscillations*, Talk, Joint theory journal club between University of California, Irvine and University of Hawaii, May 13, 2016.